

A census of symbiotic stars in the 2MASS, *WISE* and *Gaia* surveys

STAVROS AKRAS,^{1,2} LIZETTE GUZMAN-RAMIREZ,^{3,4} MARCELO L. LEAL-FERREIRA,^{5,6} AND GERARDO RAMOS-LARIOS⁷

¹*Observatório Nacional/MCTIC, Rua Gen. José Cristino, 77, 20921-400, Rio de Janeiro, Brazil*

²*Observatório do Valongo, Universidade Federal do Rio de Janeiro, Ladeira Pedro Antonio 43, 20080-090, Rio de Janeiro, Brazil*

³*Leiden Observatory, Leiden University, Niels Bohrweg 2, 2333 CA Leiden, The Netherlands*

⁴*European Southern Observatory, Alonso de Córdova 3107, Casilla 19001, Santiago, Chile*

⁵*Leiden Observatory, Leiden University, Niels Bohrweg 2, 2333 CA Leiden, Netherlands*

⁶*Argelander-Institut für Astronomie, Universität Bonn, Auf dem Hügel 71, D-53121, Bonn, Germany*

⁷*Instituto de Astronomía y Meteorología, Av. Vallarta No. 2602, Col. Arcos Vallarta, C.P. 44130 Guadalajara, Jalisco, Mexico*

(Received January 1, 2018; Revised January 7, 2018; Accepted February 6, 2019)

Submitted to ApJ

ABSTRACT

We present a new census of Galactic and extragalactic symbiotic stars (SySts). This compilation contains 323 known and 87 candidate SySts. Of the confirmed SySts, 257 are Galactic and 66 extragalactic. The spectral energy distributions (SEDs) of 348 sources have been constructed using 2MASS and AllWISE data. Regarding the Galactic SySts, 74% are S-types, 13% D and 3.5% D'. S-types show an SED peak between 0.8 and 1.7 μm , whereas D-type show a peak at longer wavelengths between 2 and 4 μm . D'-type, on the other hand, display a nearly flat profile. *Gaia* distances and effective temperatures are also presented. According to their *Gaia* distances, S-type are found to be members of both thin and thick Galactic disk populations, while S+IR- and D-types are mainly thin disk sources. *Gaia* temperatures show a reasonable agreement with the temperatures derived from SEDs within their uncertainties. A new census of the O VI $\lambda 6830$ Raman-scattered line in SySts is also presented. From a sample of 298 SySts with available optical spectra, 55% are found to emit the line. No significant preference is found among the different types. The report of the O VI $\lambda 6830$ Raman-scattered line in non-SySts is also discussed as well as the correlation between the Raman-scattered O VI line and X-ray emission. We conclude that the presence of the O VI Raman-scattered line still provides a strong criterion for identifying a source as a SySt.

Keywords: catalogs - stars: binaries: symbiotic - stars: fundamental parameters - (stars:) white dwarfs - (ISM): dust, extinction

1. INTRODUCTION

Symbiotic stars (SySts) are interacting, wide binary systems consisting of a red giant or a supergiant star that transfers matter to a much hotter companion, usually a white dwarf (WD), which can also be a neutron star. In the case of a white dwarfs as a primary, the secondary can be either a red giant or an asymptotic giant branch (AGB) star, and they are categorized as WD-symbiotics, whereas in the case of a neutron star as a

primary, the secondary can be either a giant, AGB star, or a supergiant, and they are categorized as symbiotic X-ray binaries (Masetti et al. 2006a; Luna et al. 2013). In this paper, we refer to both groups as SySts.

The optical spectrum of SySts consists of both absorption features due to the photosphere of the cool companion (e.g. TiO, VO, C₂, CN) as well as a number of high-ionization lines (e.g. He II $\lambda 4686$, [Fe VII] $\lambda\lambda 5727, 6087$, O VI $\lambda 6830$), low-/intermediate-ionization lines (e.g. [N II] $\lambda\lambda 6548, 6584$, [O III] $\lambda\lambda 4959, 5007$) and bright Balmer lines (e.g. H α , H β) due to the presence of a luminous and hot WD. Despite their spectra resembling those of planetary nebulae (PNe), they are not considered as genuine PNe. PNe are systems in which

Corresponding author: Stavros Akras
 stavrosakras@on.br, akras@astro.ufrj.br

the WD ionizes the material that the same star expelled during the AGB phase, while in case of SySts the material that the WD ionizes comes from the secondary.

The most common criteria to classify a source as a SySt are the following: (i) the presence of strong He II $\lambda 4686$ and H α lines as well as emission lines from high-excitation ions (e.g. [Fe VII] $\lambda\lambda 5727, 6087$), (ii) the presence of the absorption features TiO, VO and CN associated with the photosphere of the cool companion, and (iii) the presence of the O VI Raman-scattered lines centered at 6830 and 7088Å (e.g. Kenyon 1986; Mikolajewska et al. 1997; Belczyński et al. 2000).

The two broad O VI $\lambda\lambda 6830, 7088$ lines usually seen in SySts are interpreted as the result of the Raman-scattering of the UV O VI $\lambda 1032$ and $\lambda 1038$ resonance lines by neutral hydrogen (Nussbaumer et al. 1989; Schmid 1989). Even before the identification of these two lines, Allen (1980) and Schmid & Schild (1994) had pointed out that 50% or more of SySts exhibit the O VI $\lambda 6830$ line in their spectrum. The O VI $\lambda\lambda 6830, 7088$ Raman-scattered lines have been proven to be a powerful tool for studying jets and accretion disks in SySts (e.g. Lee & Kang 2007; Heo & Lee 2015; Heo et al. 2016). Besides the spectroscopic observations for searching SySts, O VI $\lambda 6830$ imaging polarimetry can also become a very efficient method for discovering new SySts without follow-up spectroscopic observations or additional emission line images (Akras 2017).

SySts are classified into two main categories based on their near-infrared data (Allen & Glass 1974; Webster & Allen 1975): (i) those with a near-IR color temperature of ~ 3000 - 4000 K, which is attributed to the temperature of a K, M, or G spectral-type giant (stellar or S-type SySts),¹, and (ii) those with a near-IR color temperature around 700-1000 K, indicating a warm dusty circumstellar envelope surrounding a more evolved AGB star, usually a Mira variable (dusty or D-type SySts). From the point of view of their spectral energy distributions (SEDs), S-type and D-type SySts have a peak in their SED profiles at 1-2 and 5-15 μm , respectively (Ivison et al. 1995).

Allen (1982) added a third type of SySt, namely D'-type, in order to separate those with SED profiles that peak at even longer wavelengths than the normal D-type between 20 and 30 μm . The true nature of D'-type SySts is still controversial. According to Allen (1982), the cool companions of D'-type SySts are either a K

or a G spectral type giant and their spectra exhibit a mid-IR excess due to the presence of a dusty component with temperatures lower than those of D-type SySts. On the other hand, Kenyon, Fernandez-Castro & Stencel (1988) claimed that this group of SySts have far-IR colors that resemble those of compact planetary nebulae (see also Corradi & Schwartz 1997; Pereira, Smith & Cunha 2005).

SySts are considered as potential progenitors of type Ia supernova (SNe Ia) due to the large amount of mass that WDs accrete from the winds of the cool companions, resulting in them exceeding the Chandrasekhar mass ($1.4 M_\odot$) and exploding as a SN Ia (Munari & Renzini 1992; Han & Podsiadlowski 2004; Di Stefano 2010; Dilday et al. 2012). Consequently, the interest in SySts has been gradually increasing, and many attempts have been made to discover new members in this class of objects either in our galaxy or nearby galaxies in the Local Group (e.g. Miszalski et al. 2014; Mikolajewska et al. 2014).

SySts are also important X-ray sources. The origin of X-ray emission in SySts is manifold: (i) the thermonuclear activity on the hot WDs, (ii) the colliding winds, and/or (iii) the accretion disk. Muerset, Wolff & Jordan (1997) identified 16 SySts as supersoft X-ray sources based on *ROSAT* observations. The authors proposed a classification scheme based only on their X-ray emission, dividing SySts into three groups: (a) the supersoft X-ray sources with energies ≤ 0.4 keV, likely emitted directly from the white dwarf (α -type), (b) soft X-ray objects that exhibit a peak at 0.8 kev and maximum energies up to 2.4 keV, likely originating from a hot, shocked gas where the stellar winds collide (β -type) and (c) objects with a non-thermal emission and energies higher than 2.4 keV (γ -type) due to the accretion of mass onto a neutron star.

New X-ray observations have revealed SySts with very hard X-ray emission (> 10 keV) (Chernyakova et al. 2005; Tueller et al. 2005). Recently, Luna and collaborators presented new *Swift* X-ray Telescope (XRT) data of nine SySts, and they refined the previous X-ray classification scheme by adding a new type, namely the δ -type (Luna et al. 2013). All these SySts have very hard X-ray thermal emission with energies higher than 2.4 keV likely originating from the inner regions of an accretion disk. Overall, the number of SySts with X-ray emission is increasing, and the current number is 44. Seven out of 44 are classified as α -type, 12 as β -type, 9 as γ -type, 8 as δ -type, and 8 as β/δ -type (Luna et al. 2013 and references therein; Mukai et al. 2016, Wheatley, Mukai & de Martino 2003, Nuñez et al. 2016).

¹ S-type SySts are also divided into two subgroups: (i) the yellow SySts with a K or G giant companion and (ii) the red SySts with an M-type giant companion (Schmid & Nussbaumer 1993; Frankowski & Jorissen 2007).

Over the last 20 years many new SySts have been discovered in our Galaxy and nearby galaxies. We thus decided to census the general population of known and candidate SySts, present their photometric data from the Two Micron All Sky Survey (2MASS, Cutri et al. 2003; Skrutskie et al. 2006) and the *Wide-field Infrared Survey Explorer* (*WISE*; Wright et al. 2010, Cutri et al. 2014) all-sky near-IR surveys and provide their classification in the scheme of S/D/D'-types from a wider spectral range (1-22 μm).

The paper is organized as follows: the sample selection, the description of the census, and the cross-matching between the 2MASS and AllWISE catalogs are presented in Sect. 2. The SED profiles, the black-body fitting, the temperature and distance using *Gaia* (Gaia Collaboration et al. 2016, 2018), and the classification of SySts are described in Sect 3. We present an updated census of the O VI $\lambda 6830$ Raman-scattered line in SySts in Sect. 4. We also discuss the report of the O VI Raman-scattered line in non-SySts. In Sect. 5, we explore the link of the O VI Raman-scattered lines with the metallicity and X-ray emission. We end up with our conclusions in Sect. 6.

2. SAMPLE SELECTION

The most comprehensive compilation of SySts was published by Belczyński and collaborators in 2000 (Belczyński et al. 2000, hereafter Bel2000). Their catalog includes all of the known Galactic and extragalactic SySts (188), as well as a number of candidate SySts (30). Before that catalog, two more had been already published by Allen (1984) and by Kenyon (1986).

The total number of known SySts has been continuously increasing since 2000. Most of the discoveries have been made by two independent groups: (a) Miszalski, Mikolajewska, and collaborators and (b) the INT Photometric H α Survey (IPHAS collaboration; Drew et al. 2005, see Table 5 in Appendix A for references).

Our new census of SySts lists 323 known and 87 candidate SySts. From the known SySts, 257 are Galactic and 66 extragalactic. This corresponds to a $\sim 45\%$ increase in the population of Galactic SySts and a $\sim 350\%$ increase in the population of extragalactic ones since the last SySt catalog (Table 5 in Appendix A)

Aside from the most commonly and widely used criteria presented in Bel2000, there are a number of SySts identified based on their strong UV excess and the characteristic spectrum of a red giant (e.g. SU Lyn; Mukai et al. 2016), or their strong blue-violet continuum ($U-B$ and $B-V$), and their H α line profile and orbital periods >600 days (Hen 4-18 and Hen 4-121; Van Eck & Jorissen 2002). Mukai et al. (2016) argued that the classical

criteria for identifying SySts (e.g. Bel2000) are biased toward systems with luminous WDs and that the true population is underestimated.

Despite all these new discoveries, the total number of SySts still remains very low compared to the expected number of SySts in our galaxy (3×10^3 , Allen 1984; 3×10^4 , Kenyon et al. 1993; 3×10^5 , Munari & Renzini 1992; 4×10^5 , Magrini et al. 2003; $1.2-15\times 10^3$, Lü et al. n 2006). Nevertheless, the number of SySts is expected to significantly increase over the next few years due to ongoing surveys like VPHAS+ of the southern Galactic plane and Bulge (Drew et al. 2014), J-PAS (Benítez et al. 2014)/J-PLUS (Cenarro et al. 2018, submitted) of the northern hemisphere; and S-PLUS of the southern hemisphere (Mendes de Oliveira C., et al. 2018, in preparation); as well as private survey programs (Miszalski et al. 2014; Mikolajewska et al. 2014)

2MASS data have been widely used to study SySts as well as to divide them into the S and D types (e.g Allen & Glass 1974; Phillips 2007; Corradi et al. 2008). However, the peak of the SEDs of D-type SySts is suggested to occur at wavelengths between 5 and 15 μm (Ivison et al. 1995), longer than the wavelength range covered by 2MASS (between 1 and 2.16 μm). The *WISE* survey, on the other hand, covers these longer wavelengths (between 3.6 and 22.1 μm), and it is coherent to construct and study the SED profiles of SySts using both surveys. Yet, it is well known that SySts exhibit strong flux variations. In Section 3, we discuss the impact of possible flux variations between the two surveys because of the different epochs in which they were carried out.

The first classification of SySts into S and D types by Allen and Glass (1974) was made based on observations in the J , H , K_s and L bands. The latter is centered at 3.5 μm , very close to the $W1$ band of the *WISE* survey. These authors mentioned that the $H-J$ color index alone is not a reliable criterion for classifying SySts into S and D types but the K_s-L index is. S type SySts are found to exhibit $K_s-L < 0.9$, while D type SySts exhibit $K_s-L > 1.3$. Photometric data from longer wavelengths are crucial for studying these objects and may provide a more robust classification.

Table 6 in Appendix A presents our list of SySts. The first column lists the name of SySts ordered by R.A. The second and third columns give the coordinates (R.A. and decl.) in the J2000.0 epoch of SySts. The rest of the columns list the 2MASS (from the All-Sky Catalog of Point Sources; Cutri et al. 2003) and *WISE* (from the AllWISE catalog; Cutri et al. 2014) photometric magnitudes and associated errors (except for the upper limit values).

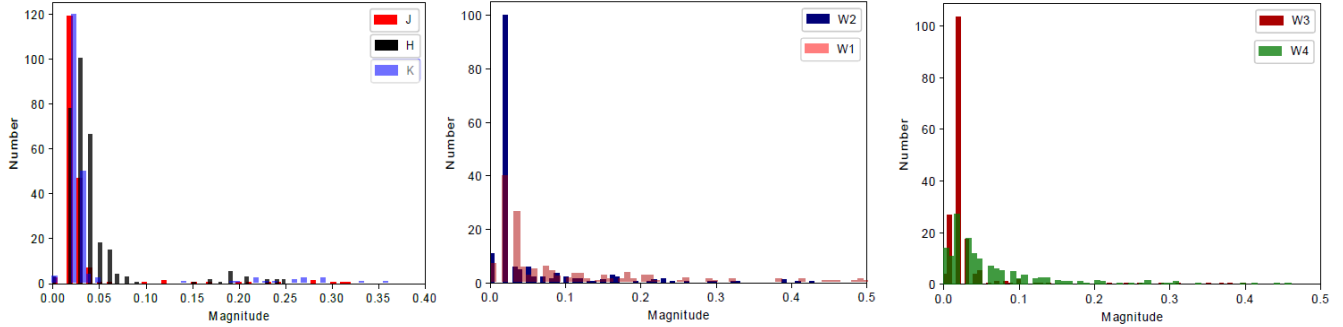


Figure 1. Histogram of the photometric errors for the 2MASS and *WISE* bands.

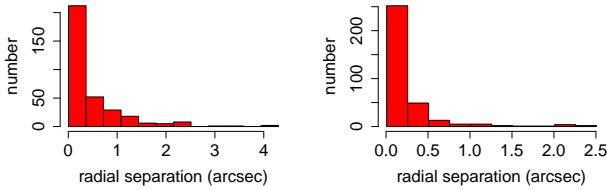


Figure 2. Radial distance separation between the positions of our list and those of AllWISE catalog (left panel) and between the *WISE* positions and the associated 2MASS counterparts (right panel).

The histogram of the photometric errors for all of the bands is illustrated in Figure 1. The vast majority of the 2MASS measurements have photometric errors lower than 0.1 mag, while those from the AllWISE catalog are lower than 0.17 mag. In particular, 95%, 92% and 93% of SySts in the *J*, *H*, and *K_s* bands, respectively, have photometric errors lower than 0.075 mag. The *WISE* measurements show higher photometric errors compared to the 2MASS data. Only 70%, 80%, 93% and 70% of SySts have photometric errors lower than 0.075 mag in the *W1*, *W2*, *W3* and *W4* bands, respectively. We also find that the *W1* and *W4* bands show systematically higher errors than the *W2* and *W3* bands.

All SySts have been cross-matched with the 2MASS and AllWISE catalogs assuming a matching radius of six arcsec due to the resolution of the *WISE* survey (Wright et al. 2010). The radial distance separation between the positions of the sources in our list and the AllWISE catalog as well as that between the AllWISE catalog and the associated 2MASS counterparts are presented in Figure 2. For the majority of the SySts, the matching between the catalogs is very good. In particular, 88% of all SySts in our list have a radial distance separation with AllWISE lower than 1 arcsec and 94% per cent lower than 2 arcsec, while 96% have a radial distance separation between the AllWISE and 2MASS

counterparts lower than 1 arcsec and 98% lower than 2 arcsec.

3. SPECTRAL ENERGY DISTRIBUTIONS

Due to the fact that the S- and D-type SySts show a peak in their SEDs between 1 and 15 μm , we constructed only the infrared SEDs of the SySts from 1 to 22 μm . To fit the 2MASS and AllWISE photometric data, we considered blackbody (BB) models. This approximation is adequate for obtaining a rough estimate of the temperature of the cool companion in S-type SySts as well as the temperature of the dust shells in D-type SySts. But not all of the SED profiles can be fitted assuming one BB model. It is known that some D-type SySts exhibit two dust components (Angeloni et al. 2010).

The majority of SySts are well fit by assuming only one BB model. But surprisingly, we found a number of SySts with an S-type SED profile and an infrared excess in the mid-infrared regime (see Fig. 3 and 4). In the case where a BB model does not fit well all the data points well, we fit the data again taking into account only the first five data points (2MASS, *W1*, and *W2*) in the calculation of the reduced χ^2 . If the reduced χ^2 of the second fitting is smaller than the first one and the visual inspection of the SED fittings indicates a possible excess at the *W3* and *W4* points, we apply the second BB model to fit the last two points.

All of these SySts, except for four display clear excesses at both *W3* and *W4* bands, which ensures the presence of the second dust component (see Fig. 3). The low *W3* and *W4* photometric errors make the detection of the dust component more confident. Upper limits on the *W3* and/or *W4* data points are not considered as possible excesses. The likelihood of false detections is small but not negligible, especially for the cases (4 out of 27) in which the excess is detected only in the *W4* band.

Regarding the D'-type SySts, three BB models (or two BB models for SySts with upper limit data) are used in order to reproduce their flat SED profiles, one for the

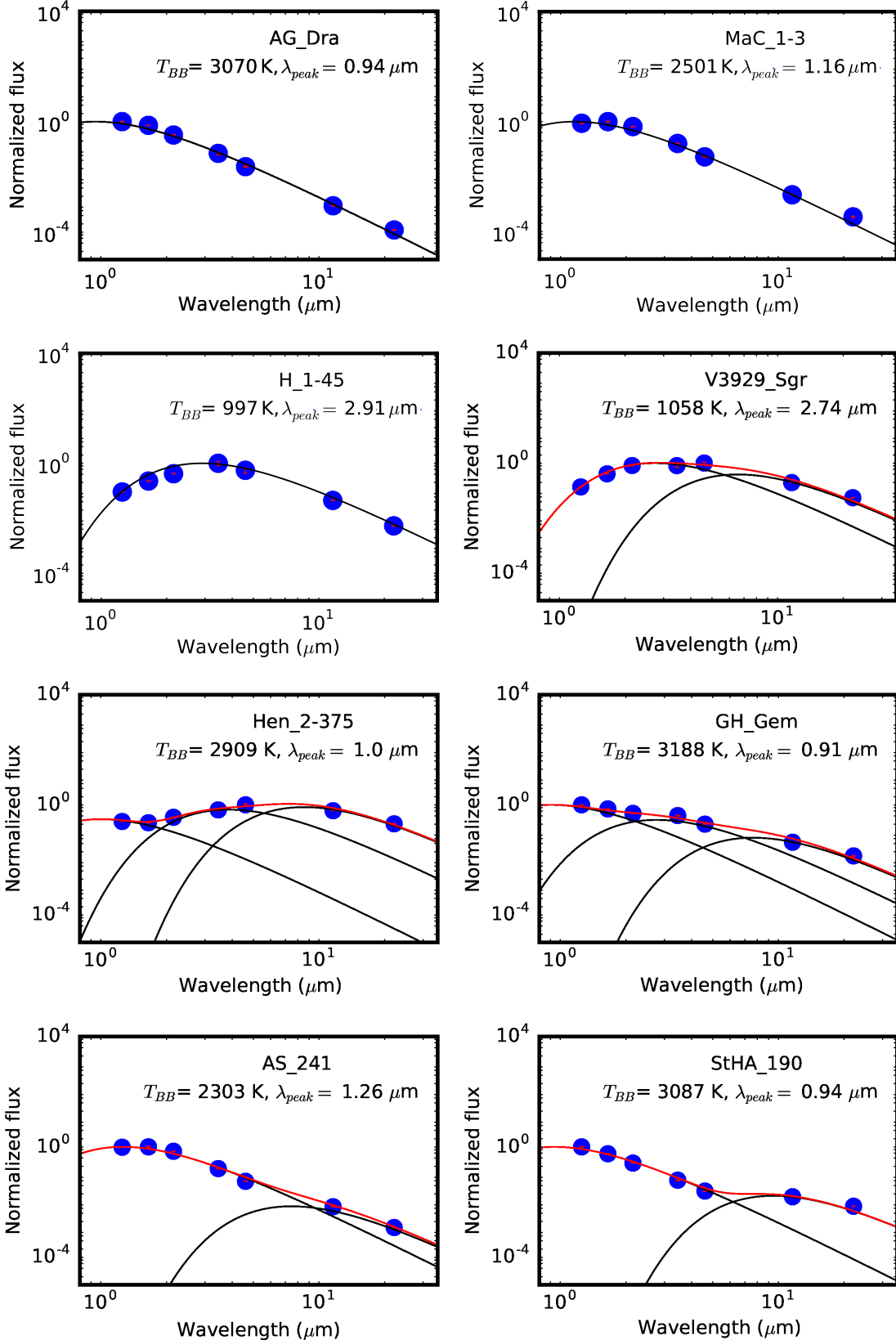


Figure 3. Examples of normalized SED profiles for two S- (first line), two D- (second line), two S+IR- (third line), and two D'-type SySts (fourth line). The blue dots correspond to the photometric data from the 2MASS and *WISE* surveys, the black lines to the BB models for each component, and the red line to the final fit only for cases of multicomponent SEDs. The errors of the data are portrayed by the vertical red bars, but in most cases are very small. (Figure set 3 presents the SED profiles for all SySts, Figures 3.1–3.348).

cold giant and two for the dust components (Figure 3). The temperatures of the BB models were varied until a good fitting was obtained by visually inspection of the SED fittings. The small number of data points used to fit each model makes the fittings for D'-type SySts less precise, although the difference in the final SED profiles between D'-type SySts and other types is still perceptible.

For a more detailed multiwavelength modeling of SySts' SEDs, we refer the reader to Skopal (2005) and Skopal (2015a,b,c). Only a handful of SySts have been modeled in such detail so far. In order to perform a similar study for all SySts, one would need data that are not available.

It should be noted that any BB model can adequately describe the temperature of a dust shell. However, the effective temperature (T_{eff}) of red giants shows a significant departure from the BB temperatures (T_{BB}), and further corrections are needed (see § 3.1).

The photometric data are not corrected for the interstellar extinction, which can alter the derived SED temperatures. However, it is very difficult to disentangle the interstellar extinction from the intrinsic extinction of SySts (e.g. Phillips 2007).

The interstellar color excess, $E(B-V)$, has been estimated for several SySts using either the 2200Å feature using UV data (Baratta & Viotti 1983; Sahade et al. 1984; Parimucha & Vaňko 2006) or recombination lines in the optical (de Freitas Pacheco & Costa 1992; Costa & de Freitas Pacheco 1994; Pereira 1995; Mikolajewska, Acker & Stenholm 1997 among others). The former method gives $E(B-V)$ values in the range of 0.2–0.67, while the latter gives values up to ~ 2 mag. The difference in $E(B-V)$ estimates between the two methods is significant. There are also cases in which the $E(B-V)$ differ by more than 0.5 mag despite using the same method.

SEDs for different $E(B-V)$ from 0.1 to 1.5 (or A_V from 3.1 to 4.65 mag, assuming $R_V=3.1$ and the interstellar extinction law from Cardelli, et al. 1989) were simulated in order to verify the effect of interstellar extinction on our SED temperatures. The final effective temperatures of the cold companions in SySts (corrected for the blackbody approximation) differ by ~ 240 K (620 K) for an extinction $A_V=3$ mag (6 mag). For the SySt with the highest $E(B-V)$ value of 0.67 (RS Oph) in the list from Parimucha & Vaňko (2006), the temperature of the cold companion is 3460 K before correcting for the interstellar extinction and 3610 K after the correction. This difference of 150 K is within the overall error of our temperature estimates. For $E(B-V)>1.6$ the temperature difference exceeds the error of our temperature

estimates (450 K). From the sample of 67 southern SySts in Mikolajewska et al. (1997), there are 13 SySts with $E(B-V)>1.5$. It is, thus, very difficult to determine the effect of interstellar extinction in SySts, and we decided to provide temperatures without correcting for the interstellar extinction.

Figure 3 portrays the normalized flux SED profiles for two examples each of S-, D-, and D'-type SySts as well as a fourth type of SySt that we call S+IR (see below). The peak of the SED profile for each SySt is normalized to one. The cool red giant clearly dominates the SED of the S-type, whereas dust emission dominates that of D-type SySts. In the case of V3929 Sgr, two dust components are required in order to reproduce the total SED profile in agreement with the results from Angeloni et al. (2010). In D'-type SySts, both components, the red giant and the dust shells, contribute to the total SED, resulting in a nearly flat profile. The common characteristic of D'-type SySts is the need for three BB components to fit the entire SED profile. D- and D'-type SySts seem to compose two different groups, which is not unambiguous when only 2MASS data are used. Figure set 3 presents all of the SED profiles.

In Figure 4, we present all of the flux density SEDs superimposed together in four individual plots. The SED fits of all known SySts are shown with black lines with 80% transparency so that one can easily notice the high density of S-type SySts close to its corresponding prediction interval. We derived polynomial fits of fourth degree to define the typical SED representation of each type. These are indicated by the red solid lines in the figures. The polynomial fits were given as input in the "predict" function in R (R Development Core Team 2008) so that the prediction interval of the corresponding SED type could be calculated. We assumed weights inversely proportional to the standard deviation of the SEDs when deriving the prediction interval. They are shown in shaded cyan in the figures and represent the regions where the SEDs of 95% of new observations are expected to occur. We also show in shaded blue the confidence intervals (where the mean of new observations is expected to be) of each type in the figures. They were derived with the R function "t.test", and a confidence level of 95% was used.

Generally, the SED profiles of S-type SySts exhibit a peak intensity at wavelengths between 0.8 and 1.7 μm with a high occurrence at 1.0–1.1 μm , while the D-type SySts have an SED peak at longer wavelengths between 2 and 4 μm , with a high occurrence between 2 and 2.5 μm (Figure 5). As for the new S+IR type, they are well spread out along the wavelength range between 0.9 and 1.7 μm (Figure 5).

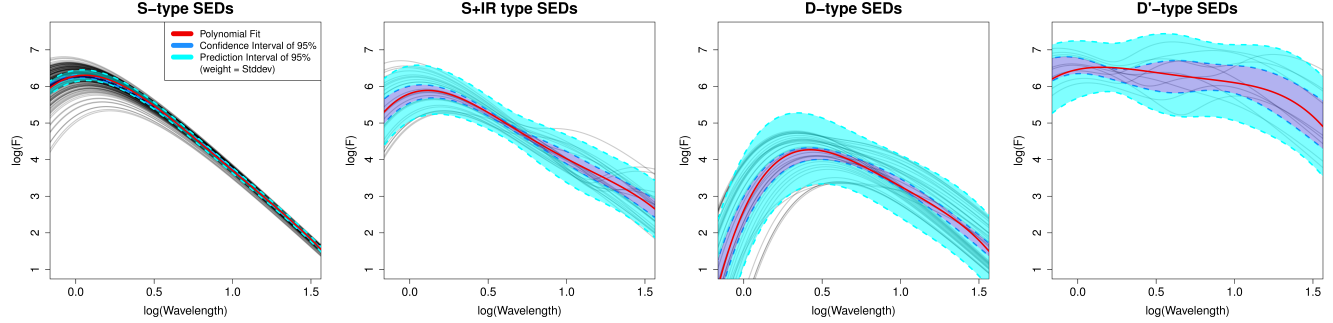


Figure 4. SED flux density profiles of all the S-, S+IR-, D- and D'-type SySts (gray lines). The typical SED profile for each type has also been determined with a confidence interval of 95% (blue dark) and prediction interval of 95% (cyan) derived with weights inversely proportional to the standard deviation. The red lines give the typical SED profile for each type by applying a polynomial fitting.

Table 7 in Appendix A lists all information obtained from the SED fitting. The first column gives the name of SySts in the same order as in Table 6 (Appendix A). The second and third columns give the old (from the literature) and the new classification (this work), respectively. The fourth column gives the temperature of the cold companions for the S-, S+IR- and D'-type SySts while the fifth column lists the temperature of the dust shells for the S+IR-, D- and D'-type SySts. The sixth column gives the effective temperature of the cold companions corrected for the blackbody approximation (see Section 3.1). The seventh and eighth columns provide the stellar effective temperatures of the secondary companions from the second *Gaia* data release (Gaia Collaboration et al. 2018) and their geometrical distances estimated from *Gaia* parallaxes (Bailer-Jones et al. 2018). The ninth column gives the wavelength at which the stellar component or the brightest dust shell shows a radiation peak. Finally, the last three columns provide information on the detection of the O VI Raman-scattered line, X-ray emission, and their respective references.

The vast majority of the SEDs are very well fitted, providing a good classification, and only around 20 of them may have a poor fitting (<7%). R Aqr, for instance, is one example with a new classification. In particular, Contini & Formiggini (2003) have pointed out that the cool companion of R Aqr is a Mira variable star surrounded by a dust envelope with a temperature of 1000 K. Our SED profile indicates an S-type SySt, but the upper limit values for the *W1*, *W2* and *W3* bands makes its classification unreliable. Another example is AS 245, which clearly exhibits an S-type SED profile rather than of a D-type SySt with a Mira companion. Gromadzki et al. (2009) also reclassified this SySt as an S-type, which means that the old classification of SySts in the S/D scheme is not always correct.

Overall, 74% of the known SySts are classified as S-types, 13% as D-types, and only 3.5% as D'-type. More-

over, only 26 SySts have obtained a new classification in this work. Fourteen S-types and two D-types are now classified as S+IR-types, three D-types are classified S-types and four as D'-types, two S-types have been reclassified as D- and D'-types, and finally, one D'-type is now classified as D-type.

As mentioned before, it is known that SySts exhibit large flux variations due to the interaction between the evolved red giant and the hot WD. The mass transfer from the red giant to the WD is the main cause of these variations together with several other phenomena like orbital motion, dust obscuration, and radial pulsations of the Mira companions in D-type or semi-regular pulsations of the red giants in S-type (see e.g. Whitelock 1987; Henden & Munari 2000, 2001, 2006; Mikolajewska 2001; Gromadzki et al. 2009, 2013, among others).

Multi-epoch photometric studies have been carried out either in the optical wavelengths or the near-infrared regime (e.g. Lorenzetti et al. 1985; Henden & Munari 2000, 2001, 2006; Mikolajewska 2001; Gromadzki et al. 2009, 2013; Jurkic & Kotnik-Karuza 2012). All of these studies have shown that flux variations can have a maximum amplitude up to 6-7 mag in the optical regime but significantly smaller at longer wavelengths. CH Cyg is a notable example with a large amplitude variations of up to 4 mag in the *U*-band but significantly lower in the near-infrared regime of 0.5 mag (Munari et al. 1996).

Therefore, it is necessary to examine how much these flux variations between the 2MASS and AllWISE data (due to the different epochs of the two surveys) affect the SED fitting and the resulting temperatures. For this exercise, we used an S- and a D-type SySt as test objects. We inferred a fluctuation in their photometric data and then we fitted their new data sets assuming six different scenarios: (1) 2MASS in the maximum brightness and *WISE* in the minimum, (2) 2MASS in the minimum brightness and *WISE* in the maximum, (3) 2MASS in the maximum brightness and *WISE* without

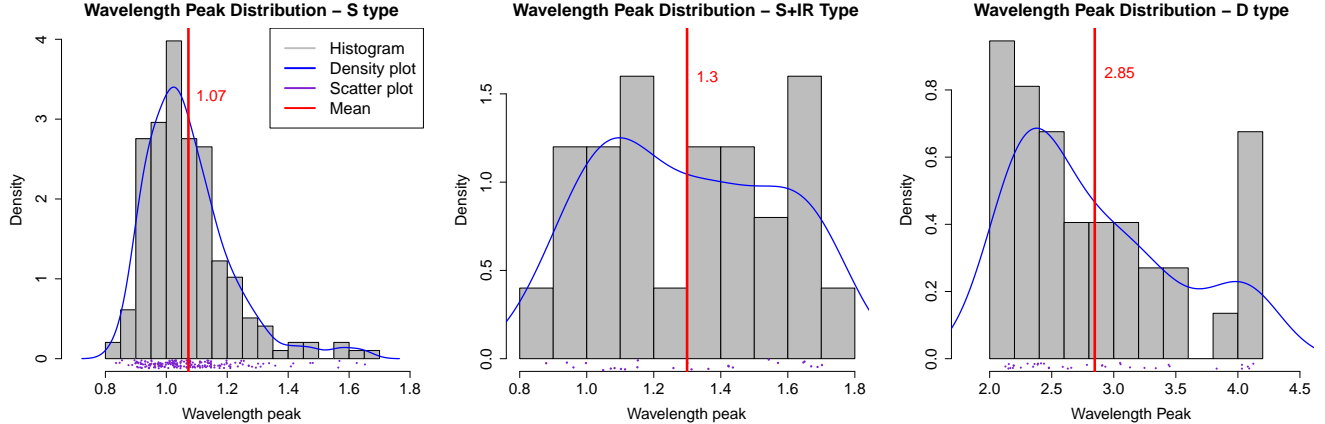


Figure 5. Histograms of the wavelengths at which the SED profiles for each type of SySt peaks, except for that of D'-type. The vertical red lines indicate the mean values for each type, the purple points portray the scattering of the sources, while the blues lines represent the density distribution.

any variation (4) 2MASS in the maximum brightness and *WISE* without any variation, (5) 2MASS without any variation and *WISE* in the minimum brightness, and (6) 2MASS without any variation and *WISE* in the minimum brightness. This was repeated for four different amplitude variations (see Appendix B). We then repeated the whole procedure for four D-type SySts, but in this case we used their observed amplitude variations taken from Gromadzki et al. (2009).

The main result from this exercise is that flux variations up to 2 mag do not significantly affect the SED fitting or the classification of SySts (see Appendix B). Moreover, by examining closely all of these artificial SEDs, we came to the conclusion that a poor fitting on the *W1* and *W2* bands or the 2MASS data may indicate some flux variability between the data. Overall, flux variations between the 2MASS and *WISE* data result in temperature variations of the order of 300-400 K which is comparable to the uncertainties of our estimates.

Only a handful of SySts exhibit noticeable signs of such variations in their SEDs (e.g. 2MASS J17391715-3546593, 356.04+03.20, AS 245, H 2-34, PN H 2-5, RT Cru, SMP LMC 88, UV Aur, BI Cru, Hen 2-127, AS 221, Hen 2-139, K 3-9, RR Tel, V347 Nor, V835 Cen, 354.98-02.87).

Nevertheless, a good agreement is found with previous studies. For instance, RR Tel is a known and well-studied variable SySt with maximum amplitudes up to 3.47 mag in *J*, 2.84 mag in *H*, 2.05 mag in *K* and 1.29 mag in *L* magnitudes (Gromadzki et al. 2009). Nevertheless, our $T_{\text{dust}}=1258$ K agrees with the temperature derived from a more detailed SED study between 1200 and 1350 K (Jurkic & Kotnik-Karuza 2012). The S-type SySt CH Cyg is another example for which our

$T_{\text{eff}}=3063$ K agrees with the value reported by Hinkle, Fekel & Joyce (2009).

Regarding the S+IR-type SySts, the excess at 11 and 22 μm cannot be attributed to possible flux variations between the 2MASS and *WISE* observations since the *W1* and *W2* bands do not present any significant deviation from the BB fitting.

Only 9 out of 42 D-type SySts have a new classification type (two as S+IR-, three as S-, and four as D'-type). The presence of a Mira variable star is not directly confirmed in all these systems. For instance, LAMOST J202629.80+423652.019 is proposed to be a D-type based only on some optical emission lines (Li et al. 2015). EF Aql, on the other hand, shows variability with amplitudes of around 2 mag and a period of 330 days (Margon et al. 2016) but its *J-H* and *H-K* color indices are not consistent with a D-type classification (Corradi et al. 2008; Rodriguez-Flores et al. 2014; Clyne et al. 2015).

Multiwavelength modeling of the SySts' SED profiles have shown that during the supersoft X-ray phase or days/weeks after an outburst event, the major contributor to the optical and near-IR spectral wavelength regimes is the nebular emission (Skopal 2015a, b, c). The duration of this active phase corresponds to a small part of the SySts' lifetime, and it is not expected to affect our SED fits.

3.1. T_{eff} vs. T_{BB}

As mentioned above, it is well known that T_{BB} does not provide the correct T_{eff} . Extensive studies on the relation between the T_{eff} and T_{BB} of K, M and G giant stars have been performed by several authors (Dyck et al. 1996; Van Belle et al. 1999; Alonso et al. 2000; Houdashelt et al. 2000; Tej & Chandrasekhar 2000, VandenBerg & Clem 2003). T_{BB} shows a significant

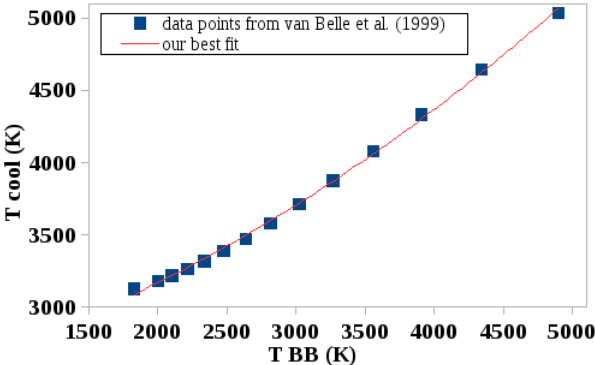


Figure 6. T_{BB} vs. T_{cool} plot. The data points have been obtained from van Belle et al. (1999). T_{BB} corresponds to the stellar temperature assuming a blackbody approximation and T_{cool} to the observed effective temperatures for spectra from M7 to G7. The red line corresponds to our best fit of the data assuming a polynomial function of second degree.

departure from T_{eff} for red giants with $T_{eff} < 4000$ K, and this difference becomes more important as T_{eff} becomes lower (see Figure 2 in van Belle et al. 1999). The discrepancy between the T_{eff} and T_{BB} is attributed to the presence of absorption features such as $^{12}\text{CO}(2,0)$ at $2.29\ \mu\text{m}$ or MgH and TiO bands (van Belle et al. 1999 and references therein).

Given that our T_{BB} range between 2200 and 4000 K, it is clear that the difference between T_{BB} and T_{eff} is significant for most SySts, and it has to be taken into consideration. To convert T_{BB} into T_{eff} , we took the values from Table 8 in van Belle et al. (1999) and applied a polynomial function of second degree to fit the data (Figure 6). This relation allows us to convert the T_{BB} of red giants to a more reliable T_{eff} . Hereafter, we refer to the effective temperature of the cool companions obtained from our best fit as T_{cool} .

The data yield the relation $T_{cool} = 6.22 * 10^{-5} * T_{BB}^2 + 0.23 * T_{BB} + 2468$ (K) with R^2 (the goodness of fit) equals to 0.9986 (Figure 6). The T_{cool} values of red giants for all SySts are given in Table 7 in Appendix A. The error of T_{cool} is estimated between 250 and 450 K due to the average standard deviation of the observed T_{eff} of 250 K (van Belle et al. 1999) and the uncertainty of our fitting.

Before we continue to the analysis of the temperatures for each type of SySts, it is necessary to compare our estimates with those from previous spectroscopic studies (T_{eff} , Table 1). The upper left panel in Figure 7 displays the difference between T_{cool} and (T_{eff}) . The blue solid line represents the average difference between the two temperatures (excluding three stars with $T_{eff} > 4400$ K), while the blue dashed lines correspond to the 1σ deviation of the distribution. The three stars with high temperature belong to the rare group of yellow SySts

with a K or G spectral-type giant. There are seven more sources with a temperature difference of around 500 K, which is comparable with our temperature error of 450 K. The upper right panel in Figure 7 illustrates the histogram of the temperature difference without including the three extreme cases.

Given that our SED fitting is restricted only to the IR regime (2MASS and *WISE* data) while other authors have used a broader spectral wavelength range from X-ray to radio (Skopal 2005, Angeloni et al. 2007), it is worth comparing our temperatures with those derived from these studies. Again, a good agreement between the two temperatures is found. The temperature difference is around 550 K. This verifies that the analysis of SEDs in this work provides a reliable classification as well as temperature within the uncertainties.

To go one step further, we also compared the temperatures of the cold companions obtained from Skopal (2005) with the equivalent observed values from Table 1. A lower temperature difference of 200 K is found. This better matching is not a result of the broader spectral wavelength range used for the SED fitting, but the use of a more robust stellar atmosphere model for the red giants, considering T_{eff} and θ_g as free parameters rather than a blackbody.

In Figure 8, we present the histograms of the T_{cool} for the red giants in S- (upper panel) and S+IR-type SySts (lower panel). The temperatures range from 3000 to 4100 K which is consistent with red giants of spectral types K, M, and G. The vast majority of the cool companions in S- and S+IR-type are M-type giants, whereas only a few are likely K- or G-type giants. The average temperatures for S- and S+IR-type SySts are 3574 and 3352 K, respectively.

3.2. *SySts in Gaia*

3.2.1. Stellar temperatures

The recent second *Gaia* data release provides the stellar temperature for 161 million stars and luminosity for 77 millions stars (Andrae et al. 2018; Gaia Collaboration et al. 2018). *Gaia* temperatures are estimated by training a machine learning algorithm (Priam algorithm)² using various samples covering a temperature range from 3000 to 10,000 K (part of DR2; Andrae et al. 2018). The typical error of the temperature is around 324 K, but it becomes as high as 550 K in the case of cold stars ($T < 4000$ K) or hot stars ($T > 8000$ K). Given that the majority of the cold companions in SySts have an M or K spectral types with temperature lower than

² T_{eff} is estimated assuming zero extinction, due to the strong degeneracy between T_{eff} and A_G .

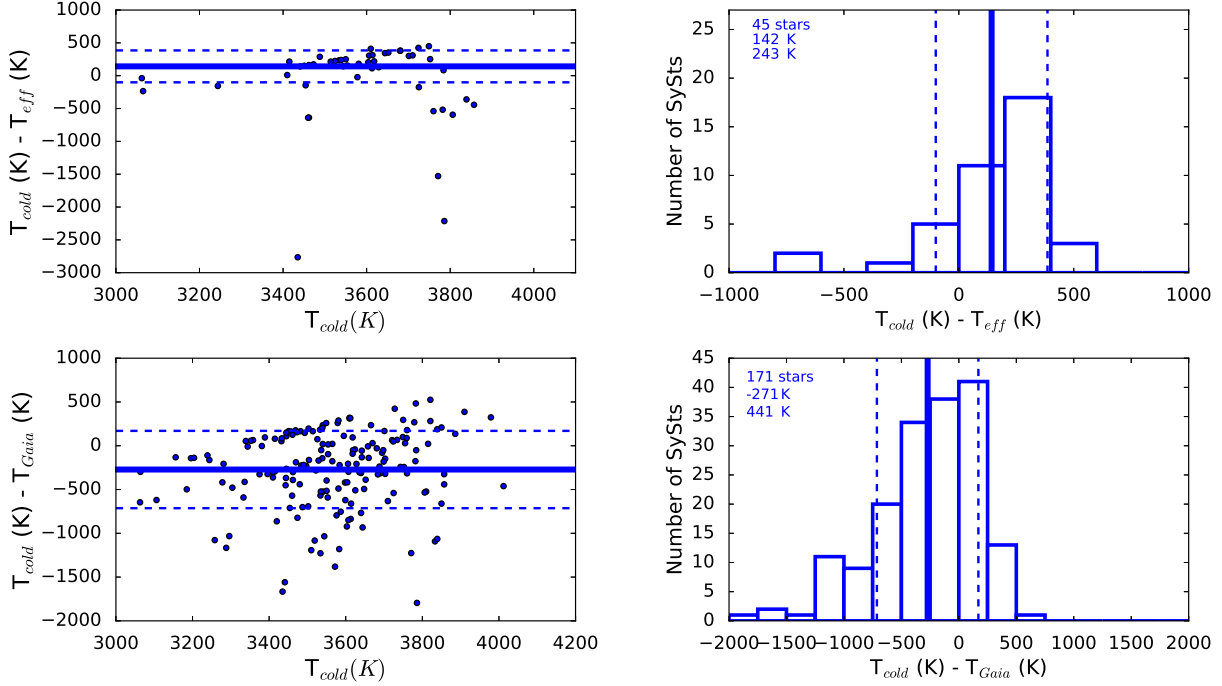


Figure 7. Left panels: difference between our temperature estimates (T_{cool}) and the effective temperatures taken from the literature (T_{eff}) for 48 SySts and those derived by *Gaia* (T_{Gaia}) for 171 SySts as a function of (T_{cool}). Right panels: histograms of the temperature difference between T_{cool} and T_{eff} (the three sources with high temperature difference are excluded from this plot), and T_{cool} and T_{Gaia} . The solid lines are the average of the temperature difference, while the dashed lines represent the 1σ of the distributions.

4000 K (expect the rare group of yellow SySts), *Gaia* temperatures estimates for SySts have errors from 324 to 550 K (Andrae et al. 2018).

In the case of colder stars, like the Mira companions in D-type SySts with $T < 3000$ K, *Gaia* temperatures are even more uncertain, and we have decided to not present them in this work. Table 7 (Appendix A) lists the stellar effective temperatures of the cold companions for 171 Galactic SySts.

A reasonable agreement within the uncertainties between our and *Gaia* temperatures is found. The difference between the estimates is presented in the lower left panel in Figure 7. Temperature estimates of only 17% (or 10%) SySts are inconsistent, and all of them have $T_{\text{Gaia}} > 4400$ K. This may imply the presence of a G-type giant in these SySts. The average temperature difference is of the order of 271 K with a standard deviation of 441 K (lower right panel in Figure 7). One can see that our T_{cool} are in better agreement with the spectroscopic estimates T_{eff} rather than with those from *Gaia*. A comparison between *Gaia* temperatures and those from the literature (Table 1) shows an agreement within the uncertainties. The majority of SySts have a temperature difference lower than 600 K which is comparable with the *Gaia* uncertainty.

Regarding the luminosity and radius parameters provided by *Gaia* DR2 for the cold companions of SySts, we decided not to present them in this work. Unfortunately, only 35 SySts have fractional parallax uncertainty $\sigma\omega/\omega > 0.2$ (i.e. signal-to-noise < 5), as it is recommended by *Gaia* (see Appendix B in Andrae et al. 2018) and therefore reliable luminosity and radius estimates (Andrae et al. 2018).

3.2.2. Geometrical distances

Besides the stellar parameters, *Gaia* DR2 also provides parallaxes for more than a billion of stars (Gaia Collaboration et al. 2018). The geometrical distances of 1.33 billion sources (without take into account the stellar type, photometry or extinction) are derived using a probabilistic approach with the advantage of providing lower and higher bounds (within $\pm 1\sigma$) either for sources with high fractional parallax uncertainties or negative parallaxes (Bailer-Jones et al. 2018).

In Table 7 (Appendix A), we list the distances of 193 SySts (155 S-, 20 S+IR-, and 18 D-types) together with their lower and higher values. At this point, it is worth mentioning that of all the sources in *Gaia* DR2 are considered to be single stars while SySts are known to be binary systems. This results in some problematic astrometric solutions like negative parallaxes because of the

Table 1. Effective Temperatures (T_{eff}) of red stars in SySts

Name	T_{eff} (K)	Type	O VI 6830Å	References.	Name	T_{eff} (K)	Type	O VI 6830Å	References.
AG Dra	4300	S	✓	1,2,14	AE Ara	3300	S	✗	8,9,14
BD-21 3873	4300	S	✗	3,2,14	SS 73 96	3400	S	✗	8
LT Del	4400	S	✗	4,2,14	AS 270	3300	S	✗	8
HD 330036	6200	D'	✗	5	Y Cra	3300	S	✓	8
AS 201	6000	D'	✗	5	Hen 2-374	3300	S	✓	8
StHA 190	5300	S+IR	✗	6	Hen 3-1761	3300	S	✗	8
CH Cyg	3100	S	✗	7	WRAY 15-1470	3600	S	✗	10
CH Cyg	2600	S	✗	14	Hen 3-1341	3500	S	✓	10
BX Mon	3400	S	✗	8,9	PN Th 3-29	3200	S	✓	10
V694 Mon	3300	S	✗	8	V2416 Sgr	3300	S	✓	10
Hen 3-461	3200	S	—	8	V615 Sgr	3300	S	✗	10
SY Mus	3400	S	✓	8	AS 281	3300	S	✓	10
Hen 2-87	3300	S+IR	✓	8	V2756 Sgr	3500	S	✓	10
Hen 3-828	3300	S	✓	8	V2905 Sgr	3600	S	—	10
CD-36 8436	3300	S	—	8	AR Pav	3400	S	✓	10,14
RW Hya	3700	S	✗	8,14	V3804 Sgr	3300	S+IR	✗	10
Hen 3-916	3400	S	✓	8	V4018 Sgr	3500	S	✗	10
Hen 3-1092	3300	S	✓	8	V919 Sgr	3400	S	✗	10
WRAY 16-202	3300	S	—	8	CD-43 14304	3900	S	✓	10,14
Hen 3-1213	4100	S	✗	8,2	CD-43 14304	4300	S	✓	2
Hen 2-173	3400	S	✓	8	Hen 3-863	4300	S	✗	2
KX Tra	3300	S	✓	8,9	StHA 176	4200	S	✗	2
CL Sco	3400	S	✗	8,9	V2116 Oph	3400	S	✗	11
V455 Sco	3200	S+IR	✓	8	RS Oph	4100	S	✓	12,13
M1-21	3300	S	✓	8	T CrB	3500	S	✗	12,14
RT Ser	3300	S	✓	8					

References: 1. Smith et al. (1996), 2. Pereira & Roig (2009), 3. Smith et al. (1997), 4. Pereira et al.(1998), 5. Pereira et al. (2005), 6. Smith et al. (2001), 7. Schmidt et al. (2006), 8. Galan et al. (2016), 9. Galan (2015), 10. Galan et al. (2017), 11. Hinkle et al. (2006), 12. Wallerstein et al. (2008), 13. Pavlenko et al. (2008), 14. Skopal(2005).

poor fitting of the single-star parallax model (Arenou et al. 2018; Lindegren et al. 2018; Luri et al. 2018). The *astrometric excess noise* < 1 mas criterion was used to select only the sources with the most reliable parallax estimates (see Lindegren et al. 2018).

Fig. 9 presents the distribution of the vertical distance from the Galactic plane (Z) for all the SySts in our list. The distance of the Sun from the Galactic center is assumed to be 8.0 ± 0.5 kpc (Reid 1993). S-type SySts show a clear Gaussian distribution around the Galactic plane extending up to 3 kpc, while S-IR and D-type SySts are more concentrated in the Galactic plane ($Z < 1$ kpc). S-type SySts appear to be members of the Galactic disk, both thin and thick (scale heights of $0.25\text{--}0.35$ kpc and 0.86 ± 0.2 kpc, respectively; Ojha

2001 and references therein), while S+IR- and D-types are mainly members of the thin Galactic disk.

A comparison of the Z distance distributions between the S-type and the S+IR-/D-type SySts shows that very few S+IR- or D-type are expected to be found at $Z > 1$ kpc. In particular, the standard deviation (1σ) of the S-, S+IR- and D-type distributions is found to be 0.97, 0.37, and 0.28 kpc, respectively. The uncertainty of the standard deviations is around 15%-20% given the error of Z distances between a few percent and up to 30%. This implies that most of the S+IR- and D-type (more than two-thirds) belong to the thin Galactic disk while the S-type are members of both disk populations. Further study of the chemical composition of these systems may provide more information about their formation and evolution as well as their link with the Galactic

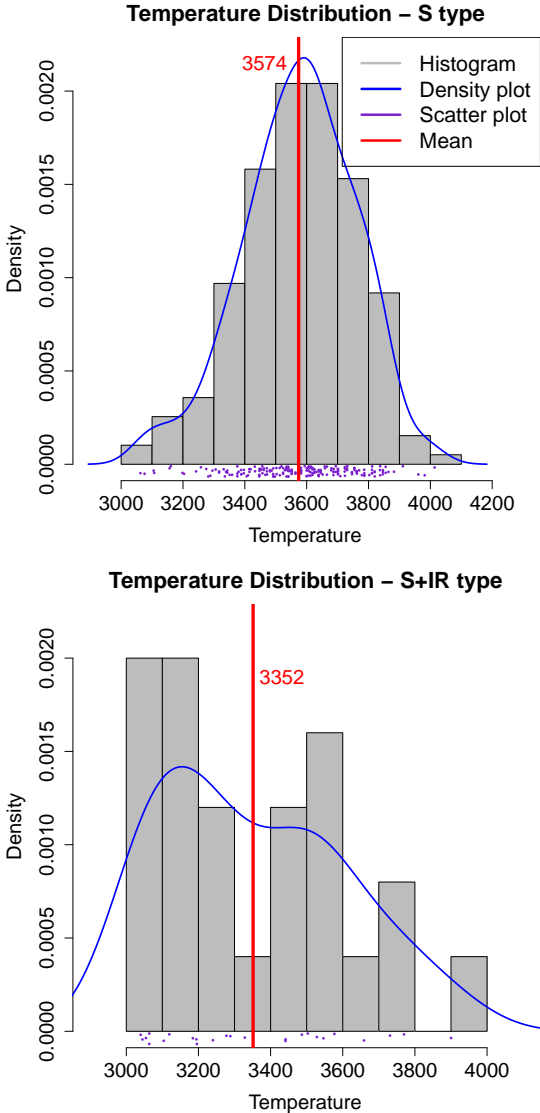


Figure 8. Histogram of the T_{cool} for the S-type (upper panel) and for the S+IR-type SySts (lower panel). The colored lines are the same as those in Figure 5.

disk populations. It should also be noted that the current population of known Galactic SySts may be biased towards the Galactic disk as the majority of them have been discovered from surveys focusing on the Galactic disk ($|d| < 10^\circ$; Munari & Renzini 1992).

Distances for a number of SySts have also been estimated before the release of *Gaia* DR2, and for most of them, a reasonable agreement is found within the uncertainties. For instance, the distance of RW Hya has been estimated to be either 0.6–0.68 kpc (Allen 1980; Muer set et al. 1991) or 1.23–1.33 kpc (Pereira et al. 2017). Its *Gaia* distance of 1217 pc with a lower and an upper bound of 1134 and 1313 pc, respectively, is consistent with the more recent estimate. The current list of SySts

distances provides more accurate values than previous studies and allow us to explore their spatial distribution in the Milky Way, and it will be very useful for many studies in this field.

3.3. S-type SySts

The majority of SySts are classified as S-type, and their SEDs show a peak between 0.8 and 1.7 μm with a mean value of 1.07 μm whereas there is a small but significant number of S-type SySts with a peak either down to 0.7 or up to 1.8 μm (Figures 3, 4, 5 and Table 7 in Appendix A). The temperature distribution of the cool companions in S-type SySts demonstrates that the majority of the SySts have a temperature between 3400 and 3800 K, which corresponds to M1–M5 spectral types with a peak at M5 (Figure 8). This is in very good agreement with the distribution reported in previous studies (Medina-Tanco & Steiner 1995; Muer set & Schmid 1999). Only a small percentage of the S-type SySts population contains a K or G spectral-type giant, i.e. yellow SySts.

Interestingly, Galactic S-type SySts are found to contain a normal red giant (M or K), but there are a number of S-type SySts in the SMC and LMC that have been found to contain a Mira companion (Muer set et al. 1996). This finding is attributed to the lower metallicity of these two galaxies compared to our Galaxy. In low-metallicity environments like the SMC and LMC, the critical mass of a star to become a carbon star is lower than that in the Milky way (Marigo et al. 2013). Stars with masses between 2–3 M_\odot become carbon stars due to the third dredge-up after only a few thermal pulses or, in other words, during the early AGB phase (Marigo et al. 2013). The mass-loss rate at this early phase is not high enough to form a dusty shell and give a D-type SED profile.

3.4. S+IR-type SySts

Besides the typical S-type SySts, we also find a statistically important number of S-type SySts with an infrared excess in the 11.6 and/or 22.1 μm bands (Figs. 3, 4, and 5, and Table 7 in Appendix A). We name this new type of SySt “S+IR-type”. Twenty-seven SySts in our list are classified as S+IR-types. Seven were previously classified as D-types, 18 as S-types, one as a D'-type, and one without a previous classification.

The SED profiles of S+IR-type SySts demonstrate a peak at longer wavelengths (1.3 μm) compared to S-type SySts (1.07 μm), indicating the presence of companions with lower temperature. For all the cases of S+IR-type SySts, two BB models were used to reproduce the total SED. This IR excess may be an indication of the existence of a dusty shell, colder temperatures compared to

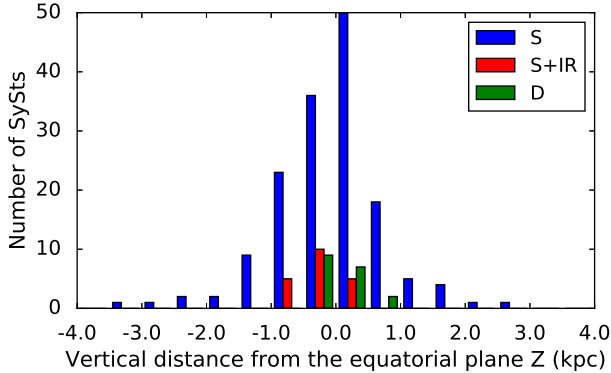


Figure 9. Distribution of the vertical distances (Z) from the galactic plane in parsecs for S-, S+IR- and D-type SySts.

those of D-types, the presence of strong amorphous silicate emission bands at ~ 10 and $\sim 18 \mu\text{m}$, or an accretion disk around the WD component.

Interestingly, all SySts, except two very bright cases (R Aqr and CH Cyg), with available *ISO* data presented by Angeloni et al. (2007), exhibit an infrared excess in the $W3$ and $W4$ bands and at the same time show strong amorphous silicate emission bands at ~ 10 and $\sim 18 \mu\text{m}$. However, only one has been classified as an S+IR-type (candidate V627 Cas), while all of the remaining ones are classified as D-type SySts. Therefore, the IR excess observed in S+IR-type SySts might not be associated with the presence of amorphous silicate emission bands.

The second possible scenario for the IR excess in S+IR-type SySts is the presence of a dusty disk that formed around the WD. The presence of a slowly expanding disk that has been proposed in order to explain the two-temperature components of high orbital inclination SySts during the active phase (Skopal 2006).

A third scenario of a much colder and tenuous dusty shell, similar to those in D-types, is also possible. In this case, the cold companion in S+IR-type SySts may have just become an AGB star. Because of its very low mass-loss rate in the early AGB phase, the stars do not have sufficient mass to form a dust shell (i.e. the shell that would obscure the star and result in a D-type SED profile). This scenario requires colder companions compared to the red giants in S-type SySts, being in a more evolved phase. This is exactly what the temperature distributions display (Figure 8). There is a significant percentage of S+IR-type SySts in which the companions have temperatures between 3000 and 3200 K, while the number of S-type SySts in the same temperature range is almost negligible.

We searched in the literature for further information on the S+IR-type SySts and variabilities with periods

between 100 and 400 days and amplitude pulsations between 0.5 and 2 mags have been reported for the several of them (e.g. EF Aql; SS 73 17; H 2-38; SS 73 122; V366 Cas, Whitelock et al. 1983; Whitelock 1987; Pojmański 2002; Matsunaga, Fukushi & Nakada 2005; Watson, Henden & Price 2006; Richards et al. 2012; Soszyński et al., 2013; Samus' et al. 2017). The pulsation periods and amplitudes from the S+IR-type SySts appear to be lower compared to those of Mira stars in D-type SySts. R Aqr has been misclassified as San +IR-type due to its uncertain photometric magnitudes while its high amplitude variations (>2 mags) are consistent with Mira stars.

Given that the pulsation period in the AGB phase increases with time (e.g. Vassiliadis & Wood 1993), it is possible that the giant companions in S+IR-type SySts are in a less evolved phase (e.g. early AGB) than the Mira in D-types (thermal pulsating in the TP AGB phase). The intense mass-loss rate during the end of the TP-AGB phase is responsible for the formation of the dusty shell in D-type SySts (e.g. Muerset et al. 1996), while in the case of S+IR-type, the companion has just entered in the AGB phase (early AGB) and its mass-loss rate is not high enough to form a similar dusty shell with high infrared excess as in D-types. In the early AGB phase, the mass-loss rate is lower compared to the more evolved TP-AGB phase (e.g. Schild 1989; Vassiliadis & Wood 1993, Rosenfield 2014), resulting in a lower infrared excess. The $K_s-[12]$ and $K_s-[22]$ color indices (or equivalently K_s-W3 and K_s-W4) are two widely used indicators of the dust mass loss in giants (e.g. Guandalini et al. 2006; Whitelock 2006; Uttenthaler 2013, Akras et al. 2017). The mean values of K_s-W3 and K_s-W4 for each type of SySts are estimated. We find that both color indices increase from 0.68 and 1.40 (the standard deviation (SD) is found to be 0.48 and 0.82, respectively) for S-type, to 2.42 and 3.83 (SD of 1.27 and 1.12, respectively) for S+IR-types, to 4.54 and 5.61 (SD of 1.01 and 1.24, respectively) for D-types and to 6.63 and 8.79 (SD of 1.31 and 1.71, respectively) for D'-types. This indicates that the red giants in S+IR-type exhibit a higher mass-loss rate than their counterparts in S-type and lower than those in D-type. Hence, S+IR-type SySts likely represent a transition phase from S-type to D-type SySts (see also Medina-Tanco & Steiner 1995).

Gromadzki et al. (2009) have claimed that AS 245 has a semi-regular star rather than a Mira, due to the low amplitudes and its certain pulsation period. From our analysis, AS 245 has been classified as an S-type, and not as an S+IR-type. However, a low excess at the $W4$ band is barely seen (see Fig. A3). Moreover, we calculate its $T_{\text{eff}}=3162 \text{ K}$, which is lower than the

average temperature of the red giants in S-type SySts by 400 K (Figs. 8). This may indicate a more evolved companion, although not as evolved as Mira stars. The K_s-W3 and K_s-W4 color indices of this SySt are found to be 1.58 and 2.38, respectively, between the values of S- and S+IR-type.

3.5. D-type SySts

From the remaining SySts, 13% of the known SySts are classified as D-types (Table 7 in Appendix A). The SEDs of D-type SySts show a peak between 2 and 4 μm with a mean value of 2.85 μm (Figure 3-5). This peak range is shorter than the one reported by Ivison et al. (1995).

An important number of D-type SySts is found for which two BB models are required in order to fit the whole SED profile. The average values of the dust temperatures for these two dusty shells are 1077 ± 35 K for the inner and 467 ± 30 K for the outer one, with SD equal to 200 and 112 K, respectively. These temperatures are in excellent agreement with the values reported by Angeloni et al. (2010). Phillips (2007) also argued that the near-IR emission emitted from a dusty shell is associated with silicate dust grains whose maximum temperature is of the order of 800 K, which is very close to the mean temperature between the two dust shells.

3.6. D'-type SySts

The typical SED profile of D'-type SySts displays a nearly flat profile (Fig. 4). Both signatures from the cool giants and the dusty shells are present, and three BB models are required to reproduce all of their SED profiles, one for the cool companion and two for the inner and outer dust shells. Because of the flat profiles, we do not present an SED peak histogram for D'-types. However, one can see that the dusty shells in D'-type SySts show two distinct peaks between 2 and 10 μm .

Only 10 D'-type SySts with a G/K spectral-type red giant are known (see Tables 6 and 7 in Appendix A). According to our classification, only five of them show the typical SED profile of D'-type SySts. The remaining are classified as a D-type (V417 Cen) and as S+IR-types (WRAY 15-157, Hen 3-1591, StHA 190 and SMP LMC 88). The classification of V417 Cen as a D-type SySt may not be correct despite the good fitting. V417 Cen shows a barely noticeable infrared excess in the J -band which could be attributed to the presence of a hotter red giant. In this case, a third BB model would be necessary to fit the SED profile to give the typical SED profile of D'-types. V417 Cen has been classified as a D'-type SySt with a G spectral-type companion (Gromadzki et al. 2011). Regarding the last four S+IR-type SySts, a

fast rotating G spectral-type companion has been found in WRAY 15-157 (Zamanov et al. 2008) and StHa 190 (Smith, Pereira & Cunha 2001), the optical spectra of SMP LMC 88 resembles that of a K giant (ilkiewicz et al. 2018) while Hen 3-1591 has a controversial classification of S or D'-type (Bel2000).

Six more SySts are found to have a typical flat SED profile, and most of them have been previously classified as D-type. One of them (GH Gem) has been previously incorrectly classified as an S-type, and our SED analysis reveals a D'-type SySt. This agrees with the classification of the red giant as K3III by Munari et al. (2007). K5-33 displays a nearly flat profile, indicating a D'-type classification, but its dust emission does not allow us to get an estimation of the temperature of the red giant. A D-type classification for K5-33 cannot be ruled out (Miszalski et al. 2013). Overall, 11 D'-type SySts are listed in our census (3.5%, Table 7) based on their SED profiles. Whether the cold companion in a SySt exhibits characteristics of a cold G/K star, it does not mean a priori that it is a D'-type since it may also be a yellow S-type (e.g. LT Del, LAMOST J12280490-014825.7, StHa 63, see also Baella et al. 2016). D'-type SySts have a G/K spectral-type companion with a strong IR excess (Allen 1982), which makes them to resemble PNe.

4. O VI RAMAN-SCATTERED $\lambda\lambda 6830, 7088$ LINES IN SYMBIOTIC STARS

An updated census of the O VI $\lambda 6830$ Raman-scattered line in SySts is required in order to determine the total occurrence of these lines in SySts. We performed a systematic search for optical spectra of SySts in all of the works listed in Table 7 as well as in the following compilations by Blair et al. (1983), Allen (1984), Acker, Lundstrom and Stenholm (1988), Medina-Tanco & Steiner (1995), Muerset, Schild & Vogel (1996), Mikolajewska, Acker, Stenholm (1997), and Gutiérrez-Moreno Moreno & Costa (1999). Whether or not the O VI $\lambda 6830$ Raman-scattered line is detected is given in Table 7. For this work, we gathered information only for the $\lambda 6830$ line since it is brighter by a factor of between 2 and 10 compared to the $\lambda 7088$ line (Allen 1980, Schmid et al. 1999) due to the different column densities of atomic hydrogen.

We gathered information from 298 optical spectra of known and candidate SySts. We end up with 165 positive confirmations of the O VI Raman-scattered line, which corresponds to 55% of the whole sample. This value is very close to the percentage calculated by Allen (1980). There are a number of SySts with spectra from different epochs, and the O VI line is not always detected. The intensity of the O VI line can signifi-

Table 2. Number of positive and negative O VI Raman-line Detections in the Milky Way, SMC, LMC, M31, and M33

Galaxy	Total number ^a	Positive detections	Negative detections	O VI Raman (%)	[Fe/H]	References ([Fe/H])
Milky Way	257	131	108	55	-0.11	1
SMC	9	9	0	100	-0.99	2
LMC	9	4	3	57	-0.60	3,4
M31	31	16	15	52	-0.45	5
M33	12	5	7	42	-0.11	6

^aTotal number of optical spectra examined in this work.

References. 1. Sadler et al. (1996), 2. Dobbie et al. (2014), 3. Cole et al. (2000), 4. Salaris & Girardi (2005), 5. Kalirai et al. (2006), 6. Gregersen et al. (2015)

cantly change during that time. A newly formed dust shell around the cool companion can absorb the O VI 1032 Å photons, resulting in the depletion of O VI $\lambda 6830$ Raman-scattered photons (e.g. V1016 Cyg, Arkhipova et al. 2016) or the presence of an optically thick disk around the WD (e.g. Skopal 2006).

The significant increase of new SySts in nearby galaxies ($\sim 350\%$) implies that the aforementioned percentage derived from the whole sample should be taken cautiously, due to the different metallicities in galaxies. The percentage of SySts with the O VI Raman-scattered line in their spectrum is determined separately for the Milky Way, SMC, LMC, M31, and M33 galaxies. In Table 2, we list the number of the positive and negative confirmations of the O VI Raman-scattered line as well as their percentages, which range from 42% to 100%. Systematic surveys of SySts in nearby galaxies are required in order to increase the sample of SySts in other galaxies.

4.1. O VI Raman-scattered versus nebular lines

The detection of the O VI Raman-scattered line implies a very hot and luminous WD able to ionize the circumstellar envelope. Hence, the recombination He II $\lambda 4686$ line (ionization potential, I.P.=54.4 eV) should also be detected when the O VI Raman-scattered line (I.P.=113.9 eV) is detected. Indeed, we find that in all of the SySts in which the O VI Raman-scattered line is detected, the He II $\lambda 4686$ line is also present, while the opposite is not true. The correlation between the two lines has been verified using the equivalent widths (e.g. Leedjärv 2004, Leedjärv et al. 2016). There are three cases in our sample for which both lines are not simultaneously detected (M31 SySt-23, Mikolajewska, Caldwell & Shara 2014; QS Nor and Th 3-29, Acker, Lundstrom & Stenholm 1988). We thus argue that the detection of the O VI Raman-scattered line in these three sources is dubious.

The average value of the O VI $\lambda 6830/\text{H}\alpha$ line ratio is determined for all Galactic SySts (113) as well as for the

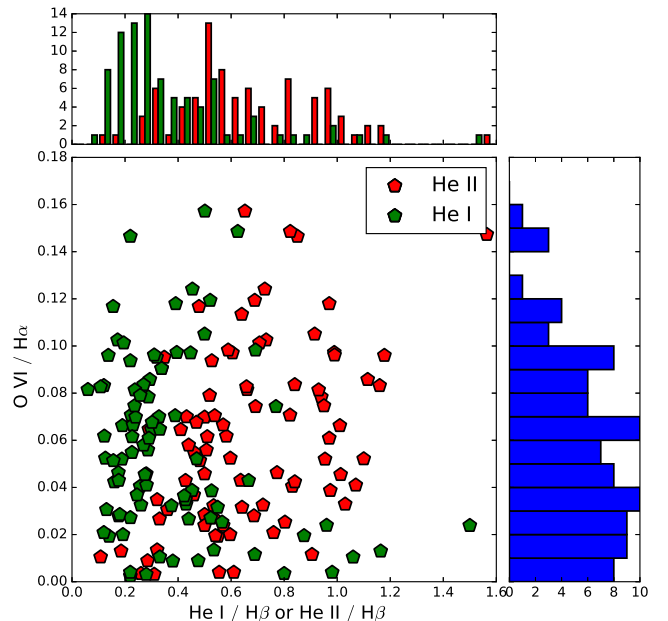


Figure 10. O VI $\lambda 6830/\text{H}\alpha$ vs. He I $\lambda 5876/\text{H}\beta$ or He II $\lambda 4686/\text{H}\beta$ line ratio plot for a number of Galactic and extragalactic SySts.

SySts in M33 and M31 (43) with available emission-lines fluxes. The total average O VI $\lambda 6830/\text{H}\alpha$ line ratio is 0.06 with SD=0.04, while for the Milky Way, M31, and M33, it is 0.06 (SD=0.04), 0.05 (SD=0.03), and 0.04 (SD=0.04), respectively. Figure 10 displays the O VI $\lambda 6830/\text{H}\alpha$ versus He I $\lambda 5876/\text{H}\beta$ and He II $\lambda 4686/\text{H}\beta$ plot for all of these SySts (see also Table 3). All the line ratios are estimated using integrated fluxes gathered from several studies in the literature. It can be seen that the He II $\lambda 4686/\text{H}\beta$ line ratio displays a lower threshold of $\sim 0.3\text{--}0.4$, while the He I $\lambda 5876/\text{H}\beta$ line ratio has an upper threshold of $\sim 0.5\text{--}0.6$.

The average values of the He II $\lambda 4686/\text{H}\beta$ and He I $\lambda 5876/\text{H}\beta$ line ratios for SySts with and without the

O VI Raman-scattered line in different galaxies are also estimated (see Table 3). In general, SySts with the O VI Raman line detected exhibit systematically higher He II $\lambda 4686/\text{H}\beta$ ratio (0.66) compared to those SySts without the O VI line detected (0.22), while the He I $\lambda 5876/\text{H}\beta$ ratio has comparable values regardless of the detection of the Raman line (0.43 and 0.38, respectively).

This implies that the O VI Raman emission is also followed by an increase of He II $\lambda 4686/\text{H}\beta$ ratio. In this case, the WD is neither luminous nor hot enough to emit a significant number of UV O VI photons, and it results in a lower He II $\lambda 4686/\text{H}\beta$ line ratio and a low-excitation nebula. On the other hand, if the O VI line is detected, the He gas is mainly doubly ionized (high He II $\lambda 4686/\text{H}\beta$) and the He I $\lambda 5876$ line becomes weaker (low He I $\lambda 5876/\text{H}\beta$). The large scatter of the point in Figure 10 reflects the complex relation between the effective temperature of the hot companion, the mass-loss rates of the stars, the density of atomic hydrogen, and the efficiency of Raman scattering.

Besides the previous line ratios, we also revise the He II $\lambda 4686/[\text{O III}]\lambda 5007$ ratio. Interestingly, this line ratio is found to decrease as a function of metallicity for SySts with the O VI Raman-scattered line detected and increase for those without Raman emission (Table 3). We have to mention that in the Milky Way, there are three SySts (AS 289, AS 316, and AS 327) with extremely high He II $\lambda 4686/[\text{O III}]\lambda 5007$ line ratio between 30 and 45, which we did not take into consideration in these calculations.

Overall, all of these line ratios provide new constraints on the identification of the O VI $\lambda 6830$ Raman-scattered line. There is, for instance, a number of sources with a He I $\lambda 5876/\text{H}\beta$ line ratio higher than 0.8, which puts them into doubt. According to Figure 10, it is clear that there is a minimum value for the He II $\lambda 4686/\text{H}\beta$ ratio and a maximum value for the He I $\lambda 5876/\text{H}\beta$ in case the O VI 6830\AA Raman-scattered line is detected.

4.2. Perplexing objects with the O VI Raman emission reported

The O VI $\lambda 6830$ Raman-scattered emission has also been reported for a few non-SySt objects, such as young PNe (Arrieta & Torres-Peimbert 2003; Sanchez-Contreras et al. 2008), NGC 6302 (Groves et al. 2002), NGC 7027 (Zhang et al. 2005) and one Be star, namely LHA 115 S-18 (Torres et al. 2012). In order to verify the presence of the Raman line in these objects, we re-examined their spectra, and below we discuss each object in more detail.

4.2.1. NGC 6302

Groves et al. (2002) reported the detection of the O VI $\lambda\lambda 6830, 7088$ Raman-scattered lines in the planetary nebula NGC 6302. Its very hot central star (150-400 kK, Pottasch et al. 1996; Groves et al. 2002) can emit a significant number of UV O VI photons. The large full-width-half-maximum (FWHM) of the $\lambda\lambda 6830, 7088$ line features in conjunction with the detection of other Raman-scattered lines at 4331\AA and 4852\AA suggests a Raman-scattering origin. Moreover, the large list of high-excitation emission-lines as well as Fe lines are consistent with what it is found in SySts. The IUE data indicate the presence of a cool G-type companion (Feibelman 2001).

However, [Kr III] $\lambda 6826.7$, He I $\lambda 6827.9$, and/or CI $\lambda 6828.1$ lines can lead to a possible misidentification (see Zhang et al. 2005; Sharpee et al. 2007). NGC 6302 has a $\lambda 6830/\text{H}\alpha$ line ratio equal to 0.001, which is more than one order of magnitude lower than the average ratio as well as the He II $\lambda 4686/[\text{O III}]\lambda 5007$ ratio.

Assuming $N_e=10000 \text{ cm}^{-3}$ and $T_e=15000 \text{ K}$, the theoretical value of the He I $\lambda 6830/\lambda 4471$ ratio is $\sim 1.1 \times 10^{-3}$ (Smits 1991), which is almost 50 times lower than the observed value (0.055). This discrepancy can be explained if the CI $\lambda 6828.1$ line is taken into account. Hence, we consider the CI $\lambda 6828.1$ line as a possible contaminant. The detection of other line from the same upper level such as CI $\lambda 6656.6$ with an intensity of 0.045 (Groves et al. 2002) supports our hypothesis.

According to this analysis, we argue that NGC 6302 is unlikely to be a SySt, and this is consistent with its very low He II $\lambda 4686/[\text{O III}]\lambda 5007$ and O VI $\lambda 6830/\text{H}\alpha$ line ratios. We claim that the identification of the $\lambda\lambda 6830, 7088$ features such as O VI Raman-scattered lines is dubious.

4.2.2. NGC 7027

NGC 7027 is a young, high-excitation nebula with a very hot central star (Middlemass 1990; Zhang et al. 2005) in which a line feature centered at 6828\AA has been detected (Zhang et al. 2005). In contrast to Groves et al. (2002), Zhang et al. (2005) identified it as [Kr III] $\lambda 6826.7$. Besides the [Kr III] line, a weaker and broader line feature is also present and blended with the former line. Zhang et al. (2005) identified this broad feature as an O VI Raman-scattered line, unlike its previous identification as a [Si II] line by Péquignot & Baluteau (1994).

Similar to NGC 6302, the aforementioned broad line is significantly weaker than He II $\lambda 4686$. Moreover, the line ratio of the two Raman-scattered lines, $\lambda 7088/\lambda 6830$, is found to be at least twice as low as the ratio found in SySts. According to this, the identification of that feature as an O VI Raman line is question-

Table 3. Emission-line ratios of SySts[†]

Galaxy	O VI $\lambda 6830/\text{H}\alpha$	He II $\lambda 4686/\text{H}\beta$		He I $\lambda 5876/\text{H}\beta$		He II $\lambda 4686/\text{[O III]} \lambda 5007$	
	O VI (✓)	O VI (✗)	O VI (✓)	O VI (✗)	O VI (✓)	O VI (✗)	O VI (✗)
All	0.06 (0.04)	0.66 (0.26)	0.22 (0.15)	0.43 (0.33)	0.38 (0.23)	1.45 (1.49)	1.21 (1.74)
Milky Way	0.06 (0.04)	0.65 (0.26)	0.21 (0.16)	0.46 (0.34)	0.40 (0.25)	1.15 (1.24)	1.42 (1.93)
M31	0.05 (0.03)	0.68 (0.27)	0.25 (0.10)	0.26 (0.22)	0.34 (0.15)	1.47 (1.40)	0.69 (0.83)
M33	0.04 (0.04)	0.81 (0.16)	0.24 (0.08)	0.35 (0.15)	0.27 (0.22)	3.78 (1.12)	0.73 (0.83)

[†] The number in parentheses corresponds to the standard deviations

able despite the broad feature. The He I $\lambda 6827.9$ line is a possibility.

Using the list of theoretical He I lines for a range of N_e and T_e by Smits (1991), we get a rough estimate of its theoretical intensity ($\text{He I } \lambda 6830/\lambda 4471 \sim 1.1 \times 10^{-3}$ for $N_e = 10^4 \text{ cm}^{-3}$ and $T_e = 15000 \text{ K}$; Smits 1991). The intensity of the $\lambda 6830$ feature is approximately three times lower than the intensity of the [Kr III] $\lambda 6826.7$ line (0.044 relative to H β =100; see Table A1 in Zhang et al. 2005). Therefore, its intensity is of order of 0.014, and that of the observed He I $\lambda 6830/\lambda 4471$ ratio of order of 0.0046. This value is almost three times higher than the theoretical value. The [Kr III] $\lambda 6826.7$ line is not corrected for the contribution of the CI $\lambda 6828.1$ line, which may result in a lower line ratio.

In conclusion, the feature detected at 6828Å in NGC 7027 may have been mistakenly classified as the O VI Raman line. The He I line centered at 6827.9Å seems a more probable identification. Looking carefully at its spectrum, one can see that other He I line centered at, e.g. 8634Å, and 8652Å also show red wings similar to the $\lambda 6828$ feature (Zhang et al. 2005).

The high-resolution spectrum of NGC 7027 by Sharpee et al. (2007) shows that the $\lambda 6830$ feature is blended with the He I $\lambda 6827.9$ and CI $\lambda 6828.1$ lines as well as with a number of telluric OH bands. After all these analyses, we conclude that the identification of the O VI Raman-scattered lines in NGC 7027 is dubious.

4.2.3. Young PNe

Arrieta & Torres-Peimbert (2003) and Sanchez-Contreras et al. (2008) also reported the detection of the O VI $\lambda 6830$ Raman line in a number of young PNe, such as M 2-9, IRAS 17395-0841, IC 4997, IRC +10420, M3-60, M1-92, IRAS 08005-2356, Hen 3-1475, and IRAS 22036+5306. We re-examined the spectra of these nine objects, and we find that (i) the $\lambda 6830$ feature is very weak compared to SySts and (ii) O VI $\lambda 6830$ and He II $\lambda 4686$ lines are not simultaneously detected. M2-9 is the only object where the He II $\lambda 4686$ line and [Fe IV] are detected.

The central stars of all these young PNe (except from M2-9) are not hot enough to emit a significant number of UV O VI photons. We, therefore, argue that the line feature at $\sim 6830\text{\AA}$ is not associated with the O VI Raman-scattered line. The [Kr III] $\lambda 6826.7$, He I $\lambda 6827.9$ or CI $\lambda 6828.1$ nebular lines are possible identifications. As for M2-9, a further study is required in order to verify whether the $\lambda 6830$ feature is associated with Raman-scattering.

4.2.4. LHA 115 S-18

LHA 115 S-18 is a highly controversial object for which the scenarios of being a luminous blue variable star, a symbiotic star, a PN, a Cygni variable, or a B[e] star have been proposed (Torres et al. 2012, Clark et al. 2013, Maravelias et al 2014, see also Lepo PhD dissertation 2015 for a detailed analysis).

The most interesting point of this likely massive star is the recent detection of the O VI Raman-scattered doublet lines $\lambda\lambda 6830, 7088$ with a simultaneous detection of the He II $\lambda 4686$ line (Torres et al. 2012). Maravelias et al. (2014) argued that the observed variations in some He II lines and in the OGLE-II data are not consistent with its previous B[e] classification. On the contrary, its optical spectrum shows a number of [Fe II], and Balmer lines, with the latter exhibiting a P Cygni profile typical for B[e] stars. Generally, P Cygni profiles imply a mass eruption event with high mass-loss rates and velocities up to 300 km s^{-1} . This event is likely responsible for the high conversion efficiency of Raman scattering and the detection of the O VI 6830 Å line.

According to the classification scheme of B[e]-type stars proposed by Lamers et al. (1998), some SySts show the B[e] phenomena and are classified as SymB[e] stars. Moreover, Skopal (2017) pointed out the similarities between B[e] stars and SySts during the active or outburst phase.

Based on *XMM-Newton* and *Chandra* data, LHA 115 S-198 is confirmed as an X-ray source. However, the low signal-to-noise ratio does not allow a spectrum to be extracted. Its X-ray luminosity is of the order of

10^{32-33} erg s $^{-1}$, and it is comparable with the luminosity of beta-type SySts but less compared to the luminosity of alpha-type SySts (Luna et al. 2013). LHA 115 S-18 is very likely a binary system with a compact object and a supergiant. The available X-ray data do not permit to identify the nature of the compact companion, which it can be either a WD or a neutron star. PU Vul is also classified as beta-type based on its X-ray spectrum and also presents the B[e] phenomena.

We thus decided to insert LHA 115 S-18 into our census as a known SySt with the O VI Raman line detected, but more studies are required. We also argue that LHA 115 S-18 may belong to the group of SymB[e] stars showing the B[e] characteristics during an active or outburst phase.

5. X-RAY EMISSION IN SYSTS

All SySts with X-ray emission detection are presented in Table 7. Only 46 have been found to be either soft or hard X-ray emission sources (see Luna et al. 2013 and references therein; Wheatley et al. 2003; Mukai et al. 2016; Nuñez et al. 2016). According to the α , β , γ , and δ classification scheme (Muerset, Wolff & Jordan 1997; Luna et al. 2013; Joshi et al. 2015; Bozzo et al. 2018), seven SySts have been classified as α -types, 12 as β -types, nine as γ -types, eight as δ -types, and eight $\beta\delta$ -types.

From these four types, only the α - and β -type SySts show the shell-burning process with or without accretion phenomena, while the last two types show only accretion phenomena (e.g. SU Lyn; Mukai et al. 2016). This implies that only α - and β -type SySts are able to emit emission-lines, which correspond to 50% of the total X-ray SySts detected so far. Mukai et al. (2016) claimed that the true population of SySts may have been significantly underestimated and that of all the published SySt catalogs are biased as they are based only on the optical emission.

Given that the shell-burning process on the hot WD's surface of α -type SySts induces the emission of supersoft X-rays, we probe for a possible link between X-ray and O VI Raman emission in SySts. We find that 12 out of 46 (or 27%) X-ray SySts emit the O VI Raman-scattered line whereas 21 of them (45%) do not (Table 7). To our knowledge, there are no available spectroscopic data for the remaining 13 X-ray SySts (27%). Moreover, 12 out of 33 (34%) SySts without detectable X-ray emission do not exhibit the Raman-scattered O VI line, whereas it is detected in 20 (60%) of them (Table 7).

In addition to that, we also explored the presence of the O VI Raman-scattered line in different X-ray-type SySts (α , β , γ and δ). None of the γ or δ types exhibit

the O VI Raman-scattered line, but only the α and β -types. Specifically, six out of seven α -type SySts, and six out of ten β -type SySts present the O VI line. The α -type SySts are expected to be hot and luminous enough due to the shell burning process, and to emit a large number of UV O VI photons that are eventually transformed to O VI Raman-scattered photons. But this is not evident in β -type SySts, in which the origin of the soft X-ray emission is from colliding winds (Muerset, Wolff & Jordan 1997, Luna et al. 2013). However, such strong winds able to produce soft X-ray emission are indicative of strong mass loss and high luminosity, which are likely associated with some shell-burning process, as in α -types. This could explain the detection of the O VI Raman line in β -type SySts. Ramsay et al. (2016) claimed that the β -type AG Peg SySt (Muerset et al. 1997) shows evidence of a quasi-shell-burning process.

The presence of the O VI Raman-scattered line in SySts may be an indication of a shell-burning process in α and β -type SySts (see also Mukai et al. 2016). Further X-ray observations are required to verify this correlation.

6. CONCLUSION

In this paper, we presented a new compilation of SySts. The total number of known SySts has been increased by 70%. For the Galactic and extragalactic SySts, the numbers have increased from 173 to 257 (~45%) and 15 to 66 (~350%), respectively.

The SED profiles of 348 SySts (known and candidates) were constructed using the 2MASS and AllWISE photometric data. These SEDs profile were used to verify their classification in the S/D/D'scheme: 74% of the known SySts were classified as S-type, 13% as D-type and only 3.5% as D'-type. A new classification was proposed for 22 SySts with no previous classification.

S-type are clearly dominated by the emission of the cool companion. Their SEDs show a peak between 0.8 and 1.7 μ m, which corresponds to an effective temperature of cool giants between 3000 and 4100 K. The majority of S-type have an M spectral-type companion. The effective temperature derived in this work can be considered reliable within the uncertainties.

A small number of SySts in the whole sample (27, or 8%) was found to display an S-type SED profile with a significant infrared excess between 10 and 22 μ m. We decided to separate this group of objects and classify them as S+IR-type. The presence of a dusty disk around the WD or a tenuous dusty envelope with temperatures lower compared to those of D-types is a possible explanation for this excess. S+IR-type SySts are likely a

Table 4. Characteristics of Different Types of SySts.

Type	All (#)	%	Known (#)	%	Peak (μm)	T_{eff}^{\dagger} (μm)	T_{dust} (K)	O VI (%)	X-Ray (#)
S	263	64	238	74	0.83-1.7	3000-4000	—	61	33
S+IR	37	9	26	8	0.88-1.7	3000-3900	150-500	39	3
D	60	15	42	13	2.1-4.1	—	200-400/700-1350	55	8
D'	31	7.5	11	3.5	“flat”	3500-4400	150-350/550-1000	50	—
No type	19	4.5	6	1.5	—	—	—	—	2

transition phase from the S- to D-type, in which the cool companion has just entered into the early AGB phase.

D-type SySts were found to have a peak at the wavelength range from 2 to 4 μm, which corresponds to a dust temperature between 700 and 1400 K. Several D-type SySts show the presence of two dusty shells, with the second one being colder between 200 and 400 K. Regarding the D'-type SySts, their SEDs reveal the characteristics of cool companions and dusty shells resulting in a nearly flat profile, clearly distinct from the other three types. The overall characteristics of the four different types of SySts are listed in Table 4.

Flux variations with amplitudes of 2 mag between the 2MASS and *WISE* surveys do not significantly affect the SED fitting, the classification, and the resulting temperatures. Moreover, we found that poor fitting of the 2MASS data or *W1* and *W2* indicate some variability among the data. In general, flux variations with amplitudes lower than 2-3 mag result in temperature variations of 400 K.

Geometrical distances of 193 SySts, using *Gaia* DR2, were also presented. The vertical distances of known SySts from the Galactic disk showed that S-type belong to the Galactic thick and thin disks, while the S+IR- and D-type belong mainly to the Galactic thin disk.

Finally, a new census of the O VI λ6830 Raman-scattered line in SySts was presented. We found 165 cases or 55% of the sample, in which the O VI λ6830 Raman-scattered line is detected. No preference for the O VI Raman-scattered line was found among the different types of SySts.

Exploring the O VI λ6830/Hα, He II λ4686/Hβ, He I λ5876/Hβ and He II λ4686/[O III] λ5007 line ratios, we came up with some additional criteria that can be used in order to identify any feature centered at 6830Å as a Raman-scattered line. According to this analysis, we were able to confirm or reject the detection of the O VI λ6830 Raman-scattered line reported in non-SySts. For most of the cases, we concluded that the line feature at 6830Å does not correspond to the Raman-scattered line but probably to the [Kr III] λ6826.7, He I λ6827.9

and CI λ6828.1 lines. Only two objects (M2-9 and LHA 115 S-18) show strong indications for a positive identification as an O VI Raman-scattered line.

Possible links between the O VI Raman-scattered line and X-ray emission were also explored. From all known X-ray SySts (46), only 12 of them emit the O VI Raman-scattered line and 21 do not. There are 13 more X-ray SySts without available optical data that merit further observations. Moreover, only α and β-type X-ray SySts were found to show the O VI Raman-scattered line. This may indicate a link between the mechanism responsible for the production of X-ray emission (shell-burning) and Raman-scattering, but further investigation is required.

In the future, more effort is needed to search for new SySts in the Milky Way and nearby galaxies. An extensive search in archive data such as the VPHAS+ survey needs to be done in order to find the hidden SySt population in the Galactic plane and bulge. X-ray observations of more SySts are also required in order to understand better the mechanisms of X-ray emission and their correlation with optical emission.

The authors thank the anonymous referee for the thorough revision and insightful comments and suggestions. S.A. and M.L.L.-F. acknowledge the support of CNPq, Conselho Nacional de Desenvolvimento Científico e Tecnológico - Brazil (grant 300336/2016-0 and 248503/2013-8, respectively). G.R.L. acknowledges support from Universidad de Guadalajara, CONACyT, PRODEP, and SEP (Mexico). L.G.R. is supported by NWO funding toward the Allegro group at Leiden University. Authors also thank Romano Corradi for helpful discussions. This publication made use of data from the Two Micron All-Sky Survey, which is a joint project of the University of Massachusetts and the Infrared Processing and Analysis Center/California Institute of Technology, funded by the NASA and the National Science Foundation, data products from the *Wide-field Infrared Survey Explorer*, which is a joint project of the University of California, Los Angeles, and the Jet Propulsion Laboratory/California Institute of

Technology, funded by the National Aeronautics and Space Administration. This work has made use of data from the European Space Agency (ESA) mission Gaia (<https://www.cosmos.esa.int/gaia>), processed by the Gaia Data Processing and Analysis Consortium (DPAC; <https://www.cosmos.esa.int/web/gaia/dpac/consortium>). Funding for the DPAC has been provided by national

institutions, in particular the institutions participating in the Gaia Multilateral Agreement. This publication made also use of many software packages in PYTHON.

Software: :Matplotlib (Hunter 2007), NumPy (van der Walt et al. 2011), SciPy (Jones et al. 2001), AstroPy Python (Astropy Collaboration et al. 2013; Muna et al. 2016), R (R Development Core Team 2008) .

REFERENCES

- Acker A., Lundstrom I., Stenholm B., 1988, *A&AS*, 73, 325
- Akras S., Ramírez Vélez J. C., Nanouris N., Ramos-Larios G., López J. M., Hiriart D., Panoglou D., 2017, *MNRAS*, 466, 2948
- Akras S., 2017, arXiv:astro-ph/17010.8898A
- Allen D. A., Glass I. S., 1974, *MNRAS*, 167, 337
- Allen D. A., 1980, *MNRAS*, 190, 75A
- Allen D. A., 1982, in Friedjung M., Viotti R., eds, *Astrophysics and Space Science Library Vol. 95*, IAU Colloq. 70: The Nature of Symbiotic Stars. pp 27-42
- Allen D. A., 1984, *PASAu*, 5, 369
- Alonso A., Salaris M., Arribas S., Martínez-Roger C., Asensio R. A., 2000, *A&A*, 355, 1060
- Andrae R., et al., 2018, *A&A*, 616, 8A
- Angeloni R., Contini M., Ciroi S., Rafanelli P., 2007, *A&A*, 472, 497
- Angeloni R., Contini M., Ciroi S., Rafanelli P., 2010, *MNRAS*, 402, 2075A
- Arenou F., et al., 2018, *A&A*, 616, 17A
- Arrieta A., Torres-Peimbert S., 2003, *ApJS*, 147, 97
- Arkhipova V. P., Taranova O. G., Ikonnikova N. P., Esipov V. F., Komissarova G. V., Shenavrin V. I., 2016, *BaltA*, 25, 35A
- Astropy Collaboration, Robitaille, T. P., Tollerud, E. J., et al., 2013, *A&A*, 558, A33
- Baella N. O., Pereira C. B., Miranda L. F., 2013, *AJ*, 146, 115
- Baella N. O., Pereira C. B., Miranda L. F., Alvarez-Candal A., 2016, *AJ*, 151, 100
- Bahramian A., Gladstone J. C., Heinke C. O., Wijnands R., Kaur R., Altamirano D., 2014, *MNRAS*, 441, 640B
- Bailer-Jones C. A. L., Rybizki J., Fouesneau M., Mantelet G., Andrae R., ApJ, 2018, AJ, 156, 58B
- Baratta G. B., Viotti R., 1983, *MmSAI*, 54, 493
- Belczyński K., Mikolajewska J., Munari U., et al., 2000, *A&AS*, 146, 407 (Bel2000)
- Benitez N., Dupke R., Moles M., Sodre L., Cenarro J., et al., 2014, arXiv:astro-ph/1403.5237
- Blair W. P., Feibelman W. A., Michalitsianos A. G., Stencel R. E., 1983, *ApJS*, 53, 573.
- Bodaghee A., Walter R., Zurita Hares J. A., et al. 2006, *A&A*, 447, 1027
- Bodaghee A., Rahoui F., Tomsick J. A., Rodriguez J., 2012, *ApJ*, 751, 113
- Bond H. E. & Kasliwal M. M., 2012, *PASP*, 124, 1262B
- Bozzo E., Bahramian A., Ferrigno C., et al., 2018, *A&A*, 613A, 22B
- Bragaglia A., Duerbeck H. W., Munari U., Zwitter T., 1995, *A&A*, 297, 759
- Cardelli J. A., Clayton G. C., Mathis J. S., 1989, *ApJ*, 345, 245
- Cenarro A. J., et al. 2018, submitted to *A&A*, arXiv e-prints, (arXiv180402667C)
- Chernyakova M., Courvoisier T. J.-L., Rodriguez J., Lutovinov A., 2005, *ATel*, 519, 1
- Clark J. S., Bartlett E. S., Coe M. J., et al. 2013, *A&A*, 560, A10
- Clyne N., Akras S., Steffen W., Redman M. P., Gonçalves D. R., Harvey E., 2015, *A&A*, 582, 60
- Cieslinski D., Elizalde F., Steiner J. E., 1994, *A&AS*, 106, 243C
- Cioni M.-R. L., et al., 2008, *A&A*, 487, 131
- Cole A., Smecker-Hane T. A., Gallagher J. S., 2000, *AJ*, 120, 1808
- Corradi R. L. M., 1995, *MNRAS*, 276, 521
- Corradi R., Schwartz H., 1997, in *Physical Processes in Symbiotic Binaries and Related Systems, Extended Optical Nebulae Around Symbiotic Stars*, ed. J. Mikolajewska (Warsaw: Copernicus Foundation for Polish Astronomy), 147
- Corradi R. L. M., Rodríguez-Flores E. R., Mampaso A., et al., 2008, *A&A*, 480, 409–419
- Corradi R. L. M., Munari U., Greimel R., et al., 2010a, *A&A*, 509, L9
- Corradi R. L. M., Valentini M., Munari U., et al., 2010b, *A&A*, 509, A41
- Corradi R. L. M., Giannanco C., 2010, *A&A* 520, A99
- Corradi R. L. M., Sabin L., Munari U., Cetrulo G., Englare A., Angeloni R., Greimel R., Mampaso A., 2011a, *A&A*, 529A, 56C

- Corradi R. L. M., Balick B., Santander-García M., 2011b, *A&A*, 529, 43
- Contini M., Formiggini L., 2003, *MNRAS*, 339, 148
- Costa R. D. D., de Freitas Pacheco J. A., 1994, *A&A*, 285, 998C
- Cutri R. M., et al., 2003, VizieR Online Data Catalog, II/246/, 2246, 0C
- Cutri R. M., et al., 2014, VizieR Online Data Catalog, II/328/, 2328, 0C
- de Freitas Pacheco J. A., Costa R. D. D., 1992, *A&A*, 257, 619
- Dilday B., Howell D. A., Cenko S. B., et al., 2012, *Sci*, 337, 942
- Di Stefano R., 2010, *ApJ*, 719, 474
- Dobbie P. D., Cole A. A., Subramaniam A., Keller S., 2014, *MNRAS*, 442, 1680D
- Downes R. A., Keyes C. D., 1988, *AJ*, 96, 777
- Drew J. E., Greimel R., Irwin M. J., Aungwerojwit A., Barlow M. J., et al., 2005, *MNRAS*, 362, 753
- Drew J. E., Gonzalez-Solares E., Greimel R., Irwin M. J., Küpcü Yoldas A., et al., 2014, *MNRAS*, 440, 2036D
- Dyck H. M., Benson J. A., van Belle G. T., Ridgway S. T., 1996, *AJ*, 111, 1705
- Feibelman Walter A., 2001, *ApJ*, 550, 785
- Frankowski A., Jorissen A., 2007, *BaltA*, 16 104.
- Frew D. J., Bento J., Bojić I. S., Parker Q. A., 2014, *MNRAS*, 445, 1605
- Gaia Collaboration et al., 2016, *A&A*, 595, 1G
- Gaia Collaboration, Brown A. G. A., Vallenari A., Prusti T., de Bruijne J. H. J., Babusiaux C., Bailer-Jones C. A. L., A&A0, 2018, *A&A*, 616, 1G
- Galan C., Mikolajewska J., Hinkle K. H., 2015, *MNRAS*, 447, 492
- Galan C., Mikolajewska J., Hinkle K. H., Joyce R. R., 2016, *MNRAS*, 455, 1282
- Galan C., Mikolajewska J., Hinkle K. H., Joyce R. R., 2017, *MNRAS*, 466, 2194
- Gonçalves D. R., Magrini L., Munari U., Corradi R. L. M., Costa R. D. D., 2008, *MNRAS*, 391L, 84G
- Gonçalves D. R., Magrini Laura, Martins L. P., Teodorescu A. M., Quireza C., 2012, *MNRAS*, 419, 854G
- Gonçalves D. R., Magrini L., de la Rosa I. G., Akras S., 2015, *MNRAS*, 447, 993G
- Gregersen D., et al., 2015, *AJ*, 150, 189
- Gutiérrez-Moreno A., Moreno H., Costa E., 1999, *PASP*, 111, 571
- Gromadzki M., Mikolajewska J., Whitelock P., Marang F., 2009, *AcA*, 59, 169G
- Gromadzki M., Mikolajewska J., Pilecki B., Whitelock P., Feast M., 2011, *apn5 confP*, 63G
- Gromadzki M., Mikolajewska J., Soszyński I., 2013, *AcA*, 63, 405G
- Groves B., Dopita M. A., Williams R. E., Hua C.-T., 2002, *PASA*, 19, 425
- Guandalini R., Busso M., Ciprini S., Silvestro G., Persi P., 2006, *A&A*, 445, 1069
- Hajduk M., Gladkowski M., Soszyński I., 2014, *A&A*, 561, 8
- Hajduk M., Gromadzki M., Mikolajewska J., Miszalski B., Soszyński I., 2015, *AcA*, 65, 139H,
- Hambach F.-J., Hümmerich S., Bernhard K., Otero S., 2015, *JAVSO*, 43, 213
- Han Z., Podsiadlowski Ph., 2004, *MNRAS*, 350, 1301
- Henden A., Munari U., 2000, *A&AS*, 143, 343
- Henden A., Munari U., 2001, *A&A*, 372, 145
- Henden A., Munari U., 2006, *A&A*, 458, 339
- Heo J.-E., Lee H.-W., 2015, *J. Korean Astron. Soc.*, 48, 105
- Heo J.-E., Angeloni R., Di Mille F., Palma T., Lee H.-W., 2016, *ApJ*, 833, 286
- Hinkle K. H., Fekel F. C., Joyce R. R., Wood P. R., Smith V. V., Lebzelter T., 2006, *ApJ*, 641, 479
- Hinkle K. H., Fekel F. C., Joyce R. R., 2009, *ApJ*, 692, 1360H
- Houdashelt M. L., Bell R. A., Sweigart A. V., Wing R. F., 2000, *AJ*, 119, 1424
- Hunter J. D., 2007, *CSE*, 9, 90
- Hynes R. I., et al., 2014, *ApJ*, 780, 11
- Ilkiewicz K., Mikolajewska J., Miszalski B., Gromadzki M., Whitelock P. A., 2015, *MNRAS*, 451, 3909
- Ilkiewicz K., Mikolajewska J., Miszalski B., Kozłowski S., Udalski A., 2018, *MNRAS*, 476, 2605
- Ivison R. J., Seaquist E. R., Schwarz H. E., Hughes D. H., Bode M. F., 1995, *MNRAS*, 273, 517I
- Jones E., Oliphant T., Peterson P., et al., 2001, SciPy: Open source scientific tools for Python, <http://www.scipy.org>
- Joshi V., Banerjee D. P. K., Ashok N. M., Venkataraman V., Walter F. M., 2015, *MNRAS*, 452, 3696J
- Jurkic T., Kotnik-Karuza D., 2012, *A&A*, 544, 35
- Kalirai J. S.; Guhathakurta P., Gilbert, Karoline M., Reitzel D. B., Majewski S. R., Rich R. M., Cooper M. C., 2006, *ApJ*, 641, 268
- Kaplan D. L., Levine A. M., Chakrabarty D., Morgan E. H., Erb D. K., Gaensler B. M., Moon D.-S., Cameron P. B., 2007, *ApJ*, 661, 437
- Kamath D., Wood, P. R., Van Winckel H., 2014, *MNRAS*, 439, 2211K
- Kamath D., Wood P. R., Van Winckel H., 2015, *MNRAS*, 454, 1468K
- Kenyon S. J., 1986, *The Symbiotic Stars*, Cambridge University Press, Cambridge

- Kenyon S. J., Fernandez-Castro T.; Stencel R. E., 1988, AJ, 95, 1817
- Kenyon S. J., Livio M., Mikolajewska J., Tout C. A., 1993, ApJ, 407, L81
- Kniazev A. Y., et al., 2009, MNRAS, 395, 1121.
- Kouveliotou C., Patel S., Tennant A., et al., 2003, IAUC, 8109,2
- Lamers H. J. G. L. M., Zickgraf F.-J., de Winter D., Houziaux L., Zorec J., 1998, A&A, 340, 117
- Lee H.-W., Kang S., 2007, ApJ, 669, 1156
- Leedjärv L., 2004, BaltA, 13, 109
- Leedjärv L., Gális R., Hric L., Merc J., Burmeister M., 2016, MNRAS, 456, 2558
- Lepo K., 2015, PhD dissertation, Univ. Toronto.
- Li J., Mikolajewska J., Chen X.-F., et al., 2015, RAA, 15, 1332
- Lindegren L., et al., A&A, 2018, A&A, 616, 2L
- Lorenzetti D., Saraceno P., Strafella F., 1985, ApJ, 298, 350
- Lü G., Yungelson L., Han Z., 2006, MNRAS, 372 1389
- Luna G. J. M., Sokoloski J. L., Mukai K., Nelson T., 2013, A&A, 559, 6
- Luri X., et al., A&A, 2018, A&A, 616, 9L
- Macfarlane S. A., et al., 2017, MNRAS, 465, 434
- Magrini L., Corradi R. L. M., Munari U., 2003, in Symbiotic stars probing stellar evolution, ASP Conf. Ser., 303, 539
- Mennickent R., Greiner J., Arenas J., Tovmassian G., Mason E., Tappert C., Papadaki C., 2008, MNRAS, 383, 845
- Maravelias G., Zezas A., Antoniou V., Hatzidimitriou D., 2014, MNRAS, 438, 2005
- Marigo P., Bressan A., Nanni A., Girardi L., Pumo M. L., 2013, MNRAS, 434, 488
- Margon B., Prochaska J. X., Tejos N., Monroe T., 2016, PASP, 128, 4201,
- Masetti N., Orlandini M., Palazzi E., Amati L., Frontera F., 2006a, A&A, 453, 295
- Masetti N., Bassani L., Dean A. J., Ubertini P., Walter R., 2006b, ATel, 715, 1
- Masetti N., et al., 2007, A&A, 470, 331
- Masetti N., Munari U., Henden A. A., Page K. L., Osborne J. P., Starrfield S., 2011, A&A, 534, 89
- Mattana F., Götz D., Falanga M., Senziani F., de Luca A., Esposito P., Caraveo P. A., 2006, A&A, 460, 1
- Matsunaga N., Fukushi H., Nakada Y., 2005, MNRAS, 364, 117
- Medina-Tanco G. A., Steiner J. E., 1995, AJ, 109, 1770
- Middlemass, D, 1990, MNRAS, 244, 294
- Mikolajewska J., Acker A., Stenholm, B. 1997, A&A, 327, 191
- Mikolajewska J., 2001, ASPC, 246, 167
- Mikolajewska J., Caldwell N., Shara M. M., 2014, MNRAS, 444, 586M
- Mikolajewska J., Shara M. M., Caldwell N., Ilkiewicz K., Zurek D., 2017, MNRAS, 465, 1699
- Miranda L. F., Vazquez R., Guerrero M. A., Pereira C. B., Iñiguez-Garín E., 2010, PASA, 27, 199M.
- Miszalski B., Acker A., Moffat A. F. J., Parker Q. A., Udalski A., 2009, A&A, 496, 813M
- Miszalski B., Napiwotzki R., Cioni M.-R. L., Groenewegen M. A. T., Oliveira J. M., Udalski A., 2011, A&A, 531, A157
- Miszalski B., Mikolajewska J., Udalski A., 2013, MNRAS, 432, 3186M
- Miszalski B., Mikolajewska J., 2014, MNRAS, 440, 1410M
- Miszalski B., Mikolajewska J., Udalski A., 2014, MNRAS, 444L, 11M
- Mróz P., et al., 2014, MNRAS, 443, 784
- Muerset U., Nussbaumer H., Schmid H. M., Vogel M., 1991, A&A, 248, 458
- Muerset U., Schild H., Vogel M., 1996, A&A, 307, 516
- Muerset U., Wolff, B., & Jordan, S. 1997, A&A, 319, 201
- Muerset U.; Schmid H. M. 1999, A&AS, 137, 473M
- Mukai K., Luna G. J. M., Cusumano G., Segreto A., Munari U., Sokoloski J. L., Lucy A. B., Nelson T., Nuñez N. E., 2016, MNRAS, 461, 1.
- Muna D., Alexander M., Allen A., et al. 2016, ArXiv e-prints, arXiv:1610.03159
- Munari U., Renzini A., 1992, AJ, 397, 87
- Munari U., Yudin B. F., Kolotilov E. A., Tomov T. V., 1996, A&A, 311, 484M
- Munari U., Zwitter T., 2002, A&A, 383, 188
- Munari U., et al., 2007, BaltA, 16, 43M
- Munari U., Corradi R. L. M., Siviero A., Baldinelli L., Maitan A., 2013a, A&A, 558A, 2
- Munari U., Valisa P., Cetrulo G., Poleski R., 2013b, IBVS, 6069, 1M
- Nespoli E., Fabregat J., Mennickent R. E., 2010, A&A, 516, 94
- Nuñez N. E., Nelson T., Mukai K., Sokoloski J. L., Luna G. J. M., 2016, ApJ, 824, 23
- Nussbaumer H., Schmid H. M., Vogel M., 1989, A&A, 211, 27
- Ojha D. K., 2001, MNRAS, 322, 426O
- Oliveira J. M., van Loon J. Th., Sloan G. C., Sewilo M., Kraemer K. E., 2013, MNRAS, 428, 3001
- Parimucha Š., Vaňko M., 2006, ASPC, 349, 309
- Pavlenko Ya. V., et al., 2008, A&A, 485, 541
- Pereira C. B., 1995, A&AS, 111, 471
- Pereira C. B., Smith V. V., Cunha K., 1998, AJ, 116, 1977

- Pereira C. B., Franco C. S., Landaberry S. J. C., 2002, A&A, 385, 900
- Pereira C. B., Franco C. S., de Araújo F. X., 2003, A&A, 397, 927
- Pereira C. B., Smith V. V., Cunha K., 2005, A&A, 429, 993
- Pereira C. B., Miranda L. F., 2005, A&A, 433, 579
- Pereira C. B., Roig F., 2009, AJ, 137, 118
- Pereira C. B., Baella N. O., Drake N. A., Miranda L. F., Roig F., 2017, ApJ, 841, 50
- Remillard R. A., Rosenthal E., Tuohy I. R., Schwartz D. A., Buckley D. A. H., Brissenden R. J. V., 1992, ApJ, 396, 668
- Péquignot D., Baluteau J.-P., 1994, A&A, 283, 593
- Phillips J. P., 2007, MNRAS, 376, 1120
- Phillips J. P. & Ramos-Larios G., 2008, MNRAS, 390, 1170
- Pojmanski G., 2002, AcA, 52, 397P
- Pottasch S. R., Beintema D., Dominguez-Rodriguez F. J., Schaeidt S., Valentijn E., Vandenbussche B., 1996, A&A, 315, 261
- R Development Core Team (2008). R: A language and environment for statistical computing. R Foundation for Statistical Computing, Vienna, Austria. ISBN 3-900051-07-0, URL <http://www.R-project.org>.
- Ramsay G., Sokoloski J. L., Luna G. J. M., Nuñez N. E., 2016, MNRAS, 461, 3599
- Reid M. J., 1993, ARA&A, 31, 345
- Reid W. A., 2014, MNRAS, 438, 2642
- Richards J. W., Starr D. L., Miller A. A., Bloom J. S., Butler N. R., Brink H., Crellin-Quick A., 2012, ApJS, 203, 32R
- Rodríguez-Flores E. R., Corradi R. L. M., Mampaso A., García-Alvarez D., Munari U., Greimel R., Rubio-Díez M. M., Santander-García M., 2014, A&A, 567, 49R
- Rosenfield P., 2014, ApJ, 790, 22
- Sadler E. M., Rich R. M., Terndrup D. M., 1996, AJ, 112, 171
- Sahade J., Brandi E., Fontenla J. M., 1984, A&AS, 56, 17S
- Salaris M., Girardi L., 2005, MNRAS, 357, 669
- Sánchez-Contreras C., Sahai R., Gil de Paz A., Goodrich R., 2008, ApJS, 179, 166
- Samus' N. N., Kazarovets E. V., Durlevich O. V., Kireeva N. N., Pastukhova E. N., 2017, ARep, 61, 80S
- Schild H., 1989, MNRAS, 240, 63S
- Schmeja S., Kimeswenger S., 2001, A&A, 377, 18S
- Schmid H. M., 1989, A&A, 211, 31.
- Schmid H. M., Nussbaumer H., 1993, A&A, 268, 159
- Schmid H. M., Schild H., 1994, A&A, 281, 145
- Schmid H. M., et al. 1999, A&A, 348, 950
- Schmidt M. R., Začs L., Mikolajewska J., Hinkle K. H., 2006, A&A, 446, 603
- Sharpee B., Zhang Y., Williams R., Pellegrini E., Cavagnolo K., Baldwin J. A., Phillips M., Liu X.-W., 2007, ApJ, 659, 1265
- Skopal A., 2005, A&A, 440, 995
- Skopal A., 2006, A&A, 457, 1003
- Skopal A., 2015a, NewA, 36, 116
- Skopal A., 2015b, NewA, 36, 128
- Skopal A., 2015c, NewA, 34, 123
- Skopal A., 2017, ASPC, 508, 313
- Skopal A., Shugarov S. Yu., Sekerás M., et al., 2017, A&A, 604A, 48S
- Skrutskie M. F., Cutri R. M., Stiening R., et al. 2006, AJ, 131, 1163 2MASS
- Smith V. V., Cunha K., Jorissen A., Boffin H. M. J., 1996, A&A, 315, 179
- Smith V. V., Cunha K., Jorissen A., Boffin H. M. J., 1997, A&A, 324, 97
- Smith V. V., Pereira C. B., Cunha K., 2001, ApJ, 556, 55
- Smits Derck P., 1991, MNRAS, 251, 316
- Soszyński I., et al., 2013 AcA, 63, 21 2013
- Srivastava M. K., Ashok N. M., Banerjee D. P. K., Sand D., 2015, MNRAS, 454, 1297
- Tang S., Grindlay J. E., Moe M., Orosz J. A., Kurucz R. L., Quinn S. N., Servillat M., 2012, ApJ, 751, 99T
- Tej A., Chandrasekhar T., 2000, MNRAS, 317, 687
- Torres A. F., Kraus M., Cidale L. S., Barbá R., Borges Fernandes M., Brandi E., 2012, MNRAS, 427, 80
- Tueller J., Gehrels N., Mushotzky R. F., et al. 2005, ATel, 591, 1
- Uttenthaler S., 2013, A&A, 556, 38
- van Belle G. T., Lane B. F., Thompson R. R., Boden A. F., Colavita M. M., et al., 1999, AJ, 117, 521
- VandenBerg D. A., Clem J. L., 2003, AJ, 126, 778
- van der Walt S., Colbert S. C., Varoquaux G., 2011, Computing in Science Engineering, 13, 22
- Van Eck S., Jorissen A., 2002, A&A, 396, 599
- Vassiliadis, E.; Wood, P. R., 1993, ApJ, 413, 641
- Viironen K., Greimel R., Corradi R. L. M., et al., 2009, A&A, 504, 291
- Wallerstein G., Harrison T., Munari U., Vanture A., 2008, PASP, 120, 492
- Watson C. L., Henden A. A., Price A., 2006, SASS, 25, 47W
- Webster B. L., Allen D. A., 1975, MNRAS, 171, 171
- Weidmann W. A., Gamen R., 2011, A&A, 526, 6
- Wheatley P. J., Mukai K., de Martino D., 2003, MNRAS, 346, 855
- Whitelock P. A., Catchpole R. M., Feast M. W., Roberts G., Carter, B. S., 1983, MNRAS, 203, 363
- Whitelock P. A., 1987, PASP, 99, 573W
- Whitelock P. A., 2006, MNRAS, 369, 751

- Wright E. L., Eisenhardt P. R. M., Mainzer A. K., et al.,
2010, AJ, 140, 1868
- Zamanov R. K., Bode M. F., Melo C. H. F., Stateva I. K.,
Bachev R., Gomboc A., Konstantinova-Antova R.,
Stoyanov K. A., 2008, MNRAS, 390, 377
- Zhang Y., Liu X.-W., Luo S.-G., Péquignot D., Barlow M.
J., 2005, A&A, 442, 249

APPENDIX

- A. LISTS OF SYSTS, NEW DISCOVERIES, 2MASS AND ALLWISE DATA, AND THEIR PHYSICAL PARAMETERS

Table 5. List of new SySt (Known or Candidate) Discoveries and Their References.

Known	Candidate	Environment	References
–	2 ^a	Galactic	Corradi (1995), Weidmann & Gamen (2011)
188	30 ^b	Catalog	Bel2000 and references therein
–	2 ^c	Galactic	Schmeja & Kimeswenger (2001), Corradi et al. (2011b)
–	1	Galactic	Feibelman (2001), Groves et al. (2002)
2 ^d	2 ^d	Galactic	Van Eck & Jorissen (2002)
4	–	Galactic	Munari & Zwitter (2002), Downes & Keyes (1988)
1	–	Galactic	Pereira et al. (2002)
1 ^e	–	Galactic	Wheatley et al.(2003)
–	1	Galactic	Pereira & Miranda (2005), Miranda et al. (2010), Weidmann & Gamen (2011)
1 ^f	–	Galactic	Mattana et al. (2006), Masetti et al. (2006a)
1 ^f	–	Galactic	Masetti et al. (2006b)
1 ^f	–	Galactic	Kaplan et al. (2007)
1 ^f	–	Galactic	Masetti et al. (2007)
3	1183 ^g	Galactic	Corradi et al (2008)
–	1	Galactic	Phillips & Ramos-Larios (2008)
1	–	IC 10	Gonçalves et al. (2008)
1	–	Galactic	Mennickent et al. (2008)
4	8 ^h	Galactic	Miszalski et al. (2009)
–	1 ⁱ	Galactic	Viironen et al. (2009)
1	–	NGC 6822	Kniazev et al. (2009)
1	–	Galactic	Corradi & Giammanco (2010)
1	–	Galactic	Corradi et al. (2010a)
8	–	Galactic	Corradi et al. (2010b)
1 ^f	1 ^f	Galactic	Nespoli et al. (2010)
–	1	Galactic	Weidmann & Gamen (2011)
1	–	Galactic	Corradi et al. (2011a)
–	5	LMC	Miszalski et al. (2011)
1 ^f	–	Galactic	Masetti et al. (2011)
1	–	SMC	Torres et al. (2012)

Table 5 continued

Table 5 (*continued*)

Known	Candidate	Environment	References
1	–	Galactic	Bond & Kasliwal (2012)
1	–	NGC 185	Gonçalves et al. (2012)
–	1	Galactic	Tang et al. (2012)
1	–	SMC	Oliveira et al. (2013)
1	–	Galactic	Baella et al. (2013)
16	13 ^h	Galactic ^j	Miszalski et al. (2013)
1 ^f	–	Galactic	Luna et al. (2013)
–	1	Galactic	Munari et al. (2013b)
–	1	SMC	Hajduk et al. (2014)
12	3	Galactic	Miszalski & Mikolajewska (2014)
1	–	SMC	Miszalski et al. (2014)
5	–	Galactic	Rodríguez-Flores et al. (2014)
31	4	M31	Mikolajewska et al. (2014)
1 ^f	–	Galactic	Bahramian et al. (2014)
–	7 ^k	LMC	Reid (2014)
–	5	SMC	Kamath et al. (2014)
1	–	Galactic	Mroz et al. (2014)
–	1	Galactic	Hynes et al. (2014)
1	–	Galactic	Joshi et al. (2015)
1	–	Galactic	Srivastana et al. (2015)
–	1	Galactic	Hambach et al. (2015)
–	2	LMC	Kamath et al. (2015)
1	2	NGC 205	Gonçalves et al. (2015)
2	–	Galactic	Li et al. (2015)
–	1 ^l	Galactic	Clyne et al. (2015)
1	–	Galactic	Margon et al. (2016)
1	–	Galactic	Baella et al. (2016)
1	–	Galactic	Mukai et al. (2016)
12	–	M33	Mikolajewska et al. (2017)
1	–	Galactic	Bozzo et al. (2018)
1	–	LMC	ilkiewicz et al. (2018)

Table 5 continued

Table 5 (*continued*)

Known	Candidate	Environment	References
323 ^m	87+1183	Total	This work
66(15)	28(2)	Extragalactic	This work (Bel2000)

NOTE—^a Corradi (1995) refers to three objects, Hen 2-25, Th 2-B and 19W32. 19W32 is included in the Belczyński et al. catalog but not the other two. Here, we refer to the discovery of the other two candidate Systs.

^b Table 2 in Bel2000 lists 28 candidate, whereas the correct number is 30 (see Belczyński’s online VizieR catalog).

^c M2-9, Mz 3.

^d These discoveries were made based on the H α line profiles. These four objects belong to the extrinsic s-type stars.

^e The X-ray properties of this object are consistent with a symbiotic binary, ruling out its previous classifications as an AM Her-type cataclysmic variable.

^f These are SySt X-ray binaries (SyXB; Luna et al. 2013 and references therein).

^g Based on the IPHAS photometric constraints in Corradi et al. (2008).

^h Miszalski et al. (2009) presented a preliminary list of 13 SySts and 11 candidate SySts. A second list is presented in 2013, with 20 SySts and 15 candidates (Miszalski et al. 2013). By cross matching the two studies, the exact number of SySts discovered in each study are given in the table. The second study provides a different but more robust classification.

ⁱ Two objects were classified as candidate SySts by Viironen et al. (2009). However, one of them (IPHASX J190438.7+021424) was excluded from the list of SySt candidates by Weidmann & Gamen (2011).

^j Towards the Galactic Bulge.

^k Two more objects are also classified as candidates, but they were first reported as candidates by Miszalski et al. (2011; [RP2006] 883 and [RP2006] 264).

^l Sh 2-71.

^m Seven previously classified candidate SySts have been confirmed.

Table 6. Known and candidate symbiotic stars

Name	R.A.	Decl.	J	H	K _s	W1	W2	W3	W4
	J2000	J2000	(mag)	(mag)	(mag)	(mag)	(mag)	(mag)	(mag)
IC10 SySt-1 ⁴	00 20 33.59	+59 18 45.9	-	-	-	13.77±0.03	13.53±0.04	12.68 [†]	9.36
SMC1 ^{1,2} (SMC SySt-1)	00 29 10.86	-74 57 39.8	13.65±0.02	12.85±0.02	12.64±0.03	12.41±0.02	12.43 ±0.02	11.88 ±0.22	9.07
Lin9 ¹³ (SMC SySt-10)	00 30 07.40	-73 37 19.1	13.29±0.03	12.44±0.03	12.27±0.03	12.14±0.02	12.17 ±0.02	12.15 ±0.26	8.90
M31 SySt-1 ¹⁶	00 38 46.16	+40 07 17.0	-	-	-	-	-	-	-
M31 SySt-2 ¹⁶	00 38 57.19	+40 31 32.2	-	-	-	-	-	-	-
NGC185 SySt-1 ²¹	00 39 00.36	+48 19 26.6	-	-	-	13.47±0.03	13.45±0.04	12.68	9.28
M31 SySt-4 ¹⁶	00 39 32.01	+40 12 24.7	-	-	-	-	-	-	-
M31 SySt-5 ¹⁶	00 39 51.85	+40 21 53.8	-	-	-	-	-	-	-
M31 SySt-6 ¹⁶	00 40 05.96	+40 16 04.3	18.26	16.62	16.75±0.24	-	-	-	-
NGC 205 SySt-1 ¹⁴	00 40 17.60	+41 41 53.3	-	-	-	-	-	-	-
M31 SySt-7 ¹⁶	00 40 21.10	+40 45 01.1	-	-	-	-	-	-	-
M31 SySt-8 ¹⁶	00 40 59.30	+40 50 03.0	-	-	-	14.88±0.08	14.66±0.06	12.95	8.81
M31 SySt-9 ¹⁶	00 41 17.11	+40 45 24.1	-	-	-	-	-	-	-
M31 SySt-10 ¹⁶	00 41 47.71	+40 57 37.1	-	-	-	-	-	-	-
M31 SySt-11 ¹⁶	00 41 55.61	+41 08 46.7	-	-	-	-	-	-	-
M31 SySt-12 ¹⁶	00 41 56.21	+41 07 35.0	-	-	-	-	-	-	-
M31 SySt-13 ¹⁶	00 42 16.70	+40 44 15.7	-	-	-	-	-	-	-
M31 SySt-14 ¹⁶	00 42 33.17	+41 27 20.7	-	-	-	-	-	-	-
M31 SySt-15 ¹⁶	00 42 35.59	+41 01 48.0	-	-	-	-	-	-	-
M31 SySt-17 ¹⁶	00 42 42.00	+41 56 56.4	-	-	-	-	-	-	-
SMC2 ^{1,2} (SMC SySt-2)	00 42 47.86	-74 42 00.2	14.04±0.03	13.34±0.03	13.10±0.03	13.00±0.02	12.94±0.03	12.33±0.24	9.14
M31 SySt-18 ¹⁶	00 43 19.98	+41 51 37.5	-	-	-	-	-	-	-
M31 SySt-20 ¹⁶	00 43 23.68	+41 37 33.6	-	-	-	15.52±0.14	14.93±0.09	12.57	9.21
M31 SySt-21 ¹⁶	00 43 34.79	+41 34 47.9	-	-	-	-	-	-	-
M31 SySt-22 ¹⁶	00 43 35.01	+41 43 58.2	-	-	-	15.66±0.18	16.28±0.30	12.23±0.42	8.60
M31 SySt-23 ¹⁶	00 43 49.54	+41 38 55.9	-	-	-	-	-	-	-
M31 SySt-24 ¹⁶	00 43 53.59	+41 53 23.3	-	-	-	-	-	-	-
M31 SySt-25 ¹⁶	00 43 58.20	+41 28 50.9	-	-	-	14.42±0.14	14.85±0.20	12.87	9.11

Table 6 continued

Table 6 (*continued*)

AKRAS ET AL.

Name	R.A.	Decl.	<i>J</i>	<i>H</i>	K _s	<i>W1</i>	<i>W2</i>	<i>W3</i>	<i>W4</i>
	J2000	J2000	(mag)	(mag)	(mag)	(mag)	(mag)	(mag)	(mag)
M31 SySt-26 ¹⁶	00 43 59.52	+41 02 53.5	-	-	-	-	-	-	-
M31 SySt-27 ¹⁶	00 44 11.71	+41 13 36.0	-	-	-	-	-	-	-
M31 SySt-28 ¹⁶	00 44 21.89	+41 51 25.6	-	-	-	-	-	-	-
M31 SySt-29 ¹⁶	00 44 32.09	+41 19 40.8	17.21	15.95	15.46±0.09	-	-	-	-
M31 SySt-30 ¹⁶	00 44 33.74	+41 44 02.8	16.97±0.08	15.98±0.10	15.52±0.08	-	-	-	-
EG And ^{1,2}	00 44 37.19	+40 40 45.7	3.82±0.24	2.93±0.17	2.58±0.26	1.11	1.39	2.45±0.01	2.29±0.02
M31 SySt-31 ¹⁶	00 44 40.50	+41 20 52.2	16.93	16.01	15.83	14.19±0.06	13.34±0.04	11.24±0.31	8.79
M31 SySt-32 ¹⁶	00 44 45.03	+41 41 56.5	-	-	-	-	-	-	-
M31 SySt-33 ¹⁶	00 45 21.55	+41 25 57.3	-	-	-	15.33±0.10	14.43±0.09	12.34±0.39	9.18
M31 SySt-34 ¹⁶	00 45 34.07	+41 30 49.0	17.61±0.14	16.55±0.15	16.15±0.15	-	-	-	-
SMC3 ^{1,2} (SMC SySt-3)	00 48 19.93	-73 31 52.0	11.94±0.03	11.04±0.03	10.80±0.03	10.56±0.02	10.63±0.02	10.22±0.05	9.28±0.52
LHA 115-S 18 ⁵⁹ (SMC SySt-16)	00 54 09.56	-72 41 43.1	12.35±0.03	11.93±0.03	11.11±0.03	9.38±0.02	8.36±0.02	6.28±0.02	4.88±0.03
[OVS2013] 19 ²² (SMC SySt-8)	00 54 19.55	-72 29 11.4	15.08±0.06	15.07±0.09	14.95±0.14	12.98±0.12	11.57±0.03	6.23±0.02	3.00±0.02
SMC N60 ^{1,2} (SMC SySt-4)	00 57 05.85	-74 13 16.6	14.04±0.02	13.17±0.03	12.62±0.03	12.14±0.02	11.74±0.02	10.83±0.08	9.02
LIN 358 ^{1,2} (SMC SySt-5)	00 59 12.26	-75 05 17.7	12.50±0.02	11.65±0.02	11.46±0.03	11.29±0.02	11.29±0.02	10.86±0.09	8.90
SMC N73 ^{1,2} (SMC SySt-6)	01 04 39.33	-75 48 24.7	12.55±0.02	11.71±0.02	11.49±0.03	11.37±0.02	11.46±0.02	11.27±0.13	9.03
M33 SySt-1 ⁵⁶	01 32 19.75	+30 37 31.7	-	-	-	-	-	-	-
M33 SySt-2 ⁵⁶	01 32 39.11	+30 38 36.5	-	-	-	-	-	-	-
M33 SySt-3 ⁵⁶	01 33 03.27	+30 35 28.3	-	-	-	-	-	-	-
M33 SySt-4 ^{56,b}	01 33 11.10	+30 15 28.2	18.7	17.79	17.48	-	-	-	-
M33 SySt-5 ⁵⁶	01 33 27.01	+30 40 45.8	-	-	-	-	-	-	-
M33 SySt-6 ⁵⁶	01 33 34.95	+30 51 08.3	-	-	-	-	-	-	-
M33 SySt-7 ⁵⁶	01 34 17.72	+30 41 19.5	-	-	-	-	-	-	-
M33 SySt-8 ⁵⁶	01 34 30.14	+30 33 46.0	-	-	-	-	-	-	-
M33 SySt-9 ^{56,b}	01 34 35.17	+30 34 09.4	17.97	17.02	16.74	-	-	-	-
M33 SySt-10 ⁵⁶	01 34 49.50	+30 47 36.9	-	-	-	-	-	-	-
M33 SySt-11 ^{56,b}	01 34 57.79	+31 00 54.2	18.90	17.96	17.92	17.11±0.12	16.739±0.29	12.69	9.06
M33 SySt-12 ⁵⁶	01 35 10.81	+30 51 46.8	-	-	-	-	-	-	-
AX Per ^{1,2}	01 36 22.70	+54 15 02.4	6.60±0.02	5.69±0.02	5.35±0.02	5.27±0.20	5.17±0.07	4.96±0.01	4.42±0.03
V471 Per ^{1,2}	01 58 49.67	+52 53 48.4	11.02±0.02	10.40±0.02	9.93±0.02	8.74±0.02	7.48±0.02	3.57±0.02	1.46±0.02

Table 6 continued

Table 6 (*continued*)

Name	R.A.	Decl.	J	H	K _s	W1	W2	W3	W4
	J2000	J2000	(mag)	(mag)	(mag)	(mag)	(mag)	(mag)	(mag)
o Ceti ^{1,2}	02 19 20.79	-02 58 39.5	-0.73±0.15	-1.57±0.19	-2.21±0.22	4.75	3.36	0.10	-3.69
BD Cam ^{1,2}	03 42 09.32	+63 13 00.5	1.40±0.32	0.53±0.17	0.27±0.20	-2.18	-1.92	0.04±0.10	-0.08±0.02
StHA 32 ^{1,2}	04 37 45.63	-01 19 11.8	10.18±0.02	9.48±0.02	9.29±0.02	9.15±0.02	9.18±0.02	8.71±0.03	7.95±0.18
LMC S154 ^{1,2} (LMC SySt-3)	04 51 50.47	-75 03 35.4	11.71±0.02	10.36±0.02	9.38±0.02	8.64±0.02	7.98±0.02	6.78±0.02	6.24±0.05
LMC S147 ^{1,2} (LMC SySt-4)	04 54 03.4	-70 59 32.2	12.87±0.02	12.04±0.03	11.79±0.03	11.66±0.02	11.64±0.02	11.02±0.08	9.50±0.46
LMC N19 ^{1,2} (LMC SySt-5)	05 03 23.74	-67 56 33.5	12.73±0.02	11.84±0.03	11.53±0.02	11.41±0.02	11.42±0.02	11.08±0.07	9.55
UV Aur ^{1,2}	05 21 48.92	+32 30 40.1	4.03 ±0.21	3.02±0.19	2.13±0.22	-1.21	-1.29	-0.30±0.38	-0.88±0.01
V1261 Ori ^{1,2}	05 22 18.64	-08 39 58.0	3.34 ±0.28	2.42±0.24	2.14±0.27	-0.09	0.52	1.85±0.03	1.72±0.02
LMC1 ^{1,2} (LMC SySt-1)	05 25 01.11	-62 28 48.9	13.55±0.03	12.01±0.02	10.71±0.02	8.82±0.02	8.24±0.02	7.50±0.02	7.37±0.06
LMC N67 ^{1,2} (LMC SySt-2)	05 36 07.65	-64 43 22.5	12.67±0.03	11.85±0.03	11.46±0.03	11.08±0.02	11.12±0.02	10.61±0.05	9.58
SMP LMC 88 ⁶³ (LMC SySt-24)	05 42 33.19	-70 29 24.1	15.34±0.06	14.74±0.07	14.33±0.09	13.53±0.03	12.79±0.03	10.59±0.05	7.62±0.09
Sanduleak's star ^{1,2} (LMC SySt-8)	05 45 19.57	-71 16 06.7	15.92±0.10	14.59	13.21	11.31±0.02	9.79±0.02	6.96±0.01	4.96±0.02
LMC S63 ^{1,2,18} (LMC SySt-6)	05 48 43.42	-67 36 10.3	12.51±0.02	11.65±0.03	11.33±0.02	11.01±0.02	11.07±0.02	10.54±0.05	9.36±0.31
SMP LMC 94 ^{1,2} (LMC SySt-7)	05 54 09.53	-73 02 34.1	14.54±0.04	12.77±0.03	11.38±0.02	9.86±0.02	8.96±0.02	6.89±0.01	5.53±0.03
SU Lyn ⁴⁷	06 42 55.14	+55 28 27.2	2.98±0.30	1.92±0.19	1.62±0.22	-1.39	-0.68	0.74±0.01	0.60±0.01
Hen 4-18 ²⁶	07 01 09.15	-29 06 25.0	6.12±0.03	5.27±0.04	4.92±0.02	4.91±0.21	4.85±0.06	4.81±0.02	4.64±0.03
GH Gem ^{1,2}	07 04 12.78	+12 03 34.3	12.07±0.02	11.32±0.02	10.69±0.03	9.10±0.02	8.55±0.02	6.36±0.02	4.75±0.03
ZZ CMi ^{1,2}	07 24 13.99	+08 53 51.8	4.41±0.31	3.39±0.25	3.05±0.24	1.93	1.43	2.49±0.01	2.03±0.02
BX Mon ^{1,2}	07 25 22.76	-03 35 50.6	7.04±0.02	6.04±0.03	5.71±0.02	5.45±0.13	5.32±0.04	4.98±0.02	4.62±0.03
V694 Mon ^{1,2}	07 25 51.28	-07 44 08.1	6.45±0.03	5.47±0.02	5.07±0.02	4.74±0.21	4.31±0.11	4.08±0.01	3.95±0.02
NQ Gem ^{1,2}	07 31 54.52	+24 30 12.6	4.72±0.23	3.64±0.19	3.26±0.29	3.02±0.49	1.79	2.79±0.01	2.71±0.02
StHA 63 ²⁷	07 58 05.87	-07 43 55.5	10.70±0.02	9.90±0.03	9.65±0.02	9.57±0.02	9.53±0.02	9.29±0.04	8.27±0.27
WRAY 15-157 ^{1,2}	08 06 34.87	-28 32 01.2	10.58±0.03	9.80±0.03	9.47±0.02	8.81±0.02	7.74±0.02	4.10±0.02	2.16±0.01
RX Pup ^{1,2}	08 14 12.31	-41 42 29.0	6.40±0.02	4.98±0.02	3.78±0.27	0.06	-0.23	-0.87±0.37	-2.33±0.00
Hen 3-160 ^{1,2}	08 24 53.14	-51 28 32.9	9.30±0.02	8.33±0.04	7.80±0.02	7.55±0.04	7.27±0.02	6.55±0.02	6.02±0.04
AS 201 ^{1,2}	08 31 42.89	-27 45 31.5	10.54±0.02	10.22±0.02	10.00±0.02	9.12±0.02	8.34±0.02	3.91±0.01	1.35±0.01
KM Vel ^{1,2}	09 41 14.00	-49 22 47.2	8.40±0.02	7.01±0.04	5.56±0.02	3.72±0.48	2.56±0.43	1.45±0.02	0.40±0.02
V366 Car ^{1,2}	09 54 43.29	-57 18 52.4	6.93±0.03	5.68±0.04	4.76±0.02	2.29	0.97	1.58±0.04	0.95±0.02
SS73 17 ^{35,48}	10 11 02.95	-57 48 13.9	5.15±0.02	4.48±0.21	3.92±0.04	3.75±0.41	3.40±0.26	3.64±0.03	0.319±0.03
Hen 3-461 ^{1,2}	10 39 08.70	-51 24 12.5	5.24±0.02	4.19±0.23	3.86±0.27	3.64±0.44	3.46±0.29	3.28±0.01	3.01±0.02

Table 6 continued

Table 6 (*continued*)

Name	R.A.	Decl.	J	H	K _s	W1	W2	W3	W4
	J2000	J2000	(mag)	(mag)	(mag)	(mag)	(mag)	(mag)	(mag)
SS73 29 ^{1,2}	11 08 27.48	-65 47 21.1	11.78±0.03	10.90±0.03	10.56±0.03	10.39±0.02	10.40±0.02	10.08±0.05	9.30
SY Mus ^{1,2}	11 32 10.00	-65 25 11.5	5.92±0.02	4.99±0.06	4.59±0.03	4.48±0.32	4.26±0.13	4.27±0.02	3.80±0.02
BI Cru ^{1,2}	12 23 26.00	-62 38 16.1	7.33±0.03	6.19±0.02	5.06±0.02	3.61±0.45	1.20	0.57±0.04	-0.58±0.01
Hen 4-121 ²⁶	12 24 32.51	-28 18 55.7	5.35±0.02	4.51±0.21	4.21±0.29	3.86±0.38	3.86±0.22	3.87±0.02	3.70±0.02
LAMOSTJ12280490-014825.7 ¹⁹	12 28 04.90	-01 48 25.7	10.03±0.03	9.18±0.02	9.03±0.02	8.92±0.02	8.95±0.02	8.72±0.03	8.39±0.31
4 Dra ^{57,58}	12 30 06.66	+69 12 04.1	1.55±0.26	0.56±0.15	0.45±0.17	-1.79	-0.76	0.13±0.10	0.09±0.01
RT Cru ^{1,2}	12 34 53.74	-64 33 56.0	6.65±0.02	5.58±0.02	5.19±0.02	5.48±0.04	4.74±0.07	4.52±0.02	4.33±0.03
TX CVn ^{1,2}	12 44 42.06	+36 45 50.6	7.47±0.02	6.58±0.04	6.25±0.03	5.79±0.14	5.25±0.06	3.54±0.02	2.78±0.02
Hen 2-87 ^{1,2}	12 45 47.03	-63 00 35.7	8.58±0.02	6.93±0.04	6.04±0.02	5.65±0.10	5.16±0.04	3.24±0.01	2.35±0.02
Hen 3-828 ^{1,2}	12 50 58.10	-57 50 46.5	8.54±0.02	7.53±0.03	7.10±0.02	6.97±0.06	7.09±0.02	6.74±0.02	6.46±0.05
SS73 38 ^{1,2}	12 51 26.20	-64 59 58.0	9.35±0.02	7.43±0.03	5.92±0.02	4.60±0.16	3.47±0.17	1.90±0.01	1.33±0.01
Hen 3-863 ^{1,2}	13 07 43.90	-48 00 19.5	9.53±0.02	8.60±0.04	8.44±0.02	8.32±0.02	8.32±0.02	7.96±0.02	7.42±0.11
Sa 3-22 ^{1,2}	13 14 30.30	-58 51 49.6	9.73±0.02	8.68±0.03	8.21±0.02	8.14±0.02	8.20±0.02	7.82±0.02	7.47±0.08
CD-36 8436 ^{1,2}	13 16 01.38	-37 00 10.7	6.59±0.02	5.71±0.05	5.35±0.02	5.22±0.19	5.13±0.07	5.02 ±0.01	4.79±0.03
V840 Cen ^{1,2}	13 20 49.47	-55 50 14.7	11.81±0.04	11.08±0.04	10.90±0.03	10.27±0.02	10.20±0.02	9.81±0.04	8.84±0.34
Hen 3-905 ^{1,2}	13 30 37.16	-57 58 20.2	9.77±0.02	8.77±0.04	8.43±0.02	8.22±0.02	8.21±0.02	7.69±0.02	6.97±0.09
RW Hya ^{1,2}	13 34 18.13	-25 22 48.9	5.73±0.03	4.92±0.03	4.61±0.03	4.57±0.30	4.34±0.16	4.28±0.01	3.73±0.02
Hen 3-916 ^{1,2}	13 35 29.95	-64 45 43.2	9.24±0.03	8.17±0.04	7.65±0.03	7.48±0.03	7.53±0.02	7.03±0.02	6.38±0.06
V704 Cen ^{1,2}	13 54 55.7	-58 27 16.6	11.76±0.03	10.07±0.03	8.63±0.02	6.87±0.05	5.79±0.04	3.82±0.02	2.30±0.02
2MASSJ14031865-5809349 ¹²	14 03 18.66	-58 09 35.0	10.42±0.02	9.32±0.02	8.94±0.02	8.70±0.02	8.67±0.02	8.15±0.03	7.22±0.12
V852 Cen ^{1,2}	14 11 52.06	-51 26 24.1	11.01±0.02	8.96±0.04	7.15±0.03	5.03±0.15	3.64±0.12	1.43±0.02	0.06±0.02
V835 Cen ^{1,2}	14 14 09.41	-63 25 46.3	9.58±0.02	7.76±0.05	6.14±0.02	3.36±0.54	1.17±-	-0.06±0.10	-1.27±0.01
V417 Cen ^{1,2}	14 15 59.68	-61 53 50.2	8.07±0.02	6.98±0.05	5.79±0.03	4.05±0.26	2.88±0.39	0.96±0.03	-0.24±0.01
BD-21 3873 ^{1,2}	14 16 34.31	-21 45 50.2	8.12±0.03	7.32±0.05	7.13±0.03	6.98±0.05	6.97±0.02	6.73±0.02	6.15±0.05
AE Cir ^{1,2}	14 44 51.34	-69 23 34.6	10.88±0.02	10.05±0.03	9.74±0.02	9.46±0.02	9.27±0.02	8.22±0.02	7.34±0.10
Hen 2-127 ^{1,2}	15 24 49.78	-51 49 52.6	10.59±0.02	9.43±0.03	8.53±0.02	6.92±0.03	6.44±0.02	5.26±0.02	3.98±0.02
2MASSJ15431767-5857221 ¹²	15 43 17.67	-58 57 22.2	11.22±0.02	10.13±0.02	9.72±0.02	9.64±0.02	9.70±0.02	9.28±0.04	9.09
Hen 3-1092 ^{1,2}	15 47 10.50	-66 29 16.2	8.97±0.02	8.04±0.03	7.72±0.02	7.50±0.03	7.43±0.02	6.96±0.02	6.23±0.04
Hen 3-1103 ^{1,2}	15 48 28.28	-44 19 01.5	9.60±0.02	8.74±0.06	8.36±0.02	8.21±0.02	8.17±0.02	7.63±0.02	7.01±0.09
HD 330036 ^{1,2}	15 51 15.92	-48 44 58.5	9.02±0.03	8.08±0.04	7.57±0.02	6.10±0.09	4.66±0.09	0.21±0.02	-1.54±0.01

Table 6 continued

Table 6 (*continued*)

Name	R.A.	Decl.	J	H	K _s	W1	W2	W3	W4
	J2000	J2000	(mag)	(mag)	(mag)	(mag)	(mag)	(mag)	(mag)
Hen 2-139 ^{1,2}	15 54 44.45	-55 29 34.1	8.38±0.02	6.92±0.02	5.95±0.02	4.89±0.20	3.85±0.16	2.57±0.02	1.49±0.02
T CrB ^{1,2}	15 59 30.16	+25 55 12.6	6.00±0.02	5.15±0.04	4.81±0.02	4.54±0.18	4.50±0.08	4.41±0.01	4.23±0.03
2MASSJ16003761-4835228 ¹²	16 00 37.61	-48 35 22.9	10.80±0.03	9.47±0.03	8.89±0.02	8.21±0.02	8.19±0.02	7.75±0.02	6.99±0.09
AG Dra ^{1,2}	16 01 41.01	+66 48 10.1	7.15±0.02	6.37±0.02	6.21±0.02	6.08±0.11	5.96±0.04	5.67±0.02	5.01±0.03
WRAY 16-202 ^{1,2}	16 06 56.98	-49 26 41.8	8.79±0.02	7.39±0.02	6.75±0.02	6.38±0.07	6.41±0.02	6.23±0.02	5.89±0.05
V347 Nor ^{1,2}	16 14 01.10	-56 59 28.0	7.20±0.02	5.81±0.03	4.94±0.02	3.93±0.29	3.09±0.24	1.90±0.02	1.32±0.02
UKS Ce-1 ^{1,2}	16 15 29.63	-22 12 15.6	12.48±0.03	11.60±0.02	11.33±0.02	10.97±0.02	11.07±0.02	10.88±0.12	8.50±0.40
IRG J16194-2810 ⁴⁰	16 19 33.35	-28 07 39.7	8.27±0.03	7.33±0.04	6.98±0.02	6.77±0.06	6.96±0.02	6.79±0.02	6.73±0.10
QS Nor ^{1,2}	16 21 07.76	-42 23 54.2	9.48±0.02	8.49±0.04	8.07±0.05	7.78±0.03	7.73±0.02	6.69±0.02	5.95±0.06
WRAY 15-1470 ^{1,2}	16 23 21.65	-27 40 10.4	9.02±0.02	8.06±0.04	7.67±0.02	7.40±0.04	7.35±0.02	6.92±0.02	6.00±0.06
Hen 2-171 ^{1,2}	16 34 04.25	-35 05 26.8	9.68±0.02	8.03±0.03	6.64±0.02	4.87±0.15	4.02±0.16	2.59±0.01	1.53±0.01
Hen 3-1213 ^{1,2}	16 35 15.08	-51 42 27.6	8.02±0.03	7.00±0.04	6.69±0.03	6.63±0.07	6.48±0.02	6.14±0.02	5.42±0.06
IGR J16358-4726 ^{38,c}	16 35 53.80	-47 25 41.1	15.41±0.11	13.39±0.05	12.52±0.02	-	-	-	-
Hen 2-173 ^{1,2}	16 36 24.64	-39 51 44.4	8.16±0.02	7.03±0.03	6.53±0.02	6.46±0.08	6.25±0.03	6.23±0.02	5.85±0.04
Hen 2-176 ^{1,2}	16 41 31.20	-45 13 04.6	8.17±0.02	6.66±0.03	5.78±0.03	5.28±0.09	4.85±0.09	4.23±0.02	2.47±0.03
2MASSJ16422739-4133105 ¹²	16 42 27.39	-41 33 10.5	10.33±0.02	8.96±0.07	7.66±0.02	6.09±0.08	4.94±0.07	3.99±0.02	3.30±0.04
KX TrA ^{1,2}	16 44 35.47	-62 37 14.1	7.33±0.02	6.41±0.03	5.98±0.02	5.86±0.12	5.57±0.05	5.22±0.02	4.72±0.03
AS 210 ^{1,2}	16 51 20.41	-26 00 26.7	9.09±0.02	7.56±0.04	6.26±0.02	4.99±0.16	3.71±0.17	2.90±0.01	2.50±0.02
HK Sco ^{1,2}	16 54 41.04	-30 23 07.6	9.02±0.02	8.12±0.08	7.70±0.03	7.70±0.03	7.69±0.02	7.37±0.02	6.83±0.15
CL Sco ^{1,2}	16 54 51.98	-30 37 18.2	8.99±0.02	8.14±0.04	7.74±0.02	7.51±0.03	7.41±0.02	6.86±0.02	6.25±0.09
SS73 71 ⁴⁵	16 59 23.41	-32 14 44.2	11.37±0.03	10.57±0.03	10.16±0.03	9.94±0.02	9.93±0.02	9.26±0.07	7.47
MaC 1-3 ^{1,2}	17 01 27.69	-47 45 35.4	9.84±0.03	8.57±0.04	7.98±0.03	7.73±0.03	7.62±0.02	7.23±0.02	6.39±0.07
V1535 Sco ⁶⁴	17 03 26.1	-35 04 17.8	13.40±0.03	12.53±0.04	12.22±0.03	11.24±0.03	11.46±0.03	11.14±0.19	8.44±0.00
2MASSJ17050868-4849122 ¹²	17 05 08.69	-48 49 12.2	10.04±0.02	8.95±0.03	8.56±0.02	8.39±0.02	8.45±0.02	8.21±0.02	7.81±0.26
V934 Her ^{1,2}	17 06 34.52	+23 58 18.6	4.17±0.20	3.32±0.19	2.99±0.23	2.22	2.85±0.41	2.96±0.01	2.84±0.02
V455 Sco ^{1,2}	17 07 21.73	-34 05 14.5	7.54±0.03	6.47±0.03	5.96±0.02	5.76±0.11	5.73±0.04	5.21±0.02	3.27±0.02
Hen 3-1341 ^{1,2}	17 08 36.58	-17 26 30.5	8.76±0.03	7.89±0.04	7.48±0.03	7.41±0.03	7.36±0.02	6.45±0.02	5.21±0.04
Hen 3-1342 ^{1,2}	17 08 54.98	-23 23 36.5	9.61±0.02	8.69±0.05	8.35±0.02	8.22±0.02	8.24±0.02	7.84±0.02	7.22±0.15
AS 221 ^{1,2}	17 12 12.87	-32 37 46.9	12.14±0.02	10.10±0.03	8.73±0.02	7.18±0.04	7.13±0.02	4.62±0.02	3.69±0.02
PN H 2-5 ^{1,2}	17 15 19.82	-31 33 53.4	7.16±0.02	6.03±0.04	5.56±0.02	4.53±0.11	5.10±0.05	5.29±0.02	5.03±0.03

Table 6 (*continued*)

AKRAS ET AL.

Name	R.A.	Decl.	J	H	K _s	W1	W2	W3	W4
	J2000	J2000	(mag)	(mag)	(mag)	(mag)	(mag)	(mag)	(mag)
V1534 Sco ⁶⁵	17 15 46.83	-31 28 30.3	11.26±0.04	10.05±0.04	9.58±0.04	8.79±0.02	8.91±0.02	8.65±0.03	8.97±0.00
PN Sa 3-43 ^{1,2}	17 17 55.78	-30 01 42.5	9.48±0.02	8.23±0.03	7.84±0.03	7.54±0.03	7.51±0.02	7.28±0.02	6.77±0.08
SWIFTJ171951.7-300206 ⁵¹	17 19 51.70	-30 02 00.6	10.88±0.03	10.19±0.03	9.97±0.02	9.58±0.03	9.53±0.02	9.45±0.05	10.88
Draco C-1 (Draco SySt-1) ^{1,2}	17 19 57.66	+57 50 05.5	14.38±0.03	13.71±0.04	13.46±0.04	13.25±0.11	13.27±0.03	12.49±0.29	9.51
PN Th 3-7 ^{1,2}	17 21 02.54	-29 22 52.8	9.75±0.02	8.49±0.06	7.88±0.03	7.53±0.03	7.67±0.02	7.32±0.02	6.95±0.09
356.04+03.20 ¹⁰	17 23 21.20	-30 31 35.0	9.79±0.02	8.46±0.06	7.87±0.03	7.24±0.03	7.61±0.02	7.21±0.02	6.58±0.07
PN Th 3-17 ^{1,2}	17 27 31.63	-29 02 56.5	9.52±0.03	8.41±0.06	7.84±0.02	7.72±0.03	7.78±0.02	7.33±0.02	6.62±0.09
358.46+03.54 ¹⁰	17 28 13.10	-28 19 38.0	9.19±0.03	8.23±0.04	7.75±0.02	7.75±0.02	7.73±0.02	7.24±0.02	6.39±0.08
PN Th 3-18 ^{1,2}	17 28 26.93	-28 38 34.6	9.82±0.03	8.67±0.03	8.23±0.03	8.01±0.02	7.98±0.02	7.71±0.02	7.10±0.14
Hen 3-1410 ^{1,2}	17 29 06.20	-29 43 17.7	10.32±0.03	9.16±0.04	8.57±0.03	7.78±0.02	7.68±0.02	7.28±0.02	6.69±0.10
357.32+01.97 ¹⁰	17 31 23.18	-30 08 44.3	10.39±0.03	9.07±0.03	8.60±0.02	8.24±0.02	8.22±0.02	7.81±0.06	4.44±0.03
V2116 Oph ^{1,2}	17 32 02.16	-24 44 44.2	10.10±0.02	8.70±0.05	7.98±0.02	7.43±0.03	7.14±0.02	6.78±0.02	6.40±0.07
PN Th 3-29 ^{1,2}	17 32 27.89	-29 05 08.8	8.92±0.02	7.57±0.04	6.92±0.02	6.61±0.08	6.65±0.02	6.20±0.01	5.59±0.05
IGR J17329-273 ⁶⁶	17 32 50.28	-27 30 04.9	9.82±0.03	8.44±0.03	7.78±0.02	7.44±0.03	7.29±0.02	6.18±0.02	5.44±0.05
PN Th 3-30 ^{1,2}	17 33 43.39	-28 07 21.1	10.17±0.03	8.86±0.06	8.33±0.03	7.94±0.03	7.90±0.02	7.43±0.02	6.66±0.08
2MASSJ17334728-2719266 ¹²	17 33 47.29	-27 19 26.7	9.32±0.04	7.91±0.03	7.26±0.02	6.32±0.08	5.87±0.05	4.73±0.01	4.03±0.03
PN Th 3-31 ^{1,2}	17 34 16.81	-29 29 12.0	9.74±0.03	8.53±0.07	7.95±0.03	7.26±0.03	7.39±0.02	6.90±0.02	6.18±0.08
M 1-21 ^{1,2}	17 34 17.22	-19 09 23.0	8.66±0.02	7.60±0.07	7.10±0.03	6.85±0.05	6.89±0.02	6.42±0.02	5.74±0.05
357.98+01.57 ¹⁰	17 34 35.5	-29 48 22.0	10.02±0.03	8.68±0.03	8.07±0.04	7.62±0.03	7.66±0.02	6.96±0.02	5.55±0.06
Hen 2-251 ^{1,2}	17 35 22.24	-29 45 19.8	10.42±0.02	8.63±0.03	6.95±0.02	4.63±0.18	3.61±0.23	1.72±0.02	0.30±0.02
NSV 22840 ¹⁰	17 35 58.47	-28 49 54.1	10.50±0.02	9.20±0.02	8.65±0.02	8.21±0.02	8.19±0.02	7.63±0.03	7.10±0.13
PN Pt 1 ^{1,2}	17 38 49.55	-23 54 05.4	10.09±0.02	8.91±0.02	8.49±0.02	8.24±0.02	8.21±0.02	7.86±0.02	7.16±0.13
2MASSJ17391715-3546593 ¹²	17 39 17.15	-35 46 59.4	9.81±0.02	8.45±0.06	7.64±0.02	7.63±0.02	6.88±0.02	5.79±0.02	4.76±0.02
K 6-6 ^{1,2}	17 39 18.28	-28 15 08.5	9.42±0.03	8.20±0.04	7.52±0.02	6.69±0.05	6.36±0.02	5.23±0.02	4.50±0.03
RT Ser ^{1,2}	17 39 51.98	-11 56 39.0	8.39±0.02	7.34±0.06	6.88±0.03	6.77±0.07	6.62±0.02	6.14±0.01	5.42±0.04
359.76+01.15 ¹⁰	17 40 34.60	-28 31 41.0	9.65±0.03	8.10±0.04	7.20±0.02	5.94±0.07	5.75±0.05	4.85±0.02	3.66±0.03
AE Ara ^{1,2}	17 41 04.92	-47 03 27.2	7.69±0.02	6.77±0.03	6.37±0.02	6.25±0.11	6.19±0.03	5.78±0.02	5.11±0.03
SS73 96 ^{1,2}	17 41 28.42	-36 47 45.2	8.19±0.02	6.91±0.03	6.42±0.02	5.57±0.07	5.93±0.03	5.59±0.02	4.67±0.03
2MASSJ17422035-2401162 ¹²	17 42 20.36	-24 01 16.3	10.20±0.02	9.00±0.03	8.44±0.02	8.26±0.02	8.23±0.02	7.56±0.02	6.69±0.08
UU Ser ^{1,2}	17 42 38.29	-15 24 26.2	10.48±0.02	9.52±0.02	9.12±0.03	9.10±0.02	9.06±0.02	8.33±0.03	7.72±0.19

Table 6 continued

Table 6 (*continued*)

Name	R.A.	Decl.	J	H	K _s	W1	W2	W3	W4
	J2000	J2000	(mag)	(mag)	(mag)	(mag)	(mag)	(mag)	(mag)
V2110 Oph ^{1,2}	17 43 33.32	-22 45 37.0	9.80±0.02	8.39±0.05	7.64±0.02	7.14±0.04	6.86±0.02	5.70±0.02	5.06±0.04
V916 Sco ^{1,2}	17 43 54.71	-36 03 26.5	13.27±0.05	12.28±0.04	12.03±0.05	11.55±0.04	11.84±0.05	11.86±0.40	9.00
K 5-33 ¹⁰	17 44 29.91	-27 20 40.8	14.45±0.12	12.80±0.08	11.24±0.04	8.70±0.03	7.24±0.02	3.25±0.01	0.68±0.01
XMMUJ174445.5-295044 ¹⁷	17 44 46.26	-29 50 56.1	-	-	-	-	-	-	-
354.98-02.87 ¹⁰	17 44 53.12	-34 42 39.6	14.55±0.12	12.57±0.08	10.75±0.03	8.01±0.02	6.58±0.02	3.95±0.01	2.25±0.02
355.39-02.63 ¹⁰	17 44 55.68	-34 14 17.9	10.01±0.02	8.79±0.05	8.29±0.05	7.97±0.02	8.12±0.02	7.73±0.02	6.90±0.11
AS 241 ^{1,2}	17 45 14.24	-38 17 25.9	9.48±0.03	8.32±0.04	7.69±0.02	7.47±0.03	7.29±0.02	5.76±0.02	4.79±0.03
Hen 2-275 ^{1,2}	17 45 30.74	-38 39 45.8	10.18±0.02	9.16±0.02	8.77±0.02	8.64±0.02	8.68±0.02	8.40±0.03	7.95±0.25
2MASSJ17463311-2419558 ¹²	17 46 33.11	-24 19 55.8	9.86±0.02	8.51±0.06	7.91±0.03	7.48±0.03	7.47±0.02	5.97±0.02	4.73±0.03
355.28-03.15 ¹⁰	17 46 48.24	-34 36 02.8	9.83±0.03	8.60±0.03	8.07±0.03	7.75±0.03	7.83±0.02	7.32±0.02	6.83±0.10
V917 Sco ^{1,2}	17 48 04.28	-36 08 17.3	9.42±0.03	8.30±0.04	7.85±0.02	7.63±0.03	7.74±0.02	7.36±0.02	6.98±0.11
PN H 1-36 ^{1,2}	17 49 48.22	-37 01 27.9	11.77	9.87±0.04	7.63±0.02	5.19±0.10	3.71±0.17	-	-0.85±0.01
JaSt2-6 ¹⁰	17 50 01.85	-29 33 25.6	10.89±0.02	8.13±0.03	6.16±0.02	3.50±0.26	2.73±0.33	0.28±0.10	-0.89±0.01
RS Oph ^{1,2}	17 50 13.20	-06 42 28.5	7.64±0.02	6.86±0.04	6.50±0.02	6.18±0.12	5.94±0.05	5.16±0.02	4.34±0.03
WRAY 16-312 ^{1,2}	17 50 16.66	-30 57 34.6	11.84±0.03	9.60±0.03	7.96±0.02	5.83±0.12	4.92±0.12	3.02±0.01	1.89±0.02
V4141 Sgr ^{1,2}	17 50 23.83	-19 53 43.2	9.81±0.02	8.61±0.04	8.01±0.03	7.75±0.03	7.80±0.02	6.43±0.02	5.63±0.04
ALS 2 ^{1,2}	17 50 51.12	-17 47 57.2	9.82±0.02	8.77±0.02	8.45±0.02	8.23±0.02	8.24±0.02	7.92±0.02	7.23±0.12
AS 245 ^{1,2}	17 51 00.92	-22 19 35.0	9.45±0.02	8.17±0.04	7.43±0.02	6.04±0.05	6.49±0.02	5.85±0.02	5.05±0.04
Hen 2-294 ^{1,2}	17 51 45.73	-32 54 51.6	10.01±0.03	8.77±0.04	8.34±0.03	7.08±0.02	7.24±0.02	7.18±0.02	6.83±0.09
JaSt79 ^{10,11}	17 51 53.55	-29 30 53.5	10.17±0.02	8.53±0.04	7.11±0.02	5.19±0.13	4.06±0.16	2.13±0.02	0.91±0.01
PN Bl 3-14 ^{1,2}	17 52 25.94	-29 45 57.0	10.42±0.02	9.18±0.02	8.68±0.02	8.31±0.03	8.36±0.02	7.97±0.03	7.05±0.14
000.49-01.45 ¹⁰	17 52 31.21	-29 15 34.6	9.86±0.02	8.48±0.05	7.73±0.02	7.31±0.03	7.50±0.02	7.29±0.02	6.48±0.10
PN Bl 3-6 ^{1,2}	17 52 56.32	-31 19 18.5	10.03±0.04	8.87±0.04	8.38±0.03	8.02±0.02	8.09±0.02	7.94±0.03	8.51±0.44
PN Bl L ^{1,2}	17 53 13.78	-30 18 05.6	9.84±0.02	8.65±0.06	8.12±0.02	7.60±0.03	7.67±0.02	7.04±0.02	5.94±0.07
V745 Sco ^{1,2}	17 55 22.22	-33 14 58.6	10.04±0.03	8.85±0.04	8.26±0.03	7.42±0.04	7.09±0.02	5.87±0.02	5.27±0.04
MaC 1-9 ^{1,2}	17 55 52.68	-14 06 49.1	9.83±0.02	8.68±0.03	8.21±0.03	7.90±0.03	7.93±0.02	7.43±0.02	6.78±0.09
AS 255 ^{1,2}	17 57 08.72	-35 15 37.8	9.58±0.02	8.61±0.03	8.36±0.03	8.09±0.02	8.11±0.02	7.89±0.02	7.40±0.12
V2416 Sgr ^{1,2}	17 57 15.99	-21 41 29.1	6.44±0.02	5.08±0.02	4.51±0.03	4.21±0.21	3.96±0.15	3.96±0.01	3.54±0.02
PHR 1757-2718 ¹⁰	17 57 32.46	-27 18 25.3	10.57±0.03	9.19±0.03	8.52±0.03	7.95±0.02	8.06±0.02	7.50±0.04	6.06±0.06
H 1-45 ¹⁰	17 58 21.87	-28 14 52.3	10.52±0.03	8.40±0.03	6.70±0.02	3.96±0.18	3.27±0.23	2.18±0.01	1.64±0.02

Table 6 (*continued*)

AKRAS ET AL.

Name	R.A.	Decl.	J	H	K _s	W1	W2	W3	W4
	J2000	J2000	(mag)	(mag)	(mag)	(mag)	(mag)	(mag)	(mag)
H 2-34 ^{1,2}	17 58 28.04	-28 33 42.0	9.42±0.03	8.13±0.03	7.61±0.03	7.04±0.04	7.38±0.02	6.94±0.02	5.77±0.06
002.86-01.88 ¹⁰	17 59 34.78	-27 25 43.5	9.98±0.02	8.68±0.03	8.10±0.03	7.92±0.03	8.00±0.02	7.68±0.03	7.57±0.20
003.46-01.92 ^{10,11}	18 01 06.31	-26 55 59.6	9.83±0.02	8.64±0.02	8.02±0.02	7.72±0.03	7.73±0.02	7.08±0.02	6.03±0.08
SS73 117 ^{1,2}	18 02 23.00	-31 59 11.0	9.22±0.03	8.05±0.05	7.37±0.02	6.65±0.11	6.19±0.04	5.46±0.01	4.91±0.04
AS 269 ^{1,2}	18 03 23.96	-32 42 24.9	12.15±0.04	11.31±0.04	9.94±0.03	6.77±0.06	5.69±0.05	3.75±0.01	1.33±0.02
ShWi 5 ^{10,11}	18 03 53.69	-29 51 22.1	13.08	12.47	11.87	9.52±0.03	8.46±0.02	4.63±0.01	2.21±0.01
001.70-03.67 ^{10,11}	18 04 04.95	-29 18 46.9	9.00±0.03	8.12±0.03	7.78±0.03	7.68±0.03	7.73±0.02	7.22±0.02	6.50±0.08
Ap 1-8 ^{1,2}	18 04 29.80	-28 21 28.0	9.35±0.02	8.31±0.04	7.90±0.02	7.71±0.02	7.75±0.02	7.18±0.02	5.56±0.04
SS73 122 ^{1,2}	18 04 41.22	-27 09 12.4	8.31±0.02	7.06±0.04	6.36±0.02	5.68±0.09	5.25±0.06	4.03±0.02	3.04±0.02
AS 270 ^{1,2}	18 05 33.74	-20 20 38.0	7.21±0.03	6.01±0.03	5.51±0.02	5.10±0.17	5.06±0.08	5.11±0.02	4.65±0.04
H 2-38 ^{1,2}	18 06 01.16	-28 17 04.2	8.27±0.02	7.24±0.05	6.48±0.02	5.55±0.18	4.83±0.11	2.93±0.01	1.77±0.02
SS73 129 ^{1,2}	18 07 05.54	-29 36 29.8	9.29±0.02	8.33±0.02	8.06±0.02	7.86±0.02	7.93±0.02	7.71±0.03	7.83±0.21
Hen 3-1591 ^{1,2}	18 07 32.02	-25 53 43.3	10.50±0.02	9.68±0.02	9.07±0.02	7.98±0.02	7.21±0.02	5.40±0.02	4.17±0.03
V615 Sgr ^{1,2}	18 07 40.01	-36 06 21.2	8.79±0.02	7.84±0.02	7.51±0.02	7.37±0.03	7.44±0.02	6.96±0.02	6.27±0.06
Ve 2-57 ^{1,2}	18 08 22.05	-24 33 45.0	8.87±0.03	7.60±0.02	7.11±0.03	6.81±0.07	6.92±0.02	6.72±0.02	5.98±0.07
AS 276 ^{1,2}	18 09 09.54	-41 13 26.7	9.19±0.02	8.28±0.02	7.96±0.02	7.89±0.03	7.91±0.02	7.47±0.02	6.84±0.09
Ap 1-9 ^{1,2}	18 10 28.94	-28 07 41.0	9.80±0.03	8.91±0.03	8.61±0.03	8.22±0.02	8.16±0.02	7.62±0.02	7.00±0.11
AS 281 ^{1,2}	18 10 43.86	-27 57 50.1	8.30±0.02	7.28±0.03	6.92±0.02	6.69±0.07	6.80±0.02	6.50±0.02	6.09±0.07
V2506 Sgr ^{1,2}	18 11 01.69	-28 32 40.4	9.53±0.02	8.60±0.02	8.17±0.02	7.95±0.02	7.98±0.02	7.48±0.02	6.60±0.07
V5590 Sgr ⁶⁷	18 11 03.70	-27 17 29.4	9.29±0.02	8.13±0.04	7.35±0.02	6.04±0.10	5.29±0.04	4.33±0.02	3.64±0.02
SS73 141 ^{1,2}	18 12 11.34	-33 10 42.5	10.26±0.03	9.27±0.03	8.94±0.03	8.72±0.02	8.79±0.02	8.25±0.03	7.30±0.13
AS 289 ^{1,2}	18 12 22.16	-11 40 07.1	6.72±0.02	5.51±0.03	4.99±0.02	4.72±0.18	4.55±0.09	4.35±0.02	3.67±0.04
2MASSJ18131474-1007218 ¹²	18 13 14.74	-10 07 21.9	10.94±0.02	9.64±0.03	9.18±0.02	8.98±0.02	9.02±0.02	8.72±0.03	7.83±0.18
Y CrA ^{1,2}	18 14 22.95	-42 50 32.4	7.77±0.02	6.84±0.03	6.48±0.02	6.31±0.09	6.25±0.03	5.94±0.02	5.55±0.05
YY Her ^{1,2}	18 14 34.19	+20 59 21.3	9.04±0.03	8.13±0.07	7.86±0.02	7.73±0.03	7.81±0.02	7.44±0.02	6.84±0.07
V2756 Sgr ^{1,2}	18 14 34.52	-29 49 23.7	9.19±0.03	8.28±0.03	7.89±0.02	7.59±0.03	7.71±0.02	7.24±0.02	6.80±0.12
FG Ser ^{1,2}	18 15 07.10	-00 18 52.2	5.91±0.02	4.87±0.02	4.40±0.03	4.27±0.32	4.00±0.15	3.96±0.02	3.54±0.03
HD 319167 ^{1,2}	18 15 24.67	-30 31 55.3	8.85±0.02	7.89±0.03	7.51±0.02	7.29±0.03	7.33±0.02	6.86±0.02	6.17±0.06
Hen 2-374 ^{1,2}	18 15 31.07	-21 35 22.8	8.01±0.02	6.85±0.03	6.40±0.02	6.02±0.10	6.06±0.04	5.92±0.02	5.62±0.05
Hen 2-376 ^{1,2}	18 15 46.31	-27 53 46.3	9.41±0.02	8.42±0.02	8.10±0.02	7.83±0.02	8.01±0.02	7.63±0.02	7.25±0.17

Table 6 continued

Table 6 (*continued*)

Name	R.A.	Decl.	J	H	K _s	W1	W2	W3	W4
	J2000	J2000	(mag)	(mag)	(mag)	(mag)	(mag)	(mag)	(mag)
V4074 Sgr ^{1,2}	18 16 05.56	-30 51 11.3	9.07±0.04	7.96±0.03	7.75±0.03	7.42±0.03	7.53±0.02	7.37±0.02	5.32±0.05
V2905 Sgr ^{1,2}	18 17 20.28	-28 09 49.2	9.23±0.02	8.26±0.04	8.00±0.02	7.08±0.06	7.32 ±0.02	6.59±0.02	5.76±0.05
Hen2-375 ¹⁰	18 18 09.03	-57 11 13.4	11.42±0.02	10.41±0.02	8.88±0.02	6.42±0.07	4.63±0.10	1.33±0.01	-0.33±0.02
StHA 149 ^{1,2}	18 18 55.87	+27 26 27.7	8.00±0.02	7.07±0.02	6.82±0.02	6.67±0.07	6.65±0.02	6.28±0.02	5.60±0.04
Hen 3-1674 ^{1,2}	18 20 19.06	-26 22 46.5	8.97±0.02	7.90±0.03	7.44±0.02	7.26±0.03	7.46±0.02	7.04±0.02	6.86±0.11
AR Pav ^{1,2}	18 20 27.88	-66 04 42.9	8.15±0.02	7.37±0.03	7.01±0.03	6.86±0.06	6.86±0.02	6.32±0.02	5.66±0.04
V3929 Sgr ^{1,2}	18 20 58.87	-26 48 25.6	11.59±0.02	9.28±0.03	7.49±0.03	5.71±0.15	4.15±0.10	2.09±0.02	0.61±0.02
V3804 Sgr ^{1,2}	18 21 28.77	-31 32 04.5	8.77±0.02	7.77±0.05	7.36±0.02	6.89±0.06	6.80±0.02	4.73±0.02	3.02±0.02
V443 Her ^{1,2}	18 22 07.85	+23 27 19.9	6.60±0.03	5.65±0.05	5.32±0.02	5.26±0.17	5.12±0.08	4.96±0.02	4.47±0.03
V3811 Sgr ^{1,2}	18 23 29.00	-21 53 09.5	10.48±0.02	9.36±0.02	8.88±0.02	8.22±0.02	8.07±0.02	7.23±0.02	6.45±0.08
V4018 Sgr ^{1,2}	18 25 26.85	-28 35 57.2	8.64±0.02	7.79±0.03	7.44±0.02	7.30±0.03	7.37±0.02	7.01±0.02	6.40±0.07
2MASSJ18272892-1555547 ¹²	18 27 28.93	-15 55 54.8	9.16±0.03	7.80±0.03	7.18±0.02	6.80±0.07	6.78±0.02	6.29±0.02	5.33±0.05
SS383 ⁹	18 27 35.40	+03 58 27.0	9.63±0.02	8.61±0.06	8.36±0.03	8.18±0.02	8.19±0.02	7.87±0.02	7.37±0.14
IPHASJ182906.08-003457.2 ⁷	18 29 06.08	-00 34 57.2	10.97±0.02	9.61±0.02	9.06±0.02	8.82±0.02	8.84±0.02	8.59±0.02	8.20±0.30
2MASSJ18300636-1940315 ¹²	18 30 06.37	-19 40 31.6	11.07±0.02	9.96±0.02	9.55±0.02	9.31±0.02	9.28±0.02	8.75±0.03	8.15±0.29
V3890 Sgr ^{1,2}	18 30 43.28	-24 01 08.9	9.83±0.02	8.77±0.03	8.26±0.02	7.88±0.03	7.89±0.02	7.36±0.02	7.02±0.12
IPHASJ183501.83+014656.0 ⁷	18 35 01.83	+01 46 55.9	10.75±0.02	9.48±0.03	8.92±0.03	8.66±0.02	8.61±0.02	7.88±0.02	7.37±0.13
Sct X-1 ³⁷	18 35 25.83	-07 36 50.1	12.06±0.03	8.52±0.02	6.55±0.02	4.81±0.15	4.01±0.14	2.26±0.03	0.96±0.03
V2601 Sgr ^{1,2}	18 38 02.06	-22 41 51.5	9.29±0.02	8.30±0.04	7.95±0.03	7.76±0.03	7.74±0.02	7.26±0.02	6.55±0.07
K 3-9 ^{1,2}	18 40 24.17	-08 43 46.4	8.19±0.02	6.62±0.03	5.55±0.03	4.53±0.29	2.23±0.09	1.70±0.03	1.01±0.01
IPHASJ184144.00-012839.5 ¹⁵	18 41 44.00	-01 28 39.5	11.45±0.02	9.99±0.03	9.33±0.02	8.98±0.02	9.00±0.02	8.65±0.05	8.45±0.41
AS 316 ^{1,2}	18 42 32.80	-21 17 46.6	9.14±0.02	8.19±0.04	7.79±0.03	7.62±0.03	7.58±0.02	7.02±0.02	6.12±0.06
StHA 154 ⁴²	18 43 27.93	+19 30 05.3	5.80±0.02	4.83±0.02	4.42±0.02	4.36±0.22	4.20±0.12	3.95±0.02	3.49±0.02
DQ Ser ^{1,2}	18 44 39.6	+05 02 49.1	9.39±0.02	8.29±0.04	7.81±0.02	7.58±0.03	7.66±0.02	7.27±0.02	6.81±0.07
IPHASJ184446.08+060703.5 ⁷	18 44 46.08	+06 07 03.6	11.04±0.02	9.88±0.02	9.41±0.02	9.00±0.02	8.99±0.02	8.46±0.03	7.88±0.20
V4368 Sgr ^{42,44}	18 54 40.32	-19 41 59.8	9.08±0.02	8.86±0.06	8.62±0.02	8.64±0.02	8.08±0.02	7.02±0.02	5.90±0.05
IPHASJ184733.03+032554.3 ⁷	18 47 33.03	+03 25 54.2	10.07±0.02	8.44±0.04	7.71±0.02	7.17±0.07	7.24±0.02	6.58±0.02	5.61±0.04
MWC 960 ^{1,2}	18 47 55.81	-20 05 50.9	8.88±0.03	8.09±0.05	7.81±0.03	7.63±0.03	7.55±0.02	6.97±0.01	5.98±0.05
AS 323 ^{1,2}	18 48 35.68	-06 41 10.4	9.30±0.02	8.29±0.02	7.85±0.03	7.59±0.03	7.73±0.02	7.48±0.02	7.26±0.14
AS 327 ^{1,2}	18 53 16.67	-24 22 58.9	8.83±0.02	7.87±0.03	7.55±0.03	7.45±0.03	7.43±0.02	7.02±0.02	6.24±0.06

Table 6 continued

Table 6 (*continued*)

AKRAS ET AL.

Name	R.A.	Decl.	J	H	K _s	W1	W2	W3	W4
	J2000	J2000	(mag)	(mag)	(mag)	(mag)	(mag)	(mag)	(mag)
FN Sgr ^{1,2}	18 53 54.77	-18 59 40.5	8.69±0.02	7.97±0.04	7.67±0.02	7.80±0.03	7.85±0.02	7.42±0.02	6.70±0.11
IPHASJ185323.58+084955.0 ⁷	18 53 23.58	+08 49 55.1	10.32±0.02	9.05±0.02	8.52±0.02	8.19±0.02	8.18±0.02	7.70±0.02	7.00±0.08
Pe 2-16 ^{1,2}	18 54 10.03	-04 38 51.9	9.63±0.02	8.50±0.06	7.93±0.02	7.26±0.02	7.35±0.02	6.81±0.02	5.83±0.05
IPHASJ185704.44+002631.7 ³	18 57 04.44	+00 26 31.9	10.43±0.02	8.86±0.03	8.09±0.02	7.60±0.03	7.54±0.02	5.75±0.02	4.29±0.04
CM Aql ^{1,2}	19 03 35.12	-03 03 14.3	9.21±0.04	8.10±0.05	7.69±0.02	7.50±0.03	7.51±0.02	6.99±0.02	6.23±0.05
V919 Sgr ^{1,2}	19 03 45.11	-16 59 55.4	8.39±0.02	7.39±0.04	7.05±0.02	6.85±0.06	6.81±0.02	6.42±0.02	5.80±0.05
V1413 Aql ^{1,2}	19 03 46.83	+16 26 17.1	8.73±0.02	7.92±0.03	7.50±0.02	6.93±0.04	6.93±0.02	6.25±0.02	5.56±0.04
NSV 11749 ⁶⁸	19 07 38.00	+00 06 09.0	-	-	-	-	-	-	-
IPHASJ190742.36+000251.1 ¹⁵	19 07 42.36	+00 02 51.1	10.79±0.02	9.73±0.03	9.35±0.03	9.07±0.02	9.10±0.02	8.67±0.03	7.83±0.23
IPHASJ190832.31+051226.5 ⁶	19 08 32.31	+05 12 26.5	10.68±0.03	9.26±0.03	8.53±0.02	8.24±0.02	8.19±0.02	7.59±0.03	6.68±0.13
IPHASJ190924.64-010910.2 ³	19 09 24.64	-01 09 10.3	11.44±0.02	10.30±0.02	9.80±0.02	9.55±0.02	9.56±0.02	9.24±0.05	8.02
PN K 3-22 ⁵	19 09 26.60	+12 00 44.6	12.34±0.02	10.33±0.02	8.82±0.02	7.02±0.04	5.94±0.03	4.14±0.02	2.72±0.02
NSV 11776 ^{1,2}	19 09 55.14	-02 47 43.81	8.06±0.02	6.97±0.03	6.45±0.02	6.35±0.08	6.09±0.03	5.43±0.02	4.50±0.03
Ap 3-1 ^{1,2}	19 10 36.13	+02 49 28.2	10.08±0.02	8.94±0.03	8.51±0.02	8.24±0.02	8.21±0.02	7.90±0.02	7.94±0.27
MaC 1-17 ^{1,2}	19 12 57.27	-05 21 20.5	10.38±0.02	9.35±0.03	8.96±0.02	8.78±0.02	8.80±0.02	8.33±0.03	7.69±0.17
V352 Aql ^{1,2}	19 13 33.69	+02 18 13.0	10.90±0.02	9.82±0.02	9.43±0.03	9.25±0.02	9.33±0.02	9.06±0.03	8.94
ALS 1 ^{1,2}	19 16 16.08	-08 17 46.0	9.24±0.03	8.29±0.05	7.98±0.02	7.79±0.03	7.89±0.02	7.54±0.02	7.01±0.11
BF Cyg ^{1,2}	19 23 53.50	+29 40 29.2	7.57±0.02	6.61±0.02	6.27±0.02	5.89±0.12	5.80±0.05	5.48±0.01	5.02±0.03
CH Cyg ^{1,2}	19 24 33.07	+50 14 29.1	1.07±0.28	0.05±0.18	-0.42±0.19	-1.02	1.77	-2.92	-3.06
StHA 164 ^{1,2}	19 28 41.64	-06 03 51.7	9.31±0.02	8.33±0.05	7.93±0.04	7.83±0.03	7.90±0.02	7.66±0.02	7.67±0.15
IPHASJ193436.06+163128.9 ⁷	19 34 36.06	+16 31 28.9	10.71±0.02	9.34±0.02	8.77±0.02	8.53±0.02	8.55±0.02	8.10±0.03	7.55±0.16
IPHASJ193501.31+135427.5 ⁷	19 35 01.31	+13 54 27.5	10.05±0.02	8.98±0.02	8.58±0.02	8.37±0.02	8.39±0.02	8.00±0.02	7.66±0.16
IPHASJ193830.62+235438.4 ¹⁵	19 38 30.62	+23 54 38.4	10.80±0.02	8.55±0.02	7.00±0.02	5.06±0.19	3.95±0.21	3.42±0.01	3.08±0.02
IPHASJ193943.36+262933.1 ^{1,2,15}	19 39 43.36	+26 29 33.1	11.79±0.03	9.43±0.02	7.35±0.02	4.86±0.20	3.03±0.39	1.13±0.02	0.33±0.01
HM Sge ^{1,2}	19 41 57.09	+16 44 39.9	7.62±0.02	6.02±0.02	4.65±0.02	1.25	-0.43	-0.48±0.35	-1.81
Hen 3-1761 ^{1,2}	19 42 25.38	-68 07 35.4	6.68±0.02	5.80±0.04	5.45±0.02	5.33±0.20	5.29±0.05	5.08±0.02	4.64±0.03
NGC6822 SySt-1 ²⁰	19 44 53.88	-14 51 46.8	16.91±	15.78±0.15	15.29	14.55±0.04	14.88±0.10	12.28	8.84
QW Sge ^{1,2}	19 45 49.54	+18 36 47.8	8.32±0.03	7.37±0.02	6.97±0.02	6.82±0.07	6.92±0.02	6.54±0.02	6.02±0.05
IPHASJ194607.52+223112.2 ⁷	19 46 07.52	+22 31 12.3	9.22±0.02	7.19±0.04	5.97±0.02	5.11±0.18	3.92±0.19	1.86±0.01	0.75±0.01
StHA 169 ^{1,2,19}	19 49 57.60	+46 15 20.6	10.10±0.02	9.17±0.02	8.93±0.02	8.83±0.02	8.90±0.02	8.59±0.02	8.47±0.21

Table 6 continued

Table 6 (*continued*)

Name	R.A.	Decl.	J	H	K _s	W1	W2	W3	W4
	J2000	J2000	(mag)	(mag)	(mag)	(mag)	(mag)	(mag)	(mag)
CI Cyg ^{1,2}	19 50 11.83	+35 41 03.0	5.76±0.03	4.76±0.02	4.41±0.02	4.29±0.26	4.07±0.17	4.01±0.02	3.57±0.02
EF Aql ²⁴	19 51 51.73	-05 48 16.6	6.95±0.02	6.00±0.04	5.36±0.02	4.71±0.20	3.82±0.16	2.49±0.02	1.47±0.02
OY Cyg ⁴²	19 54 43.85	+39 17 57.9	6.53±0.03	5.50±0.02	5.078±0.02	5.09±0.18	4.89±0.09	3.88±0.02	2.89±0.02
4U 1954+31 ^{36,46}	19 55 42.34	+32 05 49.0	4.91±0.04	3.88±0.23	3.51±0.36	3.39±0.49	3.36±0.32	3.33±0.01	3.15±0.02
V1016 Cyg ^{1,2}	19 57 05.03	+39 49 36.3	7.03±0.02	5.80±0.02	4.76±0.02	3.28±0.50	0.33	-0.29±0.14	-1.35±0.01
RR Tel ^{1,2}	20 04 18.54	-55 43 33.2	7.30±0.04	6.08±0.04	4.90±0.02	3.41±0.46	0.99	0.41±0.02	-0.62±0.01
PU Vul ^{1,2}	20 21 13.31	+21 34 18.7	7.42±0.03	6.54±0.03	6.12±0.02	5.92±0.15	5.74±0.05	5.14±0.02	4.32±0.04
StHA 176 ^{42,43}	20 22 42.26	-21 07 54.6	10.00±0.02	9.23±0.02	9.05±0.02	8.85±0.02	8.88±0.02	8.84±0.03	8.45
IPHASJ202510.58+435233.0 ³	20 25 10.59	+43 52 33.0	9.94±0.02	8.45±0.02	7.73±0.02	7.05±0.03	6.92±0.02	6.31±0.02	5.70±0.05
LAMOSTJ202629.80+423652.0 ¹⁹	20 26 29.80	+42 36 52.0	12.27±0.03	11.67±0.03	11.55±0.02	11.45±0.02	11.54±0.02	11.98	9.12
LT Del ^{1,2}	20 35 57.23	+20 11 27.5	10.46±0.02	9.67±0.02	9.50±0.02	9.32±0.02	9.34±0.02	8.95±0.03	8.16±0.27
StHA 180 ^{1,2}	20 39 20.61	-05 17 16.3	9.61±0.02	8.70±0.04	8.50±0.03	8.37±0.02	8.47±0.02	8.17±0.03	7.68±0.20
Hen 2-468 ^{1,2}	20 41 18.99	+34 44 52.3	9.40±0.02	8.31±0.03	7.95±0.03	7.78±0.03	7.85±0.02	7.50±0.02	7.11±0.14
ER Del ^{1,2}	20 42 46.50	+08 41 13.5	6.19±0.02	5.34±0.03	4.99±0.02	4.93±0.21	4.89±0.09	4.79±0.01	4.64±0.03
V1329 Cyg ^{1,2}	20 51 01.23	+35 34 54.0	8.17±0.02	7.19±0.02	6.75±0.02	6.64±0.08	6.64±0.02	6.25±0.02	5.59±0.03
IPHASJ205836.43+503307.2 ⁸	20 58 36.44	+50 33 07.4	13.49±0.02	10.50±0.02	8.16±0.02	5.14±0.06	3.50±0.30	2.12±0.01	1.50±0.01
CD-43 14304 ^{1,2}	21 00 06.36	-42 38 44.9	8.58±0.04	7.76±0.04	7.53±0.02	7.36±0.04	7.32±0.02	6.71±0.02	5.81±0.04
V407 Cyg ^{1,2}	21 02 09.81	+45 46 33.0	5.70±0.02	4.36±0.02	3.17±0.26	1.57	0.76	0.95±0.05	-0.30±0.02
StHA 190 ^{1,2}	21 41 44.89	+02 43 54.4	8.71±0.02	8.21±0.03	8.02±0.03	7.78±0.03	7.44±0.02	4.12±0.01	2.13±0.02
AG Peg ^{1,2}	21 51 01.97	+12 37 32.1	5.00±0.02	4.37±0.25	3.85±0.02	3.82±0.41	3.56±0.23	3.62±0.02	3.08±0.03
IPHASJ224834.32+582908.4 ¹⁵	22 48 34.32	+58 29 08.4	11.85±0.02	9.58±0.03	7.91±0.02	6.00±0.12	4.97±0.10	3.36±0.01	2.26±0.02
LL Cas ^{1,2}	23 09 20.16	+54 44 50.0	8.49±0.02	7.56±0.02	7.13±0.02	6.77±0.06	6.57±0.02	6.01±0.02	5.89±0.04
Z And ^{1,2}	23 33 39.96	+48 49 06.0	6.19±0.02	5.29±0.03	4.89±0.02	4.60±0.25	4.40±0.11	4.09±0.01	3.48±0.02
R Aqr ^{1,2}	23 43 49.46	-15 17 04.1	-0.16±0.17	-1.10±0.24	-1.61±0.33	1.72	2.00	-2.87	-3.20
CGCS 5926 ³⁹	23 45 44.65	+62 52 51.1	8.82±0.02	7.49±0.04	6.94±0.02	6.36±0.08	6.24±0.02	5.81±0.02	5.73±0.04
M31 SySt-3 ¹⁶	00 39 23.79	+40 05 43.4	-	-	-	-	-	-	-
NGC 205 SySt-2 ¹⁴	00 40 07.97	+41 45 23.6	-	-	-	-	-	-	-
NGC 205 SySt-3 ¹⁴	00 40 20.97	+41 41 42.6	-	-	-	-	-	-	-
M31 SySt-16 ¹⁶	00 42 37.49	+40 38 13.2	-	-	-	-	-	-	-
M31 SySt-19 ¹⁶	00 43 22.50	+41 39 40.9	17.39±0.11	16.17±0.11	15.91±0.11	15.71±0.14	15.48±0.14	12.33±0.30	9.11

Table 6 continued

Table 6 (*continued*)

AKRAS ET AL.

Name	R.A.	Decl.	<i>J</i>	<i>H</i>	K _s	<i>W1</i>	<i>W2</i>	<i>W3</i>	<i>W4</i>
	J2000	J2000	(mag)	(mag)	(mag)	(mag)	(mag)	(mag)	(mag)
M31 SySt-35 ¹⁶	00 45 45.41	+41 28 51.6	-	-	-	-	-	-	-
[JD2002]11 ^{23,55} (SMC SySt-9)	00 50 52.64	-72 52 16.5	16.06±0.08	14.07±0.04	12.51±0.02	10.66±0.02	9.70±0.02	7.99±0.02	7.34±0.09
SMC SySt-11 ⁵⁴	00 51 42.25	-72 50 27.6	13.57±0.06	13.03±0.06	12.89±0.06	-	-	-	-
SMC SySt-12 ⁵⁴	01 03 22.32	-72 04 11.1	14.98 ±0.04	14.49±0.05	14.33±0.09	14.23±0.03	14.55±0.05	12.16±0.32	8.21
SMC SySt-13 ⁵⁴	01 03 36.26	-72 04 04.2	15.02 ±0.06	14.42±0.05	14.13±0.07	13.80±0.03	13.68±0.03	11.31±0.16	6.79±0.06
SMC SySt-14 ⁵⁴	01 04 05.73	-72 07 00.5	17.15±0.21	16.48±0.15	15.88±0.14	15.53 ±0.05	15.33±0.07	12.10±0.23	8.81
SMC SySt-15 ⁵⁴	01 04 42.60	-72 10 07.4	15.99±0.10	15.70±0.15	14.99±0.14	14.37±0.04	13.78±0.04	11.55±0.16	8.84±0.41
RAW 1691 ^{1,2} (SMC SySt-7)	01 18 35.71	-72 42 21.3	12.77±0.02	11.75±0.02	11.34±0.02	10.83±0.02	10.90±0.02	10.49±0.06	9.41
[BE74] 583 ^{1,2} (LMC SySt-9)	05 26 50.141	-71 06 35.4	14.63±0.03	13.97±0.03	13.85±0.06	13.77±0.03	13.95±0.03	13.12	9.58
LMC SySt-15 ⁵²	05 24 09.89	-69 19 48.0	12.63±0.02	11.59±0.03	11.18±0.03	10.93±0.02	10.97±0.02	9.62±0.09	8.83±0.26
LMC SySt-16 ⁵²	05 28 04.93	-68 59 47.1	15.72±0.03	14.81±0.09	13.55±0.06	11.02±0.02	9.89±0.02	6.66±0.02	4.78±0.03
LMC SySt-17 ⁵³	05 31 16.75	-69 01 04.1	12.34±0.02	11.37±0.03	10.98±0.02	10.87±0.02	10.80±0.02	8.99±0.03	7.19±0.07
[RP2006] 776 (LMC SySt-10) ²⁸	05 32 39.24	-69 31 54.0	16.99	15.82	14.47±0.09	12.46±0.03	11.37±0.02	7.45±0.02	5.49±0.03
[RP2006] 774 (LMC SySt-11) ²⁸	05 32 39.70	-69 30 49.5	15.99	15.64	14.58±0.10	12.29±0.02	11.25±0.02	7.51±0.02	5.34±0.03
LMC SySt-18 ⁵²	05 32 52.21	-67 41 08.8	15.42±0.08	14.50±0.08	13.32±0.04	10.80±0.02	9.79±0.02	5.57 ±0.02	2.33±0.03
[RP2006] 883 (LMC SySt-12) ^{28,52}	05 35 56.89	-69 00 45.0	13.12	12.15	12.63±0.05	9.84±0.02	8.91±0.02	6.60±0.02	5.03±0.04
LMC SySt-19 ⁵²	05 37 46.82	-69 31 55.8	13.33±0.03	12.38±0.03	12.16±0.03	12.05±0.03	12.15±0.03	12.36±0.32	8.67
LM 2-39 (LMC SySt-13) ²⁸	05 40 14.82	-69 28 49.1	15.37±0.08	14.54±0.10	12.95±0.03	10.46±0.02	8.77±0.02	5.28±0.02	2.93±0.03
LMC SySt-20 ⁵³	05 42 18.20	-69 52 49.4	12.96±0.03	12.17±0.03	11.93±0.03	11.12±0.02	10.24±0.02	7.53±0.02	6.21±0.04
[RP2006] 264 (LMC SySt-14) ^{28,52}	05 43 30.34	-69 24 46.6	16.14±0.11	14.78±0.10	12.71±0.03	10.13±0.02	8.69±0.02	5.15±0.02	2.63±0.02
LMC SySt-21 ⁵²	05 43 37.77	-69 20 10.3	16.07±0.05	16.06±0.10	15.23	-	-	-	-
LMC SySt-22 ^{52,53}	05 45 00.16	-69 18 19.2	16.96±0.20	15.50±0.13	13.60±0.05	11.18±0.02	9.68±0.02	7.08±0.02	5.62±0.04
LMC SySt-23 ⁵³	05 48 22.28	-67 58 53.3	14.57±0.03	13.09±0.04	11.73±0.02	10.77±0.02	9.71±0.02	7.38±0.02	5.88±0.03
DASCH J075731.1+201735 ⁶⁹	07 57 31.12	+20 17 34.8	7.28±0.02	6.45±0.03	6.17±0.02	6.07±0.09	6.09±0.03	6.00±0.02	5.75±0.04
Hen 2-25 ^{32,33}	09 18 01.31	-54 39 29.2	13.41±0.03	12.12±0.03	10.41±0.02	8.20±0.02	6.58±0.02	2.81±0.01	0.64±0.01
WRAY 16-51 ^{1,2}	09 33 29.55	-46 34 50.9	6.10±0.02	4.87±0.03	4.29±0.02	3.99±0.40	3.64±0.21	3.32±0.01	3.03±0.02
Hen 2-57 ³³	10 56 03.00	-61 28 07.4	15.39±0.08	13.52±0.05	11.51±0.03	8.96±0.02	7.52±0.02	4.39±0.02	2.27±0.01
Hen 3-653 ^{1,2}	11 25 32.75	-59 56 34.1	6.88±0.02	5.83±0.04	5.34±0.02	4.95±0.18	4.87±0.08	4.24±0.02	3.87±0.02
NSV 05572 ^{1,2}	12 21 52.50	-13 53 10.0	8.66±0.03	7.89±0.03	7.34±0.02	6.21±0.08	5.91±0.05	5.26±0.02	4.73±0.04
Hen 4-134 ²⁶	13 14 36.37	-31 25 10.6	7.33±0.02	6.53±0.06	6.17±0.02	6.00±0.11	5.99±0.04	5.64±0.02	5.51±0.04

Table 6 continued

Table 6 (*continued*)

Name	R.A.	Decl.	<i>J</i>	<i>H</i>	K _s	<i>W1</i>	<i>W2</i>	<i>W3</i>	<i>W4</i>
	J2000	J2000	(mag)	(mag)	(mag)	(mag)	(mag)	(mag)	(mag)
Th 2-B ³²	13 28 38.86	-63 49 46.4	12.95±0.04	11.41±0.03	9.89±0.02	7.94±0.03	6.68±0.02	3.63±0.02	1.59±0.01
Hen 4-137 ²⁶	13 35 57.55	-51 12 14.7	5.10±0.28	3.96±0.30	3.79±0.33	3.48±0.30	3.43±0.16	3.43±0.01	3.27±0.02
V748 Cen ^{1,2}	14 59 36.68	-33 25 03.9	9.20±0.02	8.40±0.04	8.12±0.05	7.96±0.03	7.94±0.02	7.58±0.02	7.17±0.13
V345 Nor ^{1,2}	16 06 44.67	-52 03 01.4	10.45±0.02	9.27±0.02	8.86±0.02	8.46±0.02	8.71±0.02	7.94±0.04	7.17±0.15
Mz 3 ^{30,31}	16 17 13.40	-51 59 10.6	9.35±0.03	7.36±0.02	5.61±0.02	3.25±0.37	0.46	-0.97±0.34	-4.46
IGR J16393-4643 ^{38,41,d}	16 39 05.50	-46 42 24.0	-	-	-	-	-	-	-
2MASSJ16503229-4742288 ¹²	16 50 32.30	-47 42 28.9	13.99±0.05	11.55±0.03	9.48±0.02	7.08±0.05	5.57±0.05	3.23±0.01	1.52±0.02
M2-9 ³⁰	17 05 37.95	-10 08 32.6	11.20 ± 0.03	9.18±0.03	7.00±0.02	4.10±0.23	1.25	-0.22±0.39	-2.84
NGC 6302 ^{60,61}	17 13 44.34	-37 06 10.9	11.26±0.12	10.71±0.10	9.44±0.08	6.65±0.02	3.96±0.04	-0.72±0.05	-4.42±0.00
2MASSJ17145509-3933117 ¹²	17 14 55.10	-39 33 11.7	11.92±0.03	9.61±0.03	7.87±0.02	5.74±0.07	4.32±0.06	2.80±0.01	1.33±0.02
355.12+03.82 ¹⁰	17 18 32.20	-30 55 44.0	-	-	-	-	-	-	-
Hen 3-1383 ^{1,2}	17 20 31.76	-33 09 48.9	6.62±0.04	5.41±0.03	4.70±0.02	4.07±0.27	3.16±0.34	2.64±0.02	1.63±0.02
Th3-9 ¹⁰	17 23 59.25	-31 01 51.5	10.91±0.03	9.52±0.03	8.95±0.02	8.49±0.02	8.39±0.02	7.74±0.03	6.83±0.12
AI 2-B ¹⁰	17 27 47.06	-28 11 00.8	14.11	13.10	13.21±0.05	10.88±0.06	10.14±0.03	6.77±0.02	4.58±0.03
357.12+01.66 ¹⁰	17 32 04.80	-30 28 55.0	11.03±0.03	9.01±0.02	7.46±0.02	5.52±0.13	4.48±0.11	2.97±0.01	1.32±0.02
AI 2-G ¹⁰	17 32 22.67	-28 14 27.3	13.96	13.25±0.12	11.80	9.59±0.03	8.05±0.02	4.20±0.01	2.09±0.02
CXOGBS J173620.2-293338 ⁷⁰	17 36 20.20	-29 33 38.9	11.54±0.05	10.13±0.05	9.65±0.05	8.83±0.03	8.84±0.03	8.59±0.05	7.37±0.24
V503 Her ^{1,2}	17 36 40.46	+23 18 11.7	10.24±0.02	9.76±0.02	9.57±0.02	9.47±0.02	9.10±0.02	8.50±0.03	8.03±0.20
WSTB 19W032 ^{1,2,32}	17 39 02.91	-28 56 35.6	11.44±0.02	10.28±0.03	9.55±0.03	7.15±0.03	5.36±0.04	2.44±0.01	-0.47±0.01
WRAY 16-294 ^{1,2}	17 39 13.80	-25 38 05.1	10.15±0.03	9.16±0.03	8.59±0.02	8.66±0.02	8.63±0.02	8.32±0.03	8.08±0.30
001.97+02.41 ¹⁰	17 41 02.10	-25 59 34.0	10.90±0.03	9.48±0.02	8.96±0.03	8.62±0.02	8.64±0.02	8.41±0.04	7.49±0.18
PNG 006.1+04.1 ¹¹	17 44 10.65	-21 29 23.0	14.26	13.02±0.03	11.11±0.04	8.84±0.02	7.45±0.02	4.83±0.01	2.97±0.02
001.33+01.07 ¹⁰	17 44 37.80	-27 14 17.0	10.12±0.02	8.54±0.04	7.89±0.02	7.33±0.03	7.42±0.02	7.30±0.03	7.24±0.27
PHR 1744-3319 ¹¹	17 44 51.80	-33 19 30.0	-	-	-	-	-	-	-
001.71+01.14 ¹⁰	17 45 13.60	-26 52 42.0	10.28±0.03	8.75±0.05	7.94±0.02	7.62±0.03	7.70±0.02	7.41±0.03	6.65±0.10
ASAS J174600-2321.3 ⁷¹	17 46 00.18	-23 21 16.3	9.93±0.02	8.76±0.04	8.35±0.02	7.74±0.03	7.75±0.02	7.61±0.02	7.33±0.24
2MASSJ17460199-3303085 ¹²	17 46 01.99	-33 03 08.5	9.86±0.02	8.70±0.03	8.17±0.03	7.70±0.02	7.60±0.02	7.19±0.02	6.74±0.11
PPA 1746-3454 ¹⁰	17 46 51.41	-34 54 05.6	15.45	13.49±0.06	11.45±0.03	9.22±0.03	7.93±0.02	5.69±0.02	3.96±0.03
PHR 1751-3349 ^{10,11}	17 51 15.00	-33 49 11.0	14.01±0.03	11.70±0.03	9.99±0.02	8.09±0.02	6.92±0.02	5.00±0.01	3.36±0.02
OGLE-2011-BLG-1444 ⁷²	17 50 19.30	-33 39 07.0	-	-	-	-	-	-	-

Table 6 (*continued*)

Name	R.A.	Decl.	<i>J</i>	<i>H</i>	K _s	<i>W1</i>	<i>W2</i>	<i>W3</i>	<i>W4</i>
	J2000	J2000	(mag)	(mag)	(mag)	(mag)	(mag)	(mag)	(mag)
Al 2-O ¹¹	17 51 45.29	-32 03 03.9	12.71±0.04	11.73±0.04	10.84±0.03	8.97±0.02	8.12±0.02	5.42±0.01	2.30±0.02
PPA 1752-3542 ¹⁰	17 52 05.90	-35 42 06.0	-	-	-	-	-	-	-
001.37-01.15 ¹⁰	17 53 21.26	-28 20 47.2	13.65±0.07	11.82±0.05	10.26±0.03	8.39±0.03	7.14±0.02	4.67±0.02	2.95±0.03
K 5-37 ¹¹	17 57 15.66	-34 47 34.4	13.78	13.69±0.10	11.86±0.03	9.30±0.02	7.93±0.02	4.78±0.02	2.94±0.02
DT Ser ^{1,2,48,49,62}	18 01 52.19	-01 26 17.4	11.16±0.03	10.81±0.02	10.74±0.02	10.65±0.02	10.69±0.02	9.64±0.08	5.71±0.14
M 2-24 ¹⁰	18 02 02.89	-34 27 47.3	12.92 ± 0.03	11.14±0.03	9.31±0.02	6.87±0.07	5.32±0.06	2.80±0.01	0.89±0.01
PHR 1803-2746 ¹⁰	18 03 04.94	-27 46 44.0	12.23±0.04	11.37±0.06	11.02±0.04	10.23±0.04	9.59±0.03	5.56±0.02	2.97±0.02
ShWi 7 ¹¹	18 05 05.53	-29 20 15.9	13.68	13.01	13.02±0.11	10.28±0.03	8.80±0.02	5.66±0.01	3.48±0.02
PPA 1807-3158 ^{10,11}	18 07 19.09	-31 58 08.0	14.41	14.00±0.25	12.31±0.05	10.53±0.05	9.35±0.03	6.22±0.02	4.36±0.03
V618 Sgr ^{1,2}	18 07 56.90	-36 29 36.9	8.60±0.02	7.68±0.03	7.20±0.02	-	-	-	-
PHR 1809-2745 ¹¹	18 09 51.80	-27 45 54.0	-	-	-	-	-	-	-
AS 280 ^{1,2}	18 09 52.31	-33 19 49.9	12.18±0.04	11.89±0.05	11.60±0.04	10.87±0.02	10.57±0.02	9.74±0.06	8.85
AS 288 ^{1,2}	18 12 47.99	-28 19 59.7	11.47±0.02	9.75±0.03	8.31±0.03	6.76±0.07	5.82±0.05	4.06±0.02	2.73±0.02
Hen 2-379 ^{1,2}	18 16 17.34	-27 04 30.6	10.19±0.02	9.56±0.03	9.41±0.03	8.95±0.03	8.94±0.03	4.84±0.01	1.97±0.02
G025.5+00.2 ²⁵	18 37 05.21	-06 29 38.0	15.80	13.64±0.07	11.62±0.05	9.90±0.03	8.42±0.02	1.20±0.01	-2.31
Sh 2-71 ³⁰	19 02 00.28	+02 09 10.9	12.00±0.03	10.94±0.03	9.48±0.03	7.57±0.03	6.46±0.02	3.63±0.02	1.58±0.02
WISEJ192140.40+155354.6 ²⁹	19 21 40.40	+15 53 54.6	13.98	11.61	10.48±0.09	7.43±0.03	5.97±0.02	3.39±0.01	-0.70±0.01
V335 Vul ^{1,2}	19 23 14.14	+24 27 39.7	6.86±0.03	5.80±0.03	5.11±0.02	4.44±0.27	3.59±0.25	3.32±0.01	2.91±0.02
V850 Aql ^{1,2}	19 23 34.67	+00 37 58.4	7.43±0.02	6.17±0.02	5.40±0.02	4.66±0.24	3.92±0.09	1.98±0.01	1.09±0.01
IRAS 19558+3333 ^{1,2}	19 57 48.30	+33 41 20.0	-	-	-	-	-	-	-
PM1-322 ^{33,34}	20 14 51.60	+12 03 53.3	14.99±0.04	14.49±0.06	13.16±0.03	10.25±0.02	9.20±0.02	5.38±0.02	2.46±0.02
V627 Cas ^{1,2}	22 57 40.99	+58 49 12.5	5.46±0.02	4.55±0.27	3.71±0.33	0.16	-0.28	-1.39±0.39	-3.00

AKRAS ET AL.

Table 6 continued

Table 6 (*continued*)

Name	R.A. J2000	Decl. J2000	<i>J</i> (mag)	<i>H</i> (mag)	K _s (mag)	<i>W1</i> (mag)	<i>W2</i> (mag)	<i>W3</i> (mag)	<i>W4</i> (mag)
------	---------------	----------------	-------------------	-------------------	-------------------------	--------------------	--------------------	--------------------	--------------------

NOTE—^a All photometric magnitudes without errors correspond to upper limits.

^b The J, H, and K_s of SySt-4, 9, and 11 in M33 are taken from Cioni et al. (2008).

^c The offset between the X-ray and near-IR counterparts to IGR J 58-4726 is 1.2 arcsec (2MASS J16355369-4725398; Kouveliotou et al. 2003).

^d The first proposed near-IR counterpart to IGR J16393-4643 (2MASS J16390535-4642137; Bodaghee et al. 2006) was later on ruled out by Bodaghee et al. (2012) and its SyXB classification is doubtful.

^e For the extragalactic SySts, we give the naming pattern following by Gonçalves et al. (2008) and Kniazev et al. (2009).

References. 1. Bel2000, 2. Phillips (2007), 3. Corradi et al. (2008), 4. Gonçalves et al. (2008), 5. Corradi & Giannamico (2010), 6. Corradi et al. (2010a), 7. Corradi et al. (2010b), 8. Corradi et al. (2011a), 9. Baella et al. (2013), 10. Miszalski et al. (2013), 11. Miszalski et al. (2009), 12. Miszalski & Mikolajewska (2014), 13. Miszalski et al. (2014), 14. Gonçalves et al. (2015), 15. Rodriguez-Flores et al. (2014), 16. Mikolajewska et al. (2014), 17. Bahramian et al. (2014), 18. Ilkiewicz et al. (2015), 19. Li et al. (2015), 20. Kniazev et al. (2009), 21. Gonçalves et al. (2012), 22. Oliveira et al. (2013), 23. Hajduk et al. (2014), 24. Margon et al. (2016), 25. Phillips & Ramos-Larios (2008), 26. Van eck & Jorissen (2002), 27. Baella et al. (2016), 28. Miszalski et al. (2011), 29. Viironen et al. (2009), 30. Corradi et al. (2011b), 31. Schmeja & Kimeswenger (2001), 32. Corradi (1995), 33. Weidmann & Gamen (2011), 34. Pereira & Miranda (2005), 35. Pereira et al. (2003), 36. Mattana et al. (2006), 37. Kaplan et al. (2007), 38. Nespoli et al. (2010), 39. Masetti et al. (2011), 40. Masetti et al. (2007), 41. Bodaghee et al. (2012), 42. Munari & Zwitter (2002), 43. Downes & Keyes (1988), 44. Bragaglia et al. (1995), 45. Pereira et al. (2002), 46. Masetti et al. (2006a), 47. Mukai et al. (2016), 48. Masetti et al. 2006b, 49. Munari et al. (2013a), 50. Frew et al. (2014), 51. Luna et al. (2013), 52. Reid (2014), 53. Kamath et al. (2015), 54. Kamath et al. (2014), 55. Hajduk et al. (2015), 56. Mikolajewska et al. (2017), 57. Wheatley et al. (2003), 58. Nuñez et al. (2016), 59. Torres et al. (2012), 60. Feibelman (2001), 61. Groves et al. (2002), 62. Frew et al. (2014), 63. Ilkiewicz et al. (2018), 64. Srivastava et al. (2015), 65. Joshi et al. (2015), 66. Bozzo et al. (2018), 67. Mroz et al. (2014), 68. Bond & Kasliwal (2012), 69. Tang et al. (2012), 70. Hynes et al. (2014), 71. Hambach et al. (2015), 72. Munari et al. (2013b).

Table 7. New Classification of SySts, Stellar and Dust Temperatures Derived from Blackbody Fitting, Stellar Temperatures of Red Giants Corrected for the BB Approximation, λ Peak of SEDs, Effective Temperature from *Gaia* DR2, Distances of SySts Based on the Parallaxes Derived from *Gaia* DR2, and Information on the Detection of the OVI $\lambda 6830$ Raman-scattered Line and X-Ray Emission.

Name	Old	New	T _{BB}	T _{dust}	T _{cool}	λ_{peak}	T _{Gaia}	D _{Gaia}	O VI	O VI	X-ray ^a
	Type	Type	(K)	(K)	(K)	(μm)	(K)	(pc)	6830Å	Refs.	Emission
IC10 SySt-1	?	?	—	—	—	—	—	—	✗	25	
SMC1 (SMC SySt-1)	S	S	3056±142	—	3572	0.95±0.05	—	—	✓	1,5	
Lin9 (SMC SySt-10)	S	S	3150±180	—	3810	0.92±0.06	—	—	✓	14	
M31 SySt-1	S	?	—	—	—	—	—	—	✓	17	
M31 SySt-2	S	?	—	—	—	—	—	—	✗	17	
NGC185 SySt-1	S	?	—	—	—	—	—	—	✓	10	
M31 SySt-4	S	?	—	—	—	—	—	—	✓	17	
M31 SySt-5	S	?	—	—	—	—	—	—	✗	17	
M31 SySt-6	S	?	—	—	—	—	—	—	✓	17	
NGC205 SySt-1	S	?	—	—	—	—	—	—	✓	15	
M31 SySt-7	S	?	—	—	—	—	—	—	✗	17	
M31 SySt-8	S	?	—	—	—	—	—	—	✓	17	
M31 SySt-9	S	?	—	—	—	—	—	—	✓	17	
M31 SySt-10	S	?	—	—	—	—	—	—	✗	17	
M31 SySt-11	?	?	—	—	—	—	—	—	✗	17	
M31 SySt-12	?	?	—	—	—	—	—	—	✓	17	
M31 SySt-13	S	?	—	—	—	—	—	—	✗	17	
M31 SySt-14	S	?	—	—	—	—	—	—	✓	17	
M31 SySt-15	S	?	—	—	—	—	—	—	✗	17	
M31 SySt-17	D?	?	—	—	—	—	—	—	✗	17	
SMC2 (SMC Syst-2)	S	S	3193±128	—	3837	0.91±0.04	—	—	✓	1,5	✗
M31 SySt-18	S	?	—	—	—	—	—	—	✓	17	
M31 SySt-20	S	?	—	—	—	—	—	—	✓	17	
M31 SySt-21	S	?	—	—	—	—	—	—	✗	17	
M31 SySt-22	S	?	—	—	—	—	—	—	✗	17	
M31 SySt-23	S	?	—	—	—	—	—	—	✓?	17	

Table 7 continued

Table 7 (*continued*)

Name	Old	New	T _{BB}	T _{dust}	T _{cool}	λ _{peak}	T _{Gaia}	D _{Gaia}	O VI	O VI	X-ray ^a
	Type	Type	(K)	(K)	(K)	(μm)	(K)	(pc)	6830Å	Refs.	Emission
M31 SySt-24	S	?	—	—	—	—	—	—	✗	17	
M31 SySt-25	S	?	—	—	—	—	—	—	✗	17	
M31 SySt-26	S	?	—	—	—	—	—	—	✓	17	
M31 SySt-27	S	?	—	—	—	—	—	—	✓	17	
M31 SySt-28	D	?	—	—	—	—	—	—	✗	17	
M31 SySt-29	D	?	—	—	—	—	—	—	✓	17	
M31 SySt-30	S	?	—	—	—	—	—	—	✓	17	
EG And	S	S	3271±157	—	3886	0.89±0.01	3751	660 ₆₄₃ ⁶⁷⁸	✗	1	✓
M31 SySt-31	D	?	—	—	—	—	—	—	✗	17	
M31 SySt-32	S	?	—	—	—	—	—	—	✓	17	
M31 SySt-33	D	?	—	—	—	—	—	—	✓	17	
M31 SySt-34	S	?	—	—	—	—	—	—	✗	17	
SMC3 (SMC SySt-3)	S	S	3022±134	—	3731	0.96±0.05	—	—	✓	1,5	✓
LHA 115-S 18 (SMC SySt-16)	?	D'	3470±122	746±61	4015	0.84±0.06	—	—	✓	34	
[OVS2013] 19 (SMC SySt-8)	D	D'	3358±-	512±-/162±-	3942	0.81±-	—	—	✓	11	
SMC N60 (SMC SySt-4)	S,D	S	2419±281	—	3388	1.20±0.01	—	—	✓	1,5	
LIN 358 (SMC SySt-5)	S	S	3083±155	—	3768	0.94±0.05	—	—	✓	1,5	✓
SMC N73 (SMC SySt-6)	S	S	3158±208	—	3814	0.92±0.07	—	—	✓	1,5	
M33 SySt-1	S	?	—	—	—	—	—	—	✓	32	
M33 SySt-2	S	?	—	—	—	—	—	—	✗	32	
M33 SySt-3	S	?	—	—	—	—	—	—	✓	32	
M33 SySt-4	S	?	—	—	—	—	—	—	✗	32	
M33 SySt-5	S	?	—	—	—	—	—	—	✓	32	
M33 SySt-6	S	?	—	—	—	—	—	—	✗	32	
M33 SySt-7	S	?	—	—	—	—	—	—	✗	32	
M33 SySt-8	S	?	—	—	—	—	—	—	✓	32	
M33 SySt-9	D	?	—	—	—	—	—	—	✗	32	
M33 SySt-10	S	?	—	—	—	—	—	—	✓	32	
M33 SySt-11	S	?	—	—	—	—	—	—	✗	32	
M33 SySt-12	S	?	—	—	—	—	—	—	✓	32	

Table 7 continued

Table 7 (continued)

Name	Old	New	T _{BB}	T _{dust}	T _{cool}	λ _{peak}	T _{Gaia}	D _{Gaia}	O VI	O VI	X-ray ^a
	Type	Type	(K)	(K)	(K)	(μm)	(K)	(pc)	6830Å	Refs.	Emission
AX Per	S,D'	S	2951±112	–	3688	0.98±0.04	3927	2923 ³⁴⁹⁹ ₂₅₀₀	✗	1,2	✗
V471 Per	D'	D'	2752±308	758±71/359±58	3572	1.05±0.02	4954	2393 ²⁶¹⁸ ₂₂₀₃	✗	1	
o Ceti	S	S	2332±9	–	3342	1.24±0.01	–	–			✓
BD Cam	S	S	3308±31	–	3910	0.88±0.01	3523	–	✗	1	
StHA 32	S	S	3226±158	–	3857	0.90±0.05	4299	4516 ⁵²⁹⁷ ₃₈₉₉	✓	1	✓
LMC S154 (LMC SySt-3)	D	S+IR	1717±29	363±41	3046	1.69±0.02	–	–	✓	5,38	
LMC S147 (LMC SySt-4)	S	S	3078±140	–	3765	0.94±0.05	–	–	✓	5	
LMC N19 (LMC SySt-5)	S	S	3011±145	–	3724	0.96±0.05	–	–			✗
UV Aur	S	S+IR	2672±27	414±29	3526	1.46±0.02	3451	1078 ¹¹⁵⁸ ₁₀₀₈	✗	3	✓
V1261 Ori	S	S	3197±19	–	3839	0.91±0.01	3650	366 ³⁸⁶ ₃₄₇			
LMC1 (LMC SySt-1)	D	D	–	1226±32	–	2.36±0.03	–	–	✗	1,5	
LMC N67 (LMC SySt-2)	S	S	2836±88	–	3620	1.02±0.03	–	–	✓	1,5	✗
SMP LMC 88 (LMC SySt-24)	D'	S+IR	3106±122	178±17	3782	0.93±0.04	–	–			
Sanduleak's star (LMC SySt-8)	D	D'	3851±-	722±-/245±-	4276	0.75±-	–	–	✓	1,3,5	✗
LMC S63 (LMC SySt-6)	S	S	2906±115	–	3662	1.0±0.04	–	–	✗	1,3,5	
SMP LMC 94 (LMC SySt-7)	D	D	–	1347±34/417±19	–	2.15±0.03	–	–			
SU Lyn	S	S	2739±11	–	3565	1.06±0.01	3544	658 ⁷⁰⁴ ₆₁₈	✗	49	✓
Hen 4-18	S	S	3214±169	–	3850	0.90±0.05	3641	1341 ¹⁴²⁷ ₁₂₆₆			✓
GH Gem	S	D'	3188±-	1051±-/379±-	3833	0.91±-	4925	986 ¹⁰²¹ ₉₅₄	✗	1	
ZZ CMi	S	S	2817±51	–	3610	1.03±0.02	3298	1009 ¹¹⁴⁰ ₉₀₅	✗	1	✓
BX Mon	S	S	2721±54	–	3554	1.07±0.02	3539	3069 ³⁵¹² ₂₇₂₁	✗	1,3	
V694 Mon	S	S	2555±27	–	3462	1.13±0.01	3854	2414 ³⁶⁵⁸ ₁₇₂₄	✗	1	✓
NQ Gem	S	S	2870±15	–	3640	1.01±0.01	3951	922 ⁹⁶⁵ ₈₈₃	✗	1	✓
StHA 63	S	S	3152±138	–	3810	0.92±0.05	4333	8407 ⁹⁹⁸⁵ ₇₁₅₇	✗	31	
WRAY 15-157	S,D'	S+IR	2628±195	353±24	3502	1.11±0.07	4194	8045 ⁹⁸⁹⁶ ₆₆₇₂	✗	1,3	
RX Pup	D	D	–	1702±50/396±17	–	1.68±0.05	–	1552 ²⁰⁵⁵ ₁₂₄₄	✗	1	✓
Hen 3-160	S	S	2433±65	–	3395	1.19±0.03	–	12468 ¹⁶²⁹⁹ ₉₆₆₆	✓	3	
AS 201	D'	D'	3111±499	279±22	3786	0.93±0.02	5582	2490 ²⁶⁷¹ ₂₃₃₀	✗	1,3	
KM Vel	D	D	–	1242±206/549±29	–	2.33±0.04	–	7361 ⁹⁷⁷⁸ ₅₅₈₆	✗	1	

Table 7 continued

Table 7 (*continued*)

Name	Old	New	T _{BB}	T _{dust}	T _{cool}	λ _{peak}	T _{Gaia}	D _{Gaia}	O VI	O VI	X-ray ^a
	Type	Type	(K)	(K)	(K)	(μm)	(K)	(pc)	6830Å	Refs.	Emission
V366 Car	S/D	S+IR	1856±110	849±23	3109	1.55±0.09	—	4606 ⁶⁸²⁰ ₃₃₂₆	✓	1,39	✗
SS73 17	S/D	S+IR	3026±397	101±7	3734	0.96±0.11	3667	1223 ¹³¹⁰ ₁₁₄₇			✓
Hen 3-461	S	S	2817±18	—	3610	1.03±0.01	3291	837 ⁹³⁰ ₇₆₀			✓
SS73 29	S	S	2967±116	—	3698	0.98±0.04	—	—	✓,(✗)	1,(3)	
SY Mus	S	S	2971±90	—	3701	0.98±0.03	3533	1520 ¹⁶⁸⁰ ₁₃₈₈	✓	3	✗
BI Cru	D	D	—	1332±145/447±31	—	2.18±0.03	—	3212 ³⁵⁹² ₂₉₀₃	✗	1	✓
Hen 4-121	S	S	3168±15	—	3821	0.91±0.01	3296	847 ⁹⁴⁵ ₇₆₇			✗
LAMOSTJ12280490-014825.7	S	S	3214±176	—	3850	0.90±0.06	4511	5470 ⁶⁴⁷² ₄₆₇₈	✗	18	
4 Dra	S	S	3061±104	—	3755	0.95±0.07	3727	—			✓
RT Cru	S	S	2695±91	—	3540	1.08±0.03	3306	1581 ³⁵⁵² ₁₄₄₂	✗	33	✓
TX CVn	S	S+IR	2771±63	406±18	3583	1.05±0.03	4764	2476 ²⁷⁸³ ₂₂₂₆	✗	1	✗
Hen 2-87	S	S+IR	1758±114	354±10	3065	1.65±0.07	—	4024 ⁵⁶³¹ ₃₀₆₃	✓	3,39	
Hen 3-828	S	S	2937±108	—	3680	0.99±0.04	—	—	✓,(✗)	3,(19)	
SS73 38	D	D	—	950±39	—	3.05±0.04	—	2736 ³⁵⁵² ₂₂₁₄	✓,(✗)	1,(3)	
Hen 3-863	S	S	3106±114	—	3782	0.93±0.04	3958	3218 ⁴³⁴⁷ ₂₅₀₆	✗	1,3	✗
Sa 3-22	S	S	2841±109	—	3624	1.02±0.04	3666	6398 ⁸⁶⁷⁸ ₄₈₆₁	✗	39	
CD-36 8436	S	S	3051±100	—	3749	0.95±0.03	3650	1795 ²¹¹⁷ ₁₅₅₅			
V840 Cen	S	S	2862±65	—	3636	1.01±0.02	3941	2275 ²³⁹⁰ ₂₁₇₀	✗	1	
Hen 3-905	S	S	2797±92	—	3598	1.04±0.03	4019	6028 ⁸⁰⁰⁹ ₄₇₀₄	✓	1,3,19	
RW Hya	S	S	3109±112	—	3784	0.93±0.04	3835	1217 ¹³¹³ ₁₁₃₄	✗	1,3	✗
Hen 3-916	S	S	2702±91	—	3544	1.07±0.03	4578	3828 ⁴⁷⁷⁴ ₃₁₈₀	✓	3	
V704 Cen	D	D	—	1347±88/484±19	—	2.15±0.06	—	6397 ⁹⁰⁴⁵ ₄₅₅₅	✗	1,3,33,39	
2MASSJ14031865-5809349	S	S	2659±94	—	3519	1.09±0.04	4602	8166 ¹⁰⁷⁶⁴ ₆₃₀₃	✗	13	
V852 Cen	D	D	—	997±31/423±11	—	2.91±0.04	—	4061 ⁵¹⁷³ ₃₃₁₆	✗	1,39	✓
V835 Cen	D	D	—	708±24	—	4.09±0.03	—	—	✓	1,3,39	✗
V417 Cen	D'	D	—	1347±89/497±16	—	2.15±0.07	—	1228 ¹³⁰⁵ ₁₁₆₀	✗	1,33	
BD-21 3873	S	S	3226±97	—	3857	0.90±0.03	4182	2793 ³¹⁹⁰ ₂₄₈₀	✗	1,3	✗
AE Cir	S	S	2778±131	—	3587	1.04±0.05	4340	9867 ¹²⁵⁴⁰ ₇₉₄₇	✓	41	
Hen 2-127	D	D	—	1234±81	—	2.35±0.06	—	5479 ⁸²⁵⁶ ₃₆₈₅	✓	1,3,39	

Table 7 continued

Table 7 (continued)

Name	Old	New	T _{BB}	T _{dust}	T _{cool}	λ _{peak}	T _{Gaia}	D _{Gaia}	O VI	O VI	X-ray ^a
	Type	Type	(K)	(K)	(K)	(μm)	(K)	(pc)	6830Å	Refs.	Emission
2MASSJ15431767-5857221	S	S	2806±152	–	3603	1.03±0.06	4525	7055 ⁹⁵⁰⁵ ₅₄₄₅	✓	13	
Hen 3-1092	S	S	2811±98	–	3606	1.03±0.03	3812	4773 ⁶¹⁵⁸ ₃₈₅₇	✓	1,3,39	
Hen 3-1103	S	S	2907±94	–	3662	1.00±0.03	–	10874 ¹⁴²⁹⁶ ₈₄₃₅	✓	3,19	
HD 330036	D'	D'	2507±142	878±-/358±-	3435	1.16±0.07	5101	–	✗	1,3,39	
Hen 2-139	D	D	–	1170±68	–	2.48±0.06	–	2423 ³⁸⁵⁶ ₁₇₂₀	✗	1,3	
T CrB	S	S	3041±89	–	3743	0.95±0.03	3985	806 ⁸⁴⁰ ₇₇₆	✗	1,2	✓
2MASSJ16003761-4835228	S	S	2259±48	–	3304	1.28±0.02	3783	5028 ⁷⁰⁵⁵ ₃₇₅₁	✓	13	
AG Dra	S	S	3070±118	–	3760	0.94±0.04	4075	3888 ⁴³¹⁵ ₃₅₃₁	✓	1,2	✓
WRAY 16-202	S	S	2535±105	–	3451	1.14±0.04	3285	4145 ⁶²⁶⁸ ₂₈₈₆	–		
V347 Nor	D	D	–	1287±51	–	2.25±0.04	–	6115 ⁹⁵³⁶ ₃₉₉₁	✗	1,3,39	✓
UKS Ce-1	S	S+IR	2903±129	117±-	3660	1.00±0.04	3799	9178 ¹²²²⁸ ₇₀₈₃	✓,(✗)	1,(3)	✗
IRG J16194-2810	S	S	3100±152	–	3779	0.93±0.05	3511	2293 ³⁰⁴¹ ₁₈₃₂	–		✓
QS Nor	S	S	2570±125	–	3470	1.13±0.05	3659	7163 ⁹⁷⁴¹ ₅₄₄₂	✓?,(✗)	4,(39)	
WRAY 15-1470	S	S	2763±73	–	3578	1.05±0.03	–	8617 ¹¹⁸⁹⁶ ₆₄₂₅	✗	3,20	✗
Hen 2-171	D	D	–	1347±31/703±46	–	2.15±0.03	–	–	✓,(✗)	1,3,39,(20)	
Hen 3-1213	S	S	2872±93	–	3462	1.01±0.03	3763	3972 ⁵²⁴⁸ ₃₁₆₁	✗	3,19	✗
IGR J16358-4726	S?	?	–	–	–	–	–	–	–	–	✓
Hen 2-173	S	S	2767±104	–	3581	1.05±0.04	4070	3547 ⁵⁰⁴⁵ ₂₆₇₉	✓,(✗)	3,20,(39)	
Hen 2-176	S,D	S	1849±91	–	3106	1.57±0.05	3726	5184 ⁷⁷³⁶ ₃₅₃₆	✓	1,3,39	
2MASSJ16422739-4133105	D	D	–	1090±45	–	2.66±0.04	–	7001 ⁹⁷⁹¹ ₅₀₈₅	✓	13	
KX TrA	S	S	2685±52	–	3534	1.08±0.02	4101	4582 ⁶⁰²⁸ ₃₆₄₉	✓	3,19,39	✗
AS 210	D	D	–	1169±30	–	2.48±0.03	–	7946 ¹¹⁵¹¹ ₅₇₂₀	✓	1,3,20	✗
HK Sco	S	S	3053±104	–	3750	0.95±0.03	3455	3713 ⁴⁸²⁰ ₃₀₀₅	✓	3,20	
CL Sco	S	S	2808±77	–	3604	1.03±0.03	4022	8715 ¹²¹⁹⁷ ₆₅₀₃	✗	1,2,3,20	
SS73 71	S	S	2921±89	–	3670	0.99±0.04	3640	–	✗	22	
MaC 1-3	D	S	2501±58	–	3432	1.16±0.02	3380	–	✓	39	
V1535 Sco	S	S	2523±73	–	3443	1.15±0.03	3894	4558 ⁶²⁵⁷ ₃₅₂₃	–		
2MASSJ17050868-4849122	S	S	2834±119	–	3619	1.02±0.04	3670	8340 ¹¹⁸²⁹ ₅₉₂₇	✓	13	
V934 Her	S	S	3415±17	–	3979	0.85±0.01	3655	536 ⁵⁴⁶ ₅₂₆	–		✓

Table 7 (*continued*)

Name	Old	New	T _{BB}	T _{dust}	T _{cool}	λ _{peak}	T _{Gaia}	D _{Gaia}	O VI	O VI	X-ray ^a
	Type	Type	(K)	(K)	(K)	(μm)	(K)	(pc)	6830Å	Refs.	Emission
V455 Sco	S	S+IR	2603±172	103±-	3488	1.11±0.07	-	2383 ³⁴⁶² ₁₈₀₀	✓	3,20,39	
Hen 3-1341	S	S	2823±178	-	3613	1.03±0.06	4449	4422 ⁶¹⁷⁵ ₃₃₉₁	✓	1,3	✓
Hen 3-1342	S	S	2975±109	-	3703	0.97±0.04	4024	7484 ¹⁰⁵⁷⁹ ₅₅₈₄	✓	1,3,20	
AS 221	S	D	-	1347±66/363±23	-	2.15±0.05	-	7346 ¹¹¹¹³ ₄₉₆₅	✓,(✗)	3,39,(20)	
PN H 2-5	S,D	S	2821±115	-	3612	1.03±0.04	3296	2816 ⁵⁴²⁶ ₁₇₉₉	✓,(✗)	3,39,(20)	
V1534 Sco	S	S	2595±109	-	3484	1.12±0.05	3709	7339 ¹¹⁴³² ₄₇₂₉			✓
PN Sa 3-43	S	S	2697±78	-	3541	1.07±0.03	4065	5517 ⁸⁸⁶² ₃₇₃₉			
SWIFTJ171951.7-300206	?	S	3068±70	-	3759	0.94±0.02	3671	187 ¹⁸⁹ ₁₈₅			✓
Draco C-1 (Draco SySt-1)	S	S	3240±125	-	3866	0.89±0.04	-	-	✗	1	✓
PN Th 3-7	S	S	2592±79	-	3482	1.12±0.03	3316	-	✓,(✗)	3,39,(20)	
356.04+03.20	S	S	2547±95	-	3457	1.14±0.04	3295	-	✓	12	
PN Th 3-17	S	S	2683±103	-	3533	1.08±0.04	3349	5546 ⁹⁶⁵⁹ ₃₂₈₈	✗	3,39	
358.46+03.54	S	S	2872±117	-	3642	1.01±0.04	3698	8606 ¹³⁰²⁷ ₅₇₅₃	✓	12	
PN Th 3-18	S	S	2693±80	-	3539	1.08±0.03	3683	2017 ²⁴⁶⁸ ₁₇₀₂	✓	3,20,39	
Hen 3-1410	S	S	2166±31	-	3258	1.34±0.02	4336	7245 ¹⁰⁹⁶⁵ ₅₀₄₇	✓,(✗)	1,3,(20)	
357.32+01.97	S	S+IR	2523±151	101±-	3444	1.15±0.08	3812	11185 ¹⁶⁰⁴⁴ ₇₇₃₀	✗	12	
V2116 Oph	S	S	2137±39	-	3244	1.36±0.02	3407	7611 ¹¹⁸⁸⁷ ₄₈₅₄	✗	1	✓
PN Th 3-29	S	S	2469±74	-	3415	1.17±0.03	3709	4565 ⁸³⁰³ ₂₇₇₀	✓	3,4,39	
IGR J17329-273	S	S	1923±88	-	3140	1.51±0.05	-	-			✓
PN Th 3-30	S	S	2459±63	-	3410	1.18±0.03	3772	6355 ¹⁰⁴⁵⁴ ₄₀₀₂	✓	1,3,20,39	
2MASSJ17334728-2719266	S	S+IR	1881±95	399±31	3121	1.54±0.08	-	-	✗	13	
PN Th 3-31	S	S	2335±50	-	3344	1.24±0.02	3354	-	✓,(✗)	3,(39)	
M 1-21	S	S	2668±71	-	3524	1.09±0.03	-	6867 ¹⁰⁷⁴² ₄₄₉₉	✓	1,3,39	
357.98+01.57	S	S	2362±80	-	3358	1.23±0.03	3294	-	✓ [†]	12	
Hen 2-251	D	D	-	999±51/389±31	-	2.90±0.08	-	7327 ¹¹⁴²² ₄₈₃₆	✓	1,33,39	
NSV 22840	S	S	2393±67	-	3375	1.21±0.03	3701	5798 ⁹⁷⁸⁷ ₃₆₁₆	✗	12	
PN Pt 1	S	S	2643±87	-	3510	1.10±0.03	4704	6107 ⁹¹²¹ ₄₃₆₃	✓	1,3	
2MASSJ17391715-3546593	S	S	2044±111	-	3198	1.42±0.06	-	-	✓	13	
K 6-6	S	S	1782±77	-	3075	1.63±0.04	-	4077 ⁷⁴⁸⁶ ₂₅₄₂	✓	39	

Table 7 continued

Table 7 (continued)

Name	Old Type	New Type	T _{BB} (K)	T _{dust} (K)	T _{cool} (K)	λ _{peak} (μm)	T _{Gaia} (K)	D _{Gaia} (pc)	O VI 6830Å	O VI Refs.	X-ray ^a Emission
RT Ser	S	S	2650±68	–	3514	1.09±0.03	3348	3683 ⁶¹⁷⁷ ₂₆₇₁	✓	1,3	
359.76+01.15	S	S+IR	1756±36	328±24	3064	1.65±0.02	3363	7399 ¹¹⁷¹⁷ ₄₇₂₈	✗	12	
AE Ara	S	S	2825±92	–	3614	1.03±0.03	4275	1285 ¹⁴⁹⁸ ₁₁₂₄	✗	3,19,20,39	
SS73 96	S	S	2454±78	–	3410	1.18±0.03	3709	2138 ³⁶²⁵ ₁₄₈₉	✗	3,20	
2MASSJ17422035-2401162	S	S	2525±94	–	3445	1.15±0.04	–	–	✓	13	
UU Ser	S	S	2899±142	–	3658	1.00±0.05	3666	6596 ⁸⁷⁵⁶ ₅₂₀₄	✓, (✗)	39,(3)	
V2110 Oph	S/D	S	1956±101	–	3156	1.48±0.05	3289	–	✗	1,3	
V916 Sco	S	S	2797±157	–	3598	1.04±0.06	–	–			
K 5-33	D	D'	1137±148	598±-/194±-	–	2.55±0.33	–	–	✓	12	
XMMUJ174445.5-295044	?	?	–	–	–	–	–	–			✓
354.98-02.87	D	D	–	1047±-/644±-/349±-	–	2.77±0.45	–	–	✓	12	
355.39-02.63	S	S	2675±84	–	3529	1.08±0.03	3698	–	✓	12	
AS 241	S	S+IR	2303±124	388±25	3328	1.26±0.07	–	1838 ²¹⁷⁴ ₁₅₉₁	✓ [†] ,(✗)	3,(39)	
Hen 2-275	S	S	2869 ±131	–	3640	1.01±0.05	4408	7412 ¹¹²⁵⁴ ₄₉₅₈	✓	4,39	
2MASSJ17463311-2419558	S	S+IR	2206±151	301±17	3278	1.31±0.08	3696	6420 ⁹⁸⁵⁸ ₄₃₅₄	✗	13	
355.28-03.15	S	S	2568±81	–	3469	1.13±0.03	3293	–	✗	12	
V917 Sco	S	S	2740±100	–	3565	1.06±0.04	3743	–	✓	3	
PN H 1-36	D	D	–	1043±-/617±-/278±-	–	2.78±-	–	–	✓,(✗)	1,(3,20)	
JaSt2-6	D	D	–	840±19/218±16	–	3.45±0.03	–	–			
RS Oph	S	S	2552±94	–	3460	1.14±0.04	4030	2137 ²⁴¹⁶ ₁₉₁₄	✗,(✓)	1,2,(3)	
WRAY 16-312	D	D	–	842±60	–	3.44±0.07	–	–	✓	1,3	
V4141 Sgr	D,S	S	2393±146	–	3375	1.21±0.06	3655	3174 ⁵⁶⁹¹ ₂₀₃₆	✗	39	
ALS 2	S	S	2618±121	–	3497	1.11±0.07	3728	6981 ⁹⁴⁰⁹ ₅₄₁₃	✓	4,39	
AS 245	S,D	S	1968±59	–	3162	1.47±0.03	–	6620 ⁹³⁹⁴ ₄₈₉₃	✓	3,39	
Hen 2-294	S	S	2241±73	–	3296	1.29±0.03	4328	6463 ⁹⁸⁰⁵ ₄₅₅₈	✓	3,39	
JaSt79	D	D	–	1259±87/498±29	–	2.34±0.08	–	–	✗	12	
PN Bl 3-14	S	S	2524±91	–	3445	1.15±0.04	3709	–	✓	3	
000.49-01.45	S	S	2525±101	–	3445	1.15±0.04	3336	–	✗	12	
PN Bl 3-6	S	S	2631±97	–	3504	1.10±0.04	3367	7359 ¹¹⁵¹² ₄₈₄₉	✓	4,39	

Table 7 continued

Table 7 (*continued*)

Name	Old	New	T _{BB}	T _{dust}	T _{cool}	λ _{peak}	T _{Gaia}	D _{Gaia}	O VI	O VI	X-ray ^a
	Type	Type	(K)	(K)	(K)	(μm)	(K)	(pc)	6830Å	Refs.	Emission
PN Bl L	S	S	2393±68	–	3375	1.21±0.03	–	5813 ¹⁰⁰⁴⁵ ₃₄₃₈	✓	3	
V745 Sco	S	S+IR	2039±29	398±22	3196	1.42±0.02	3338	–	✗	1	
MaC 1-9	S	S	2577±73	–	3474	1.12±0.03	4297	3969 ⁶⁶⁵⁷ ₂₆₅₅	✗	39	
AS 255	S,D	S	2955±95	–	3691	0.98±0.03	4004	6963 ¹⁰⁶¹¹ ₄₈₂₅	✓,(✗)	1,19,20,(3)	
V2416 Sgr	S	S	2576± 84	–	3473	1.13±0.03	3319	2738 ⁵¹⁷¹ ₁₇₀₁	✓	3,20,39	
PHR 1757-2718	S	S	2211±97	–	3281	1.31±0.06	3488	–	✓	12	
H 1-45	D	D	–	997±48	–	2.91±0.05	–	–	✗	12	
H 2-34	S	S	2607±101	–	3490	1.11±0.04	3709	–	✓	4	
002.86-01.88	S	S	2663±113	–	3522	1.09±0.04	–	–	✓	12	
003.46-01.92	S	S	2434±84	–	3396	1.19±0.04	3719	4310 ⁶⁹²² ₂₉₈₀	✗	12	
SS73 117	S	S	1853±36	–	3108	1.56±0.02	–	–	✗,(✓)	3,(20)	
AS 269	D'	D'	2639±139	617±70	3508	1.11±0.06	–	–	✗	39	
ShWi 5	D'	D'	3653±-	801±-/210±-	4138	0.79±-	–	–	✗	12	
001.70-03.67	S	S	3026±130	–	3734	0.96±0.04	–	2106 ⁶⁶⁰³ ₈₉₀	✗	12	
Ap 1-8	S	S	2767±137	–	3581	1.05±0.05	–	–	✓	3,20,39	✗
SS73 122	S/D?	S+IR	1844±48	444±13	3104	1.57±0.03	–	10222 ¹⁴³¹⁵ ₇₄₂₃	✓,(✗)	1,20,36,39(3)	
AS 270	S	S	2714±99	–	3550	1.07±0.04	4065	3229 ⁴⁵¹⁴ ₂₇₄₇	✗	3,19,20	
H 2-38	S/D	S+IR	2639±55	474±28	3508	1.1±0.03	–	10515 ¹⁵⁰⁸⁸ ₇₃₀₆	✓	1,3,20,39	✗
SS73 129	S	S	2975±145	–	3703	0.97±0.05	3851	5918 ⁸⁴⁶² ₄₄₃₂	✓	1,3,20,39	
Hen 3-1591	S/D'?	S+IR	2225±133	504±19	3288	1.31±0.08	4454	1171 ¹²⁷² ₁₀₈₄	✗	1,3,20	✓
V615 Sgr	S	S	2938±125	–	3681	0.99±0.04	3710	7117 ¹⁰⁴¹⁸ ₅₁₅₂	✗	3,20,39	
Ve 2-57	S	S	2711±125	–	3549	1.07±0.05	3290	6064 ⁹²⁸⁴ ₄₁₀₀	✓ ?	3	
AS 276	S,D	S	3005±130	–	3721	0.96±0.04	3657	6503 ⁹³¹⁹ ₄₈₃₂	✓	3,20	
Ap 1-9	S	S	2765±68	–	3580	1.05±0.03	–	8866 ¹²⁶⁷⁷ ₆₄₀₃	✓,(✗)	3,(20,39)	✗
AS 281	S	S	2889±114	–	3652	1.00±0.04	4040	8744 ¹²⁷⁹⁴ ₆₀₈₄	✓	3,20,36,39	✗
V2506 Sgr	S	S	2799±97	–	3599	1.04±0.04	4220	4143 ⁶⁶⁹⁹ ₂₈₇₅	✓	3,20,39	
V5590 Sgr	S	S+IR	1757±99	644±53	3064	1.65±0.05	–	8892 ¹²⁵¹⁶ ₆₅₂₆			
SS73 141	S	S	2873±118	–	3642	1.01±0.04	3774	9168 ¹³³⁹⁷ ₆₄₄₇	✗	3,20	
AS 289	S	S	2524±84	–	3445	1.15±0.03	3295	1664 ²¹²⁵ ₁₃₆₄	✗,(✓)	1,2,3,(19,20)	✗

Table 7 continued

Table 7 (continued)

Name	Old Type	New Type	T _{BB} (K)	T _{dust} (K)	T _{cool} (K)	λ _{peak} (μm)	T _{Gaia} (K)	D _{Gaia} (pc)	O VI 6830Å	O VI Refs.	X-ray ^a Emission
2MASSJ18131474-1007218	S	S	2696±116	–	3540	1.07±0.04	3521	6137 ₄₃₀₅ ⁸⁸⁵⁴	✓	13	
Y CrA	S	S	2876±81	–	3644	1.01±0.03	4577	2682 ₂₀₉₇ ³⁶⁸⁵	✓	3,19,20	✗
YY Her	S	S	3070±120	–	3760	0.94±0.04	3581	5507 ₄₅₁₆ ⁶⁹¹⁰	✗	1,2,3	✗
V2756 Sgr	S	S	2850±100	–	3629	1.02±0.04	–	8881 ₆₂₉₇ ¹²⁹¹²	✓,(✗)	3,20,(39)	
FG Ser	S	S	2764±87	–	3579	1.05±0.03	3319	1214 ₁₀₄₀ ¹⁴⁵⁶	✗	1,3	✗
HD 319167	S	S	2829±95	–	3617	1.02±0.03	–	10433 ₇₄₀₈ ¹⁴⁹⁰⁴	✗	3,20,39	
Hen 2-374	S	S	2693±92	–	3539	1.08±0.03	3335	4003 ₂₆₀₂ ⁶⁶¹⁵	✓, (✗)	3,(20,39)	
Hen 2-376	S	S	2913±132	–	3666	0.99±0.05	3431	6727 ₄₇₆₁ ¹⁰⁰⁴⁷	✗	4,33,39	
V4074 Sgr	S	S+IR	2759±211	139±15	3576	1.05±0.08	4371	1930 ₁₇₇₉ ²¹⁰⁸	✓	3	
V2905 Sgr	S	S	2540±86	–	3454	1.14±0.03	4165	5263 ₄₂₂₃ ⁶⁸⁷⁵	✗	39	
Hen 2-375	D	D'	2909±-	755±-/339±-	3663	1.01±-	–	5947 ₄₀₉₆ ⁸⁹⁴⁵	✓	12	
StHA 149	S	S	2961±129	–	3695	0.98±0.04	3775	3727 ₃₂₇₀ ⁴³⁴⁰	✓	6	
Hen 3-1674	S	S	2832±129	–	3618	1.02±0.05	3709	–	✓	1,3	
AR Pav	S	S	2982±119	–	3710	0.97±0.04	4342	5544 ₄₆₉₇ ⁶⁷⁰⁸	✓	3	✗
V3929 Sgr	D	D	–	1058±52/442±32	–	2.74±0.08	–	–	✗	1,3,20	
V3804 Sgr	S	S+IR	2517±71	301±17	3441	1.15±0.03	5000	5823 ₃₈₈₆ ⁹³⁵⁷	✗	3,20	
V443 Her	S	S	2967±103	–	3698	0.98±0.04	3749	1999 ₁₈₄₄ ²¹⁸²	✗	1,3	✗
V3811 Sgr	S	S	2201±52	–	3276	1.32±0.03	–	8225 ₅₈₁₈ ¹¹⁷⁵⁶	✓,(✗)	1,3,(20)	
V4018 Sgr	S	S	3056±115	–	3752	0.95±0.04	–	edw	✗	1,3,19	
2MASSJ18272892-1555547	S	S	2406±78	–	3381	1.20±0.03	3384	–	✓	13	
SS383	S	S	2953±87	–	3690	0.98±0.03	–	–	✗	28	
IPHASJ182906.08-003457.2	S	S	2611±109	–	3493	1.11±0.04	3346	6626 ₄₇₇₈ ⁹²¹⁸	✓	9	
2MASSJ18300636-1940315	S	S	2614±99	–	3494	1.11±0.04	–	8182 ₅₇₈₂ ¹¹⁷²¹	✓	13	
V3890 Sgr	S	S	2530±63	–	3448	1.15±0.03	–	4357 ₃₀₃₆ ⁶⁸⁹⁶			
IPHASJ183501.83+014656.0	S	S	2469±81	–	3415	1.17±0.03	3335	3361 ₂₃₈₆ ⁵⁰⁸⁰	✗	9	
Sct X-1	S,D	D	–	925±31	–	3.13±0.03	–	–			✓
V2601 Sgr	S	S	2813±85	–	3607	1.03±0.03	3904	5011 ₃₅₀₁ ⁷⁷⁹²	✗	3,20,39	
K 3-9	D	D	–	1040±47	–	2.79±0.05	–	3549 ₂₄₆₉ ⁵⁶²⁸	✓	1,4,39	
IPHASJ184144.00-012839.5	S	S	2421±106	–	3389	1.20±0.04	3294	5703 ₃₉₈₄ ⁸¹⁸⁹	✓	16	

Table 7 continued

Table 7 (*continued*)

Name	Old	New	T _{BB}	T _{dust}	T _{cool}	λ _{peak}	T _{Gaia}	D _{Gaia}	O VI	O VI	X-ray ^a
	Type	Type	(K)	(K)	(K)	(μm)	(K)	(pc)	6830Å	Refs.	Emission
AS 316	S	S	2792±94	—	3595	1.04±0.03	3482	6568 ⁹³⁴⁵ ₄₈₈₉	✓	3,19,20,39	
StHA 154	?	S	2767±91	—	3581	1.05±0.03	3293	2825 ³⁸⁶⁰ ₂₂₀₁	✓	1	
DQ Ser	S	S	2688±98	—	3536	1.08±0.04	3586	5675 ⁷⁸⁹³ ₄₂₀₄			
IPHASJ184446.08+060703.5	S	S	2479±74	—	3420	1.17±0.03	4283	7816 ¹⁰⁵⁸³ ₅₈₄₇	✓	9	
V4368 Sgr	?	S+IR	3299±287	338±22	3904	0.88±0.09	—	5044 ⁷¹²⁰ ₃₈₂₁	✗	1	
IPHASJ184733.03+032554.3	S	S	2225±104	—	3288	1.30±0.05	—	—	✗	9	
MWC 960	S	S	2969±120	—	3699	0.98±0.04	3880	4433 ⁶⁰⁵⁷ ₄₃₅₂	✓	1,3	✗
AS 323	S	S	2849±119	—	3628	1.02±0.04	3836	4614 ⁶⁵¹² ₃₄₈₅	✓	4,39	
AS 327	S	S	2943±112	—	3684	0.98±0.04	—	—	✓	1,3,19,20,39	✗
FN Sgr	S	S	3394±218	—	3965	0.85±0.06	—	5422 ⁷⁴¹⁰ ₄₂₀₁	✓	1,3,20	
IPHASJ185323.58+084955.0	S	S	2502±74	—	3433	1.16±0.03	3349	2766 ⁴⁴⁶⁴ ₁₉₁₂	✓	9	
Pe 2-16	S	S	2320±62	—	3336	1.25±0.03	3749	5210 ⁷⁹⁴⁰ ₃₅₈₁	✓,(✗)	39,(1,3)	
IPHASJ185704.44+002631.7	S	S+IR	2127±174	412±18	3239	1.36±0.11	3349	—	✗	26	
CM Aql	S	S	2686±88	—	3535	1.08±0.03	4058	5870 ⁸⁷⁷⁰ ₄₀₈₀	✗	1,3	
V919 Sgr	S	S	2832±80	—	3618	1.02±0.03	3523	6072 ⁹¹⁵⁶ ₄₂₃₇	✗	1,3	
V1413 Aql	S	S	2601±82	—	3487	1.11±0.03	4188	5557 ⁶⁹⁸⁸ ₄₅₇₃	✗	1,3,39	
NSV 11749	S	?	—	—	—	—	—	—	✓	40	
IPHASJ190742.36+000251.1	S	S	2721±94	—	3554	1.07±0.04	3650	9133 ¹²²⁵⁰ ₆₉₀₀	✓	16	
IPHASJ190832.31+051226.5	S,D?	S	2350±85	—	3352	1.23±0.04	3295	—	✗	9	
IPHASJ190924.64-010910.2	S	S	2588±102	—	3480	1.12±0.04	3920	5332 ⁸²⁵⁷ ₃₅₂₅	✗	26	
PN K 3-22	D	D	—	1154±92/484±25	—	2.51±0.20	—	—	✓	8	
NSV 11776	S	S	2419±84	—	3388	1.20±0.04	—	—	✓	33	
Ap 3-1	S	S	2630±82	—	3503	1.10±0.03	3307	6282 ⁹⁰⁴⁴ ₄₃₇₅	✗	1	
MaC 1-17	S	S	2772±110	—	3584	1.05±0.04	3805	7788 ¹¹⁰⁷⁴ ₅₆₁₅	✗	39	
V352 Aql	S	S	2813±134	—	3607	1.03±0.05	4456	7231 ¹⁰⁰⁹⁴ ₅₂₆₁	✓	39	
ALS 1	S	S	2718±192	—	3553	1.07±0.08	4145	7862 ¹¹⁰²⁴ ₅₇₄₂	✓?,(✗)	39,(4)	
BF Cyg	S	S	2685±61	—	3534	1.08±0.02	4762	4236 ⁴⁷⁶⁹ ₃₈₀₇	✗	1	
CH Cyg	S	S	1754±105	—	3063	1.65±0.07	3709	—	✗	1, 2	✓
StHA 164	S	S	3017±104	—	3728	0.96±0.04	3305	4851 ⁶⁸²¹ ₃₆₃₈	✓	6	

Table 7 continued

Table 7 (continued)

Name	Old Type	New Type	T _{BB} (K)	T _{dust} (K)	T _{cool} (K)	λ _{peak} (μm)	T _{Gaia} (K)	D _{Gaia} (pc)	O VI 6830Å	O VI Refs.	X-ray ^a Emission
IPHASJ193436.06+163128.9	S	S	2553±106	–	3461	1.14±0.04	3335	4729 ₃₃₀₆ ⁷⁰²²	✗	9	
IPHASJ193501.31+135427.5	S	S	2713±109	–	3550	1.07±0.04	3947	7349 ₅₅₉₃ ⁹⁹⁰⁵	✗	9	
IPHASJ193830.62+235438.4	D	D	–	1120±13	–	2.59±0.01	–	–	✓	16	
IPHASJ193943.36+262933.1	D	D	–	719±29	–	4.03±0.04	–	–	✗	1,16	
HM Sge	D	D	–	1218±254/407±15	–	2.38±0.16	–	–	✓,(✗)	1,2,(3)	✓
Hen 3-1761	S	S	3010±95	–	3724	0.96±0.03	3675	3712 ₃₀₃₅ ⁴⁷⁰⁵	✗	3	
NGC6822 SySt-1	S	S	2285±92	–	3318	1.27±0.04	–	–	✓	7	
QW Sge	S	S	2944±118	–	3684	0.98±0.04	4011	3972 ₃₁₈₀ ⁵¹⁹⁴	✓	1,3	
IPHASJ194607.52+223112.2	D	D	–	892±75	–	3.25±0.08	–	5174 ₃₆₂₅ ⁷⁶⁶⁹	✓	9	
StHA 169	S	S	3056±183	–	3752	0.95±0.06	3995	8759 ₇₀₉₁ ¹¹⁰⁹⁹	✗,(✓)	6,(18)	
CI Cyg	S	S	2882±102	–	3648	1.01±0.04	4142	1716 ₁₅₇₅ ¹⁸⁸⁴	✓,(✗)	2,(1)	✗
EF Aql	D	S+IR	2017±58	345±15	3185	1.44±0.04	3683	1765 ₁₃₀₁ ²⁶⁶⁹			
OY Cyg	?	S	2324±96	–	3339	1.25±0.04	3285	1932 ₁₆₅₂ ²³²²	✗	1	
4U 1954+31	S	S	3107±115	–	3783	0.93±0.04	3300	3295 ₂₆₆₄ ⁴²⁸⁰	✗	24	✓
V1016 Cyg	D	D	–	1338±127/404±15	–	2.17±0.10	–	–	✓	1,2	✓
RR Tel	D	D	–	1258±107/414±16	–	2.30±0.10	–	–	✓	1,3	✓
PU Vul	S	S	2611±64	–	3493	1.11±0.03	–	1851 ₁₅₇₂ ²²⁴⁴	✗	1	✓
StHA 176	?	S	3197±167	–	3839	0.91±0.05	4903	6392 ₅₀₈₀ ⁸³⁰²	✗	1	
IPHASJ202510.58+435233.0	S	S	2056±56	–	3204	1.41±0.03	3342	5471 ₄₀₄₈ ⁷⁵⁸⁶	✗	26	
LAMOSTJ202629.80+423652.0	D	S	3466±236	–	4012	0.84±0.07	4473	1266 ₁₂₃₈ ¹²⁹⁵	✓	18	
LT Del	S	S	3144±146	–	3806	0.92±0.05	4340	5801 ₄₆₁₂ ⁷⁵³³	✗	1,3	✗
StHA 180	S	S	3158±153	–	3815	0.92±0.05	3793	6050 ₄₉₂₄ ⁷⁶²⁰	✗	6	
Hen 2-468	S	S	2843±111	–	3625	1.02±0.04	4134	6248 ₅₁₆₂ ⁷⁷⁴⁹	✓	1	
ER Del	S	S	3168±142	–	3821	0.91±0.05	3539	1936 ₁₇₅₈ ²¹⁵²	✗	1	✓
V1329 Cyg	S	S	2796±115	–	3597	1.04±0.04	–	3375 ₂₈₃₂ ⁴¹⁴¹	✓	1,2	✓
IPHASJ205836.43+503307.2	D	D	–	757±20	–	3.83±0.03	–	4531 ₃₃₆₉ ⁶⁴²⁵	✗	27	
CD-43 14304	S	S	3012±144	–	3725	0.96±0.05	4265	6532 ₅₃₇₉ ⁸¹²⁷	✓	1,3,19	✓
V407 Cyg	D	D	–	1362±78	–	2.13±0.06	–	3548 ₂₄₅₇ ⁵³⁰⁴	✗	1	
StHA 190	S,D'	S+IR	3087±131	306±16	3771	0.94±0.05	4997	1216 ₁₁₅₇ ¹²⁸⁰	✗	1,6,18	

Table 7 continued

Table 7 (*continued*)

Name	Old Type	New Type	T _{BB} (K)	T _{dust} (K)	T _{cool} (K)	λ _{peak} (μm)	T _{Gaia} (K)	D _{Gaia} (pc)	O VI 6830Å	O VI Refs.	X-ray ^a Emission
AG Peg	S	S	3114±137	–	3787	0.93±0.04	–	2295 ²⁸⁰¹ ₁₉₃₂	✗,(✓)	1,2,3,(37)	✓
IPHASJ224834.32+582908.4	D	D	–	868±64	–	3.34±0.07	–	6808 ⁹¹¹¹ ₅₁₅₂	✗	16	
LL Cas	S	S	2547±41	–	3457	1.14±0.02	–	6430 ⁸³⁷⁵ ₅₀₁₂			
Z And	S	S	2663±59	–	3522	1.09±0.02	3804	1844 ¹⁹⁵⁴ ₁₇₄₅	✓	1,2	✓
R Aqr	D	S	2279±15	–	3315	1.27±0.01	–	321 ³⁵³ ₂₉₃	✗	1	✓
CGCS 5926	S,D	S	2314±45	–	3333	1.25±0.02	3924	3677 ⁴⁹³⁴ ₂₈₈₀	✗	29	✓
M31 SySt-3	?	?	–	–	–	–	–	–	✗	17	
NGC 205 SySt-2	?	?	–	–	–	–	–	–	✗	15	
NGC 205 SySt-3	?	?	–	–	–	–	–	–	✗	15	
M31 SySt-16	?	?	–	–	–	–	–	–	✗	17	
M31 SySt-19	?	S+IR	2547±133	275±11	3457	1.14±0.08	–	–	✗	17	
M31 SySt-35	?	?	–	–	–	–	–	–	✗	17	
[JD2002]11 (SMC SySt-9)	D	D	–	915±60	–	3.17±0.07	–	–	✗	30	
SMC SySt-11	?	?	–	–	–	–	–	–			
SMC SySt-12	?	S	3191±333	–	3835	0.91±0.11	–	–			
SMC SySt-13	?	S+IR	2888±63	124±9	3651	1.01±0.03	–	–			
SMC SySt-14	?	S+IR	2888±49	201±11	3651	1.01±0.03	–	–			
SMC SySt-15	?	S+IR	2775±88	215±10	3585	1.04±0.04	–	–			
RAW 1691 (SMC SySt-7)	S	S	2586±83	–	3479	1.12±0.03	–	–	✗	1	✗
[BE74] 583 (LMC SySt-9)	S	S	3267±91	–	3883	0.89±0.04	–	–			
LMC SySt-15	?	S+IR	2587±131	371±14	3480	1.12±0.07	–	–			
LMC SySt-16	?	D'	3211±-	781±-/278±-	3848	0.90±-	–	–			
LMC SySt-17	?	S+IR	2781±139	278±11	3589	1.04±0.08	–	–			
[RP2006] 776 (LMC SySt-10)	?	D'	–	892±32/233±9	–	3.25±0.06	–	–			
[RP2006] 774 (LMC SySt-11)	?	D'	–	856±38/233±10	–	3.39±0.06	–	–			
LMC SySt-18	?	D'	3128±-	802±-/179±-	3796	0.93±-	–	–			
[RP2006] 883 (LMC SySt-12)	?	D'	–	777±59/233±11	–	3.73±0.09	–	–			
LMC SySt-19	?	S	3076±200	–	3764	0.94±0.07	–	–			
LM 2-39 (LMC SySt-13)	?	D'	3122±-	754±-/221±-	3792	0.93±-	–	–			

Table 7 continued

Table 7 (*continued*)

Name	Old Type	New Type	T _{BB} (K)	T _{dust} (K)	T _{cool} (K)	λ _{peak} (μm)	T _{Gaia} (K)	D _{Gaia} (pc)	O VI 6830Å	O VI Refs.	X-ray ^a Emission
LMC SySt-20	?	S+IR	2702±142	418±16	3544	1.07±0.05	—	—			
[RP2006] 264 (LMC SySt-14)	?	D'	3059±-	743±-/232±-	3754	0.95±-	—	—			
LMC SySt-21	?	?	—	—	—	—	—	—			
LMC SySt-22	?	D'	3031±-	922±-/459±-	3737	0.88±-	—	—			
LMC SySt-23	?	D	—	1313±157	—	2.21±0.10	—	—			
DASCH J075731.1+201735	S?	S	3076±111	—	3763	0.94±0.05	—	—			
Hen 2-25	?	D'	3301±-	975±-/362±-	3905	0.88±-	—	—	x	21	
WRAY 16-51	S	S	2349±31	—	3352	1.23±0.01	—	—			x
Hen 2-57	?	D	—	982±43/349±15	—	2.95±0.05	—	—			
Hen 3-653	S	S	2369±26	—	3362	1.22±0.01	—	—	x	3	
NSV 05572	S	S	2129±104	—	3240	1.36±0.05	—	—			
Hen 4-134	S?	S	3008±62	—	3723	0.96±0.02	—	—			
Th 2-B	?	D'	—	1223±88/387±11	—	2.37±0.10	—	—	x	21	
Hen 4-137	S?	S	3053±101	—	3750	0.95±0.03	—	—			
V748 Cen	S	S	3091±80	—	3773	0.94±0.03	—	—	x	1	x
V345 Nor	S	S	2638±141	—	3508	1.10±0.05	—	—			
Mz 3	?	D	—	1013±67/501±24	—	2.86±0.07	—	—			
IGR J16393-4643	?	?	—	—	—	—	—	—			✓
2MASSJ16503229-4742288	D?	D	—	888±27/392±15	—	3.26±0.04	—	—	x	13	
M 2-9	?	D	—	1085±61/512±23	—	2.67±0.05	—	—			
NGC 6302	S,D'?	D'	4043±-	624±-/318±-	4415	0.72±-	—	—	✓ ?	35	
2MASSJ17145509-3933117	D?	D	—	857±65	—	3.38±0.08	—	—	x	13	
355.12+03.82	S?	?	—	—	—	—	—	—			
Hen 3-1383	S	S	1732±61	—	3053	1.67±0.03	—	—			
Th3-9	S?	S	2325±65	—	3339	1.25±0.03	—	—			
Al 2-B	D?	D'	—	1001±71/252±13	—	2.90±0.31	—	—			
357.12+01.66	D?	D	—	879±74	—	3.30±0.08	—	—			
Al 2-G	D?	D'	—	1023±86/335±16	—	2.83±0.07	—	—			
CXOGBS J173620.2-293338	S?	S	2103±83	—	3227	1.38±0.05	—	—			✓
V503 Her	S	S	3249±177	—	3872	0.89±0.06	—	—	x	1	

Table 7 continued

Table 7 (*continued*)

Name	Old Type	New Type	T_{BB} (K)	T_{dust} (K)	T_{cool} (K)	λ_{peak} (μm)	T_{Gaia} (K)	D_{Gaia} (pc)	O VI 6830Å	O VI Refs.	X-ray ^a Emission
WSTB 19W032	D	D'	3387±-	752±-/203±-	3961	0.86±-	-	-	x	21	
WRAY 16-294	S	S	2851±139	-	3629	1.02±0.05	-	-			
001.97+02.41	S?	S	2554±109	-	3461	1.13±0.04	-	-			
PNG 006.1+04.1	?	D	-	909±179/389±16	-	3.19±0.11	-	-			
001.33+01.07	S?	S	2407±127	-	3382	1.20±0.05	-	-			
PHR 1744-3319	?	?	-	-	-	-	-	-			
001.71+01.14	S?	S	2427±114	-	3393	1.19±0.05	-	-			
ASAS J174600-2321.3	S?	S	2387±69	-	3371	1.21±0.03	-	-			
2MASSJ17460199-3303085	S?	S	2388±42	-	3372	1.21±0.02	-	-	x	13	
OGLE-2011-BLG-1444	S?	?	-	-	-	-	-	-			
PPA 1746-3454	D?	D	-	933±39/361±15	-	3.11±0.06	-	-			
PHR 1751-3349	D?	D	-	1037±82/442±21	-	2.79±0.08	-	-			
Al 2-O	?	D'	3106±-	1013±-/159±-	3782	0.93±-	-	-			
PPA 1752-3542	S?	?	-	-	-	-	-	-			
001.37-01.15	D?	D	-	1144±85/409±17	-	2.53±0.08	-	-			
K 5-37	?	D	-	902±41/379±16	-	3.21±0.08	-	-			
DT Ser	?	S	3697±354	-	4168	0.78±0.09	-	-			
M 2-24	D?	D	-	922±119/361±14	-	3.14±0.09	-	-			
PHR 1803-2746	D?	S+IR	2331±98	222±11	3342	1.24±0.04	-	-			
ShWi 7	?	D'	-	855±152/326±13	-	3.39±0.10	-	-			
PPA 1807-3158	D?	D'	-	1067±73/332±14	-	2.73±0.12	-	-			
V618 Sgr	?	?	-	-	-	-	-	-			
PHR 1809-2745	?	?	-	-	-	-	-	-			
AS 280	S	S	2984±157	-	3708	0.97±0.05	-	-	x	39	
AS 288	D	D	-	1227±32/448±20	-	2.36±0.03	-	-			
Hen 2-379	S	S+IR	3101±157	182±7	3780	0.93±0.04	-	-			
G025.5+00.2	D	D	-	921±171/202±13	-	3.16±0.21	-	-			
Sh 2-71	?	D'	3459±-	962±-/255±-	4008	0.84±-	-	-			
WISEJ192140.40+155354.6	?	D	-	711±189/120±11	-	4.08±1.01	-	-			
V335 Vul	D	S	1911±29	-	3135	1.52±0.02	-	-	x	1	

Table 7 continued

Table 7 (continued)

Name	Old	New	T_{BB}	T_{dust}	T_{cool}	λ_{peak}	T_{Gaia}	D_{Gaia}	O VI	O VI	X-ray ^a
	Type	Type	(K)	(K)	(K)	(μm)	(K)	(pc)	6830Å	Refs.	Emission
V850 Aql	S	S+IR	1756±23	422±14	3064	1.65±0.02	—	—	—	—	—
IRAS 19558+3333	D	?	—	—	—	—	—	—	—	—	—
PM1-322	?	D'	315 2±-	722±-/202±-	3811	0.92±-	—	—	✗	23	—
V627 Cas	D	S+IR	2923±-	385±-	3672	0.99±-	—	—	✗	1	✗

NOTE—^a Muerset et al. (1997), Luna et al. (2013) and references therein.

References. 1. Munari & Zwitter (2002), 2. Blair et al. (1983), 3. Allen (1984), 4. Acker et al. (1988), 5. Muerset et al. (1996), 6. Downes & Keyes (1988), 7. Kniazev et al. (2009), 8. Corradi & Giammanco (2010), 9. Corradi et al. 2010b, 10. Gonçalves et al. 2012, 11. Oliveira et al. (2013), 12. Miszalski et al. (2013), 13. Miszalski & Mikolajewska (2014), 14. Miszalski et al. (2014), 15. Gonçalves et al. (2015), 16. Rodriguez-Flores et al. (2014), 17. Mikolajewska et al. (2014), 18. Li et al. (2015), 19. Gutiérrez-Moreno et al. (1999), 20. Medina Tanco & Steiner (1995), 21. Corradi (1995), 22. Pereira et al. (2002), 23. Pereira & Miranda (2005), 24. Massetti et al. (2006a), 25. Gonçalves et al. (2008), 26. Corradi et al. (2008), 27. Corradi et al. (2011a), 28. Baella et al. (2013), 29. Masetti et al. (2011), 30. Hajduk et al. (2014), 31. Baella et al. (2016), 32. Mikolajewska et al. (2017), 33. Cieslinski et al. (1994), 34. Torres et al. (2012), 35. Groves et al. (2002), 36. Macfarlane et al. (2017), 37. Skopal et al. (2017), 38. Remillard et al. (1992), 39. Mikolajewska et al. (1997), 40. Bond & Kasliwal (2012), 41. Mennickent et al. (2008).

B. EXPLORING FLUX VARIATIONS IN THE SED PROFILES OF SYSTS

Due to the large flux variations of SySts and the different epochs in which the 2MASS and *WISE* observations were performed, we had to explore how possible flux variations between the two surveys can alter the SED fittings. For this exercise, we used one S-type (V694 Mon) and one D-type (IPHAS J205836.43+503307.28) SySt as test objects assuming four different maximum amplitude variations ($\text{mag}_{\text{maximum}} - \text{mag}_{\text{minimum}}$; Figures 11 and 12, panels a to d) and six different scenarios: (1) 2MASS in the maximum brightness and *WISE* in the minimum, (2) 2MASS in the minimum brightness and *WISE* in the maximum, (3) 2MASS in the maximum brightness and *WISE* without any variation (4) 2MASS in the maximum brightness and *WISE* without any variation, (5) 2MASS without any variation and *WISE* in the minimum brightness, and (6) 2MASS without any variation and *WISE* in the minimum brightness.

For the S-type SySt, we assumed maximum amplitude variations in the *J* band of 0.2, 0.6, 1.0, and 3.0 mag. Figure 11 illustrates the SEDs and BB fitting of each of the 24 examples. Apparently, the SED profile, as well as the classification of SySts, does not change significantly due to possible flux variations between the two surveys. Only for an amplitude variation of 3 mag does the SED fitting show some deviations from the BB fitting. In the case of a 1 mag amplitude variation, a poor fitting of the 2MASS data or *W1* and *W2* bands can be seen in only two cases (c1 and c2). In general, the SED fitting for most of the cases is good, and possible flux variations between the two surveys result in a temperature variation of 300–350 K.

Regarding the D-type SySt, maximum amplitude variations of 2, 3, 4, and 6 mag in the *J*-band were considered. A poor fitting of the 2MASS data (e.g., c1, d2, d4) or the *W1* and *W2* bands (e.g., b2, c2, d1, d2, d4, and d6) is an evidence of flux variation between the data of the two surveys (Fig. 12). Nevertheless, we can say that only amplitude variations higher than 3 mag result in significant deviations from the BB fitting. The resulting temperatures show a variation of 250 K.

Then, we applied the same exercise to four D-type SySts (a) AS 210, (b)V347, (c) SS 73 38, and (d) RR tel, using their observed maximum amplitude variation in the *J*, *H*, *K* and *L* bands from Gromadzki et al. (2009). The amplitude variation for the *W2*, *W3* and *W4* bands were calculated by extrapolating a power law. The generated SED profiles are presented in Figure 13. The derived dust temperatures of these four sources show a variation of only of 350, 210, 400, and 230 K, respec-

tively, if the poorly fitting SEDs are taken out of consideration (amplitude flux variation >3 mag).

RR Tel is a special case for which two BBs are required in order to fit the SED, and our dust temperature estimate agrees with the previous work from Jurkic & Kotnik-Karuza (2012). Moreover, the upper limit of the *W2* magnitude makes this SySt quite more uncertain. In general, SySts with upper limit *W1* and *W2* magnitudes are more uncertain but there are fewer than 20 objects in our list. In these real cases, we verify that a poor fitting on the *W1* and *W2* bands (e.g., a2, a4, b2, b4, c2, c6, etc.) or the 2MASS bands (e.g. a1, a2, b3, b5, c2, d3, d5. etc.) is likely associated with flux variations between the data.

All of these examples represent extreme cases given that the possibility that the 2MASS and *WISE* observations were performed during the maximum and minimum phases is not relatively high. Scrutinizing the SED profiles of all SySts in our list, we found that fewer than 20 exhibit some evidence of variability among the 2MASS and *WISE* data.

Overall, the effective temperatures of cold giants or the dust temperatures are reliable within their uncertainties. The agreement of our temperature estimates with previous spectroscopic studies supports our approach. Flux variations in SySts results in temperature variations of the order of 250–350 K, which are comparable with their uncertainties. This analysis is not possible if a source has been observed during or close to an outburst event, which is true for the vast majority of the SySts in our list.

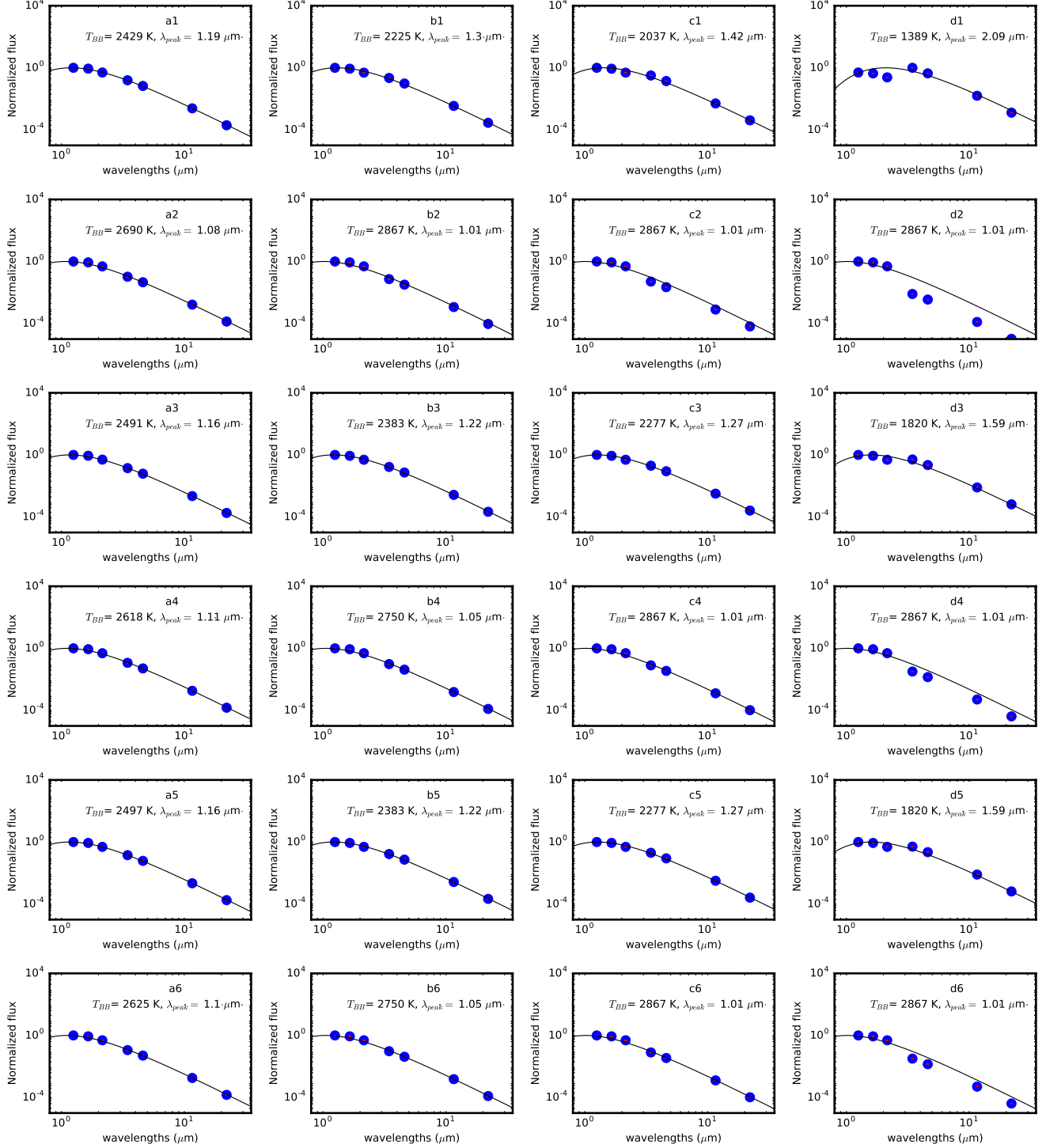


Figure 11. SEDs profiles of V694 Mon for four cases of variation amplitude variations: (a) 0.2 mag (observed), (b) 0.6 mag, (c) 1 mag, and (d) 3 mag, assuming six different cases: (first row) 2MASS in the maximum brightness and WISE in the minimum, (second row) 2MASS in the minimum brightness and WISE in the maximum, (third row) 2MASS in the maximum brightness and WISE without any variation (fourth row) 2MASS in the maximum brightness and WISE without any variation, (fifth row) 2MASS without any variation and WISE in the minimum brightness, and (sixth row) 2MASS without any variation and WISE in the minimum brightness.

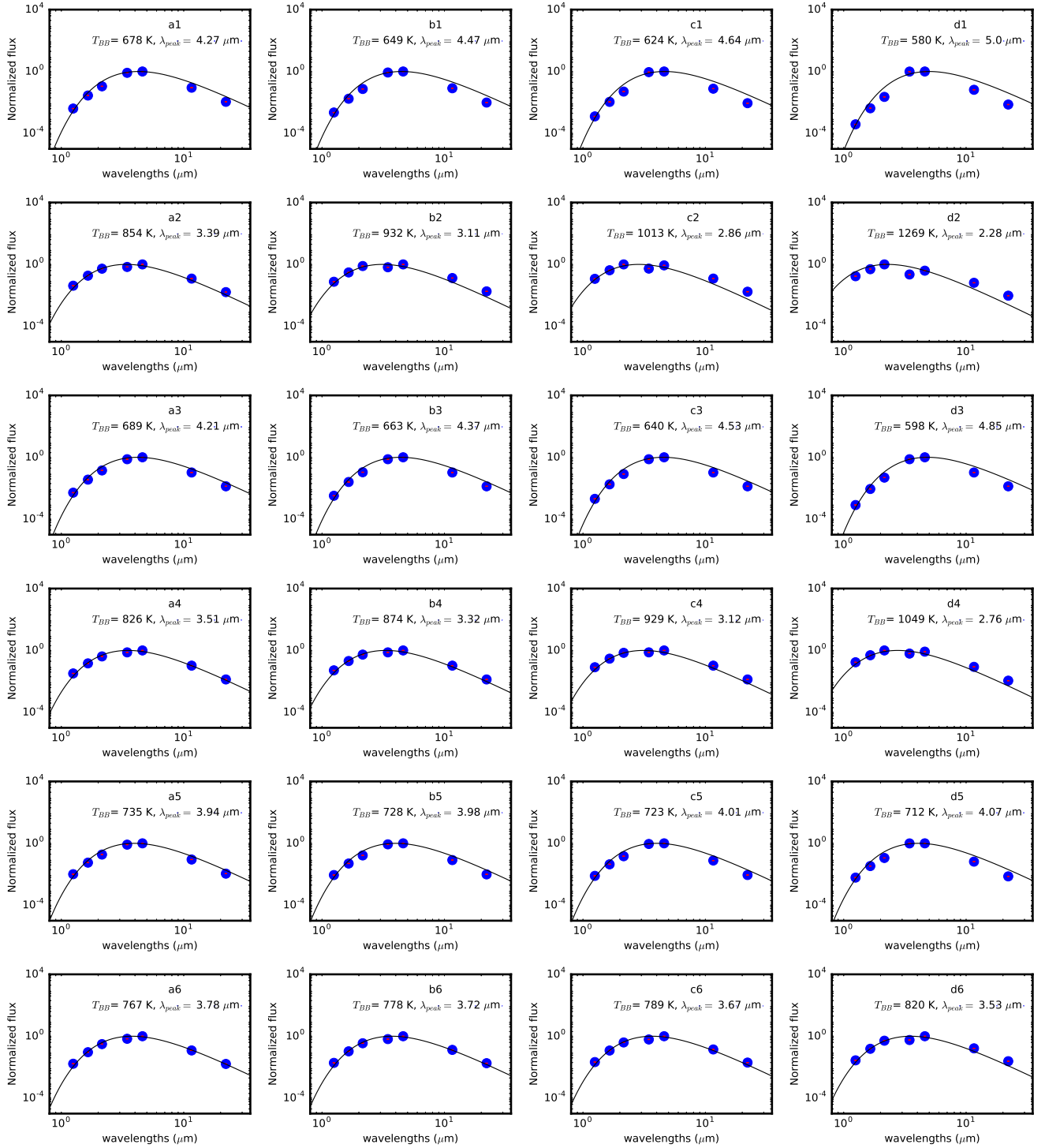


Figure 12. The same as in Figure 11 for the S-type SySt IPHAS J205836.43+503307.28 and four cases of variation amplitude variations: (a) 2 mag (observed), (b) 3 mag, (c) 4 mag, and (d) 6 mag.

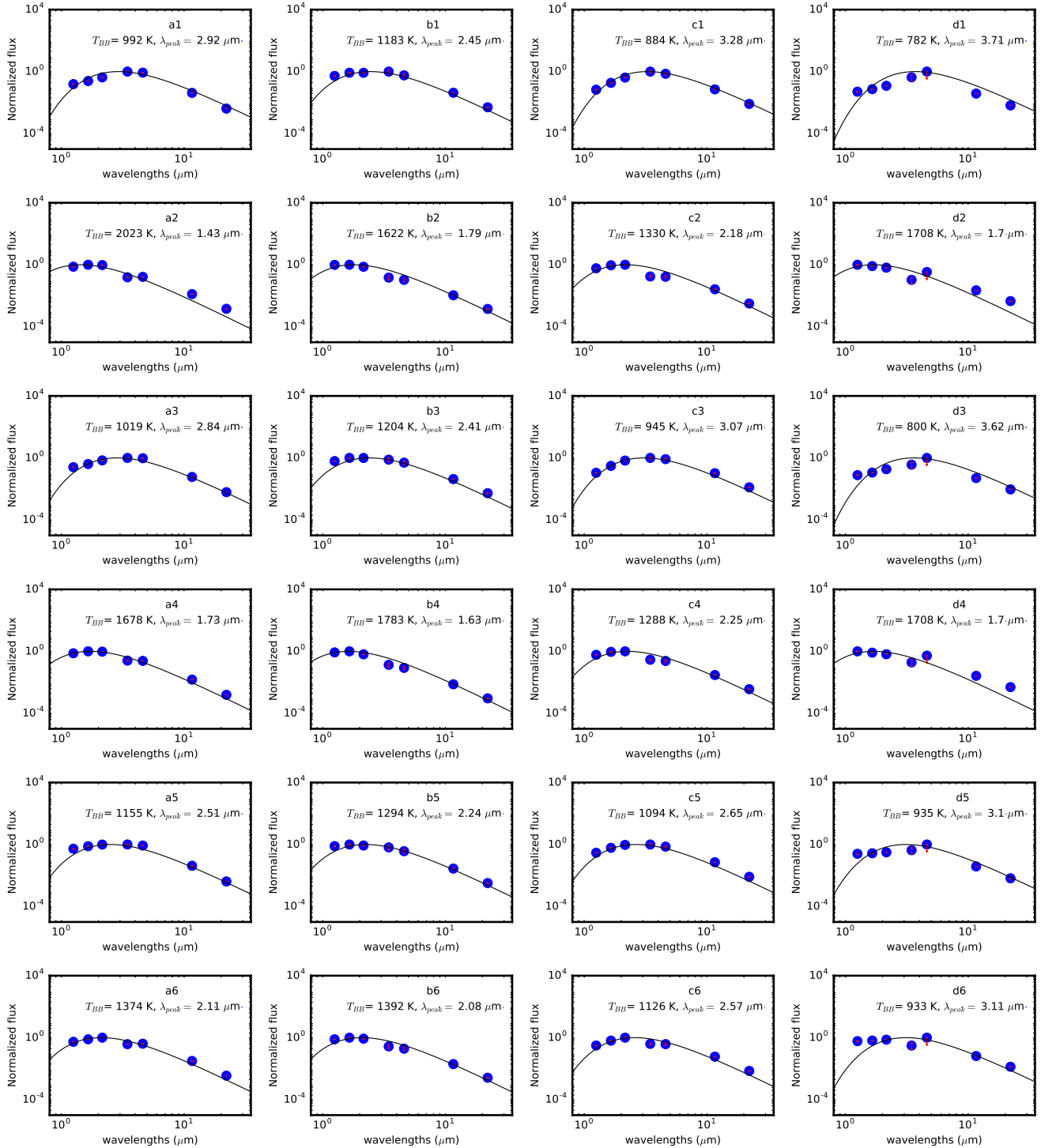


Figure 13. The same as in Figure 11 for four D-type SySts: (a) AS 210, (b)V347, (c) SS!73 38, and (d) RR tel. The maximum amplitude variations of these SySts were obtained from Gromadzki et al. (2009).